Morphology of the feeding apparatus in shorebirds (Charadriiformes): a comparative analysis

A thesis presented in partial fulfilment of the requirements for the degree of

Master of Science
in
Zoology

At Massey University, Palmerston North, New Zealand

Chieh-Ting Lin
2022

Abstract

Shorebirds (Charadriiformes) have developed diverse foraging strategies to feed in different niches. These foraging strategies are associated with morphological variation in their feeding apparatus. This variation among species is complex, with different morphological features reflecting different aspects of foraging ecology. These traits are also presumed to relate to the evolutionary history of the species. Here I attempt to untangle the mystery of the development of diverse feeding apparatus in shorebirds through a series of morphological and phylogenetic comparative analyses using 20 species.

First, I used landmark-based geometric morphometrics to compare skull shapes between species. The results showed that the major variation was the bill length, and there were also other variations. The results suggest that bill and cranial shapes vary phylogenetically, but do not suggest that visual foragers have larger eyes than tactile foragers.

Second, I compare the interspecific variation of bill forms, including the length and curvature of bills, and the bony sensory pit under the rhamphotheca. Individuals of the family Scolopacidae (sandpipers and allies) possess various bill-tip organs with large numbers of concentrated sensory pits. The variety of bill shapes and sensory pits is suggested to relate to different foraging behaviours. Moreover, I test the relationship between distal rhynchokinesis (the ability of some species to bend the tip of the upper mandible) and bill forms. The results suggest that rhynchokinesis may enhance the grabbing capability of some species with bill-tip organs.

Third, I documented and compared the morphology of tongues and palates, including the gross anatomy of oropharyngeal cavities and scanning electron microscopy of micro tongue tip spines. Tongue lengths generally increased with mandible lengths, though there were some exceptions. The spines were significantly associated with small size (light weight) and with a short distance between the tongue tip and the mandible tip. The variety of the forms of tongue tip spines may relate to different foraging behaviours and diets.

Finally, I used the taxonomic distribution of three traits (sensory pits, micro tongue tip spines and distal rhynchokinesis) to test for a role of phylogeny on the evolution of these traits. Different evolutionary models were tested with the traits, and the phylogenetic signal was measured to determine which model best fit the partial phylogeny of charadriiform shorebirds. The results suggest that sensory pits were present in the common ancestor of all

shorebirds, but that the number of pits has rapidly accumulated during the evolution of the Scolopacidae. Micro tongue tip spines were suggested to be absent at the root and to have independently evolved twice across the partial phylogeny. Distal rhynchokinesis was present in some species throughout the phylogeny, and it was suggested to be lost more rapidly than it was gained.

Together, these results provide new insights into how the fundamental structures of the feeding apparatus have been modified during the diversification of the shorebirds.

Acknowledgements

Firstly, I would like to express my great appreciation to my supervisors Phil Battley and Daniel Thomas. Thank you for sharing your knowledge, experience, and enthusiasm. Phil's passion in shorebirds really got me interested in them during a field trip to the Manawatū Estuary Bird Sanctuary, Foxton Beach. Also, I was impressed by the various fascinating bird specimens that he showed us in an undergraduate ornithology course. Phil played a good role as a supervisor that he not only gave appropriate guidance to my research but also introduced me to the resource and the staff I need, including contact with Daniel. Daniel helped me a lot with the method to digitalise and analyse the structures of avian skulls, and phylogenetic analysis. I really enjoyed discovering new things with you.

Thank you to Cleland Wallace for preparing the essential materials and some handy parts to make the experiment achievable. I also want to thank Shaun Nielsen and Tracy Harris for arranging the experiment equipment.

Assistance provided by Raoul Solomon and Yanyu He from the Manawatū Microscopy and Imaging Centre was greatly appreciated for preparing numerous fixative samples and demonstrating how to use the electronic microscope step by step.

I am also very grateful to the other academic staff members, Steven Trewick and Paul Barrett, for helping me set up the camera system and the dissection microscope. The advice given by past students Susan Cunningham was really helpful in experimental design.

Finally, I wouldn't have completed my study without the support from my family and friends. A huge thank you to my parents who have always encouraged and funded me to do the great work. Thank you to my sister for cheering me up, and congratulations on your wedding. I wish you all the best. Thanks to my flatmates Max and Robert and his cats. Special thanks to my lovely cat Sardine (RIP), and my sweet girlfriend Rebecca Tsai and her kittens for their company throughout my study.

2021 and 2022 has been tough years because of the worldwide Covid-19 pandemic and the war in Eastern Europe. I was lucky to do my research in New Zealand where the place was less affected by the disease and the warfare. Hence, I would like to extend my thanks to all the people who work hard to protect us from the viral infection and fight for peace.

Table of Contents

1 General introduction

1.1 Introduction

The shorebirds of the order Charadriiformes often forage on wetland or mudflat habitats for invertebrate prey, and they have developed diverse foraging strategies for different dietary niches (Baker, 1979; Barbosa & Moreno, 1999; Colwell, 2010; Dann, 1987; Hayman, Marchant, & Prater, 1986; Hockey & Douie, 1995; Kuwae *et al.*, 2012; Nebel, Jackson, & Elner, 2005). Interspecific competition among shorebirds feeding in the same habitat is reduced due to resource partitioning (Lourenço *et al.*, 2016). Such partitioning is facilitated by anatomical traits associated with foraging (i.e. feeding apparatus), including a diversity of bill lengths and shapes which apparently correlate well with particular diets and foraging strategies (Baker, 1979; Barbosa & Moreno, 1999; Colwell, 2010; Dann, 1987; Nebel, Jackson, & Elner, 2005). Several comparative studies of the feeding apparatus in shorebirds exist. The work of Burton (1974) focused on muscular systems; Barbosa and Moreno (1999) measured morphological variations in bills and hindlimbs; R. J. Thomas *et al.* (2006) and Hughes (2015) have studies about eye sizes. However, recent studies have indicated that the feeding apparatus and foraging strategies of many shorebird species are not yet fully understood, (Elner *et al.*, 2005; Hughes, 2015; Kuwae *et al.*, 2012; Rico-Guevara *et al.*, 2019), and the role of evolutionary history in the taxonomic distribution of these traits is under explored (Barbosa & Moreno, 1999; Hughes, 2015; Mayr, 2011).

Part of the variation in foraging structures comes from skull morphology (Pecsics *et al.*, 2020; Sun *et al.*, 2018). It was suggested that the large eyes within large orbits benefited the visual foragers to feed at night (Martin & Piersma, 2009; R. J. Thomas *et al.*, 2006). Statistical analyses for describing biological shape (i.e. geometric morphometrics) are a potentially valuable way of quantifying interspecific variation among skull morphologies and correlating this variation with foraging behaviour (Mitteroecker & Gunz, 2009; Profico *et al.*, 2019; Webster & Sheets, 2010). By using geometric morphometrics, we might easily gain the information that reflects the adaptation of bill and cranial shapes for different foraging methods among shorebirds.

In addition to the apparent features of bills such as length and curvature, the bony sensory pits under the rhamphotheca are related to foraging strategies (Baker, 1979; Berkhoudt, 1979; Colwell, 2010; Cunningham *et al.*, 2013; Nebel, Jackson, & Elner, 2005; Piersma *et al.*,

1998; Rico-Guevara *et al.*, 2019). The sensory pits contain mechanoreceptors for detecting function (Berkhoudt, 1979; Rico-Guevara *et al.*, 2019). The bill-tip organ is a particular organ present in the distal portions of maxillae and mandibles in some shorebirds (Colwell, 2010; Cunningham *et al.*, 2013; Nebel, Jackson, & Elner, 2005; Piersma *et al.*, 1998). The organ is composed of mechanoreceptors embedded in the cluster of sensory pits, and it is considered a tool for vibration detection and remote touching (Colwell, 2010; Cunningham *et al.*, 2013; Nebel, Jackson, & Elner, 2005; Piersma *et al.*, 1998; Rico-Guevara *et al.*, 2019; van de Kam *et al.*, 2004). The "remote touch" foraging method can detect the pressure gradients caused by bill probing and the reflection of the prey in the sediment (Piersma *et al.*, 1998; van de Kam *et al.*, 2004). Because various forms of sensory pits and bill-tip organs have been found in the probe feeding in birds within more distantly related families (Cunningham *et al.*, 2010; Cunningham *et al.*, 2013), and the bill-tip organ is not present in every shorebird species, it has been suggested that the bill-tip organ is an independent morphological adaptation for probing under specific ecological pressures (Cunningham *et al.*, 2010; Cunningham *et al.*, 2013; Martin & Piersma, 2009). Previous studies of the bill-tip organ in shorebirds focused on sandpipers in the genus *Calidris* (Cunningham *et al.*, 2013; Nebel, Jackson, & Elner, 2005; Piersma *et al.*, 1998). The organ has been mentioned in other shorebird species (Schäfer & Schmitz, 2016), and my study would investigate the organ of the genera under the family Scolopacidae, including *Numenius, Limosa, Xenus, Tringa, Arenaria,* and *Calidris,* and the relationship between bill features and phylogeny.

Another feature of the bill is distal rhynchokinesis. It is a type of cranial kinesis, and it indicates the flexibility of the distal part of the upper jaw (Estrella & Masero, 2007; Zusi, 1984). The function of distal rhynchokinesis in shorebirds is unclear yet. Some studies suggested that the flexible distal part can help the birds with long bills to grab the prey (van de Kam *et al.*, 2004; Zusi, 1984). Some studies proposed the mechanism of the kinesis is to increase the efficiency in surface tension transport (STT), and furthermore may play a role in biofilm feeding (Elner *et al.*, 2005; Estrella & Masero, 2007). It is also unclear if distal rhynchokinesis is also evolutionarily correlated with other foraging traits.

The morphological features of tongues and palates are associated with food collection, manipulation and swallowing in birds (Erdoğan & Iwasaki, 2014; Erdoğan & Perez, 2015). The gross structures of shorebird tongues include elongated tongue bodies and diverse "V" shape conical papillae to prevent regurgitation (Erdoğan & Iwasaki, 2014; Erdoğan & Perez, 2015; Johnston, 2014). As for microstructures, recent studies proposed that some smaller shorebirds use the micro keratinised spines on the tongue tips to feed on biofilm (Beninger

& Elner, 2020; Elner *et al.*, 2005; Kuwae *et al.*, 2008; Mathot, Lund, & Elner, 2010). Also, it has been suggested that the surface pecking behaviour and STT were related to the usage of micro tongue spines (Colwell, 2010; Elner *et al.*, 2005; Kuwae *et al.*, 2012; Rubega & Obst, 1993). Although the tongue tip structure could be observed by optical microscopes, a scanning electron microscope (SEM) could provide high magnification images to further check the detail and texture of the micro tongue tip spines (Beninger & Elner, 2020; Elner *et al.*, 2005). However, the SEM methods have not been used on the tongues of many species yet.

Finally, in order to understand the evolutionary events that have resulted in the taxonomic distribution of feeding apparatus traits we observe today, evolutionary scenarios for three traits were modelled and tested (Barbosa & Moreno, 1999; Burnham & Anderson, 2002; Mayr, 2011). A Brownian motion model and a Pagel's lambda model were selected to test with the number of sensory pits to show which one better fit (Colwell, 2010; G. H. Thomas & Freckleton, 2012); the equal-rates (ER) model and the all-rates-different (ARD) model were selected to test with the data of micro tongue tip spines and distal rhynchokinesis (Elner *et al.*, 2005; Estrella & Masero, 2007; Pennell *et al.*, 2014). The Brownian motion model is based on the random distribution of the independent trait over time (Cavalli-Sforza & Edwards, 1967; G. H. Thomas & Freckleton, 2012). Different from the random development of Brownian motion, the Pagel's lambda model is based on the phylogenetic signal that describes the tendency of related species to resemble each other dependently (Pagel, 1999; G. H. Thomas & Freckleton, 2012). The ER model is based on the same transition rate of a trait across the phylogeny, whereas the ARD model has different transition rates (Pennell *et al.*, 2014).

This research attempts to untangle the mystery of the complex foraging strategy and the interspecific variation in shorebirds through the morphological and phylogenetic analyses of the skulls, bills and tongues. I would like to answer the question of how phylogeny and foraging methods shape the morphology of feeding apparatus in charadriiform shorebirds.

1.2 Charadriiformes (Shorebird) species and their diets

In this study I analysed morphological features of the skull and tongue in 14 species in the family Scolopacidae (suborder Scolopaci), one species in the family Glareolidae (suborder Lari), three species in the family Charadriidae (suborder Charadrii), one species in the family Recurvirostridae (suborder Charadrii), and one species in the family Haematopodidae (suborder Charadrii) (Fig. 1.1). The taxonomy was based on the three prime untranslated region (3'-UTR) mRNA section (Kuhl *et al.*, 2021). Specimens had been either found dead or were accidental catching casualties from Australia or New Zealand. Basic biological information about the species is given below.

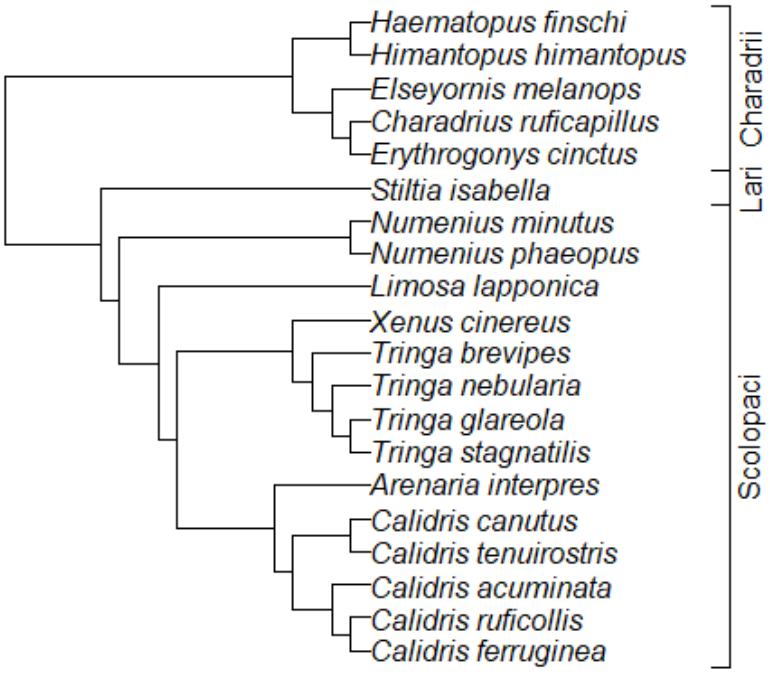

Fig. 1.1: Phylogeny of the charadriiform shorebirds used in this study. The phylogenetic tree was built using the operational taxonomic units (OTUs) (Jetz *et al.*, 2012) with reference to the phylogenetic result of multiple gene sequences (Gibson & Baker, 2012) and other previous studies (Christian, Christidis, & Schodde, 1992; Mayr, 2011). The bars on the right show the suborder.

1.2.1 Scolopacidae

1.2.1.1 Bar-tailed godwit (*Limosa lapponica*)

Bar-tailed godwit specimens were from Australia and New Zealand and represent the subspecies *baueri*, which breeds in Alaska and whose non-breeding grounds are principally in eastern Australia and New Zealand (Hayman, Marchant, & Prater, 1986).

The body length of bar-tailed godwit is 37–41 cm,[1] and the body mass is 275–400 g, and 325–600 g in females (Hayman, Marchant, & Prater, 1986). They are large waders with a long, slightly upturned bill and long legs (Medway, 2000). Females are distinctly larger than males, and the bill of the females is also longer than the males' (Conklin *et al.*, 2011). The bill length of the subspecies *baueri* is <99 mm for males and >88 mm for females with little overlap between males and females (Conklin *et al.*, 2011; Conklin, Lisovski, & Battley, 2021). Females with bills longer than males can reach deeper prey (van de Kam *et al.*, 2004). The hypothesis of resource partitioning suggested that the sexual dimorphism of bill length in shorebirds reduced intersexual competition (Mancini *et al.*, 2013; Nebel & Thompson, 2011). There is evidence of intersexual competition in bar-tailed godwits in The Netherlands: males and females foraged in different intertidal areas, and females seem to dominate the better-quality foraging areas (Both, Edelaar, & Renema, 2003). In addition, the foraging strategies are different between males and females in that males tended to tap the mud surface for small prey with slightly higher and less variable intake rates and higher feeding success, whereas females tended to probe more for deeply buried prey (Pierre, 1994; Ross, 2018).

Bar-tailed godwits are usually found foraging on mudflats and sandflats of harbours, estuaries and sandy coasts, but sometimes on saltmarshes and coastal pastures (Medway, 2000). They prefer to feed along broad intertidal edges (Medway, 2000). They are gregarious, often foraging in huge flocks with red knots (Medway, 2000). The godwits mainly eat polychaetes in deep straight burrows, but they also take benthos such as mud snails, bivalves, crustaceans, cumaceans and juvenile flounder (Choi *et al.*, 2017; Duijns, Hidayati, & Piersma, 2013; Ross, 2018). Also, terrestrial invertebrates, cranefly larvae and some berries have been recorded in their diets in the breeding grounds (Woodley, 2022). The long bill enables the godwits to probe into mud and sand in deep water, but shallow and surface prey are also taken (Esselink & Zwarts, 1989; Zharikov & Skilleter, 2011). Relatively shorter-billed males predominantly use a 'sewing machine' method by rapidly and repeatedly jabbing mud

[1] The measurement of overall body size is the length between the tip of bill and the tip of tail when the bird is flattened out.

or wet sand especially for catching mud snails (Ross, 2018). Visual cues are also used by the birds especially for targeting the retreating worms and crabs (Ross, 2018). They may make the prey more visible with movement by vibrating their bills against the surface (Hockey & Douie, 1995). Males preferred to use the sewing method while females preferred to use visual cues to search for active prey (Ross, 2018). Nocturnal feeding in bar-tailed godwits has been confirmed through radiotelemetric data and direct observation (Scheiffarth *et al.*, 2002; Zwarts, Anne-Marie, & Roelof, 1990). It has been suggested that they spend substantial time feeding at night on the same habitat during daytime (Rohweder & Baverstock, 1996; Zwarts, Anne-Marie, & Roelof, 1990). However, Jourdan *et al.* (2021) recently demonstrated the intraspecific variation of the night-time habitat selection in godwits.

1.2.1.2 Red knot (*Calidris canutus*) (other common name: lesser knot)

Red Knots analysed were from Australia and New Zealand, where the most numerous subspecies is *rogersi* with smaller numbers of *piersmai* (Battley, 2022). The subspecies *rogersi* breed in Chukchi Peninsula in eastern Russia, and the subspecies *piersmai* breed on the New Siberian Islands (Battley, 2022). The non-breeding range for both species extends from northwest Australia to New Zealand (Battley, 2022; Yang *et al.*, 2013).

The body length of red knot is 23–28.5 cm, and the body mass is 100–200 g (Medway, 2000). They are medium-sized waders with a short, slightly decurved black bill and short, dull greenish-grey legs (Powlesland, 1998). Females are on average slightly larger than males (Hayman, Marchant, & Prater, 1986).

Red knots are usually found foraging on coastal areas, including mudflats, sandflats, sandy estuaries, beaches, and rocky shores, but sometimes on saltmarshes and coastal pastures (Hayman, Marchant, & Prater, 1986; Hockey & Douie, 1995; Medway, 2000). They are gregarious, often foraging in huge flocks with other species (Hockey & Douie, 1995; Medway, 2000; Powlesland, 1998). Red knots mainly eat small bivalves on intertidal mudflats, but also take polychaetes, crustaceans, gastropods, and rhizomes (Choi *et al.*, 2017). They eat bivalves and snails by swallowing them whole (Zwarts & Blomert, 1992). Some thin-shelled preys live deeply in mud where the knots cannot reach with their bills, whereas the thick-shelled preys live at the surface are hard to be ingested by knots (Zwarts & Blomert, 1992). Therefore, the medium-sized *Limecola balthica* (synonyms as *Macoma balthica*) is a major prey of the compromise (Zwarts & Blomert, 1992). The bivalve *Potamocorbula laevis* is also an important prey in Asia that is small enough to be swallowed and crushed in a high intake

rate by red knots (Choi *et al.*, 2017; Yang *et al.*, 2013). Red knots mostly forage on the falling tide with a 'sewing machine' method by rapidly and repeatedly jabbing mud or wet sand (Medway, 2000; Powlesland, 1998). They also probe shallow burrows and peck the surface for food (Hayman, Marchant, & Prater, 1986; Hockey & Douie, 1995). Nocturnal feeding in red knots has been confirmed through radiotelemetric data and direct observation (Sitters *et al.*, 2001; Zwarts, Anne-Marie, & Roelof, 1990). Sitters *et al.* (2001) have demonstrated that they tend to spend the night feeding on the sandflats, instead of rocky platforms in Patagonia where they forage in daylight. They show great capability to find bivalves through probing in darkness (Sitters *et al.*, 2001).

1.2.1.3 Great knot (*Calidris tenuirostris*)

Great knots breed in the subarctic highlands in north-eastern Siberia (Hayman, Marchant, & Prater, 1986). After breeding, they migrate to south-eastern Asia, Indian subcontinent, the Philippines and Australasia (Hayman, Marchant, & Prater, 1986; Powlesland, 1998).

The body length of great knot is 26–28 cm, and the body mass is 115–261 g (Hayman, Marchant, & Prater, 1986). They are medium-sized waders with black bill and grey legs (Powlesland, 1998). Females are on average larger than males (Hayman, Marchant, & Prater, 1986).

Great knots are found foraging on large sandy or muddy estuaries and coasts (Hayman, Marchant, & Prater, 1986). They prefer to feed along broad intertidal edges (Hayman, Marchant, & Prater, 1986). They are gregarious, foraging in huge flocks at favoured sites (Hayman, Marchant, & Prater, 1986; Powlesland, 1998).

Great knots mainly eat small to medium-sized bivalves, but they also take gastropods, brachiopods, crustaceans, polychaetes, and small sea cucumbers (Battley, 2017; Choi *et al.*, 2017; Tulp & Degoeij, 1994; Zhang *et al.*, 2011). On the breeding grounds they also take berries (Zhang *et al.*, 2011). Great knots exhibit an opportunistic foraging strategy. Their diet varies opportunistically with the composition of prey in different habitats (Zhang *et al.*, 2011). A dietary study at Roebuck Bay, Australia, in 1991 revealed a complex diet with a diversity of prey species (Tulp & Degoeij, 1994). The bivalve *Corbicula fluminea* and the gastropod *Assiminea violacea* were important prey at Chongming Dongtan, China, during the spring stopovers of 2009 and 2010 (Zhang *et al.*, 2011). Dropping analysis at Chongming Dongtan showed that more than 70% of the diet of great knots consisted of bivalves and gastropods (Zhang *et al.*, 2011). At the Dandong Yalu Jiang Estuary in 2011 and 2012, the

major prey was *Potamocorbula laevis,* which had high densities and accessibility (Choi *et al.*, 2017). The medium-sized *P. laevis* were small enough to be swallowed whole in a high intake rate with high energy gain by great knots (Choi *et al.*, 2017). The thin-shelled bivalves *Macoma* and *Siliqua* were also considered good prey for the knots to ingest and crush (Tulp & Degoeij, 1994; Zwarts & Blomert, 1992).

However, thick-shelled *Anomalocardia* was also taken by great knots probably because *Anomalocardia* were easy to be detected and handled at Roebuck Bay in Australia (Tulp & Degoeij, 1994). *Quadrans pristis* was another preferred prey, but great knots might have switched from *Quadrans* to *Modiolus* when *Modiolus* were available (Tulp & Degoeij, 1994). Great knots mainly probe for food (Hayman, Marchant, & Prater, 1986). In addition to tactile cues, great knots may also use visual cues to detect the tubeworms and their holes for the attached bivalves *Modiolus* spp. underneath (Tulp & Degoeij, 1994). Great knots are assumed to forage at night based on the calculation of energy intake (Tulp & Degoeij, 1994).

1.2.1.4 Red-necked stint (*Calidris ruficollis*)

Red-necked stints breed on tundra at low altitude in northern Siberia and north-western Alaska (Hayman, Marchant, & Prater, 1986; Medway, 2000; Powlesland, 1998). After breeding, they migrate to Malaysia, the Philippines and Australasia (Hayman, Marchant, & Prater, 1986; Medway, 2000; Powlesland, 1998).

The body length of red-necked stint is 13–16 cm, and the body mass is 21–51 g (Medway, 2000). They are tiny waders with short straight black bill and short black legs (Medway, 2000; Powlesland, 1998). Females are on average slightly larger than males (Hayman, Marchant, & Prater, 1986).

Red-necked stints are usually found foraging on tidal mudflats, sandflats, saltmarshes and coastal lagoons (Medway, 2000). They prefer coastal areas, but sometimes feed at inland wetlands (Hayman, Marchant, & Prater, 1986). They are gregarious, often foraging in huge flocks with other species (Medway, 2000). The stints mainly eat small marine invertebrates, molluscs, crustaceans and insects (Medway, 2000). They mostly forage with a 'sewing machine' method by rapidly and repeatedly jabbing mud or wet sand (Medway, 2000). They also probe shallow burrows and peck the surface for food (Hayman, Marchant, & Prater, 1986; Powlesland, 1998). Nocturnal feeding in red-necked stints has been confirmed through direct observation (Dann, 1999; Rohweder & Baverstock, 1996). Rohweder and Baverstock (1996) have demonstrated that they tend to spend the night feeding on the

ocean beaches at low tides, instead of the mudflats where they forage in daylight, but Dann (1999) observed that they also feed on the mudflats at night.

1.2.1.5 Curlew sandpiper (*Calidris ferruginea*)

Curlew sandpipers breed on high-arctic coastal tundra in central Siberia, although a few in northern Alaska (Hayman, Marchant, & Prater, 1986; Medway, 2000). After breeding, they migrate to Africa, southern Asia and Australasia (Medway, 2000; Powlesland, 1998).

The body length of curlew sandpiper is 18–23 cm, and the body mass is 44–117 g (Medway, 2000). They are small waders with a long, decurved, black bill and long black legs (Medway, 2000; Powlesland, 1998). Females are average larger than males, and the bill of the females is also longer than the males' (Hayman, Marchant, & Prater, 1986; Hockey & Douie, 1995).

Curlew sandpipers are usually found foraging on tidal flats, brackish pools, coastal lakes and lagoons, wet mud, and shallow water (Medway, 2000; Powlesland, 1998). They are gregarious, often foraging in huge flocks with other species (Hayman, Marchant, & Prater, 1986; Hockey & Douie, 1995; Medway, 2000; Powlesland, 1998). When prey is abundant, curlew sandpipers form single-sex foraging groups (Hockey & Douie, 1995). Females forage faster and their longer bills enable them to reach deeper prey than males (Hockey & Douie, 1995). Sexual segregation may reduce intraspecific competition and allow females to store enough energy for breeding (Hockey & Douie, 1995). The sandpipers mainly eat polychaetes, molluscs, crustaceans, and insect larvae (Medway, 2000). In addition, they eat many seeds of the salt marsh plant *Salicornia* to store enough energy before migration (Hockey & Douie, 1995). Curlew sandpipers forage in many ways. They can probe deeply and peck from the surface (Hayman, Marchant, & Prater, 1986; Medway, 2000; Powlesland, 1998). In addition, they can submerge the head in water or use the 'stitching' method by rapidly and repeatedly probing the mud (Hockey & Douie, 1995). Nocturnal feeding in curlew sandpipers has been confirmed through direct observation (Dann, 1999; Rohweder & Baverstock, 1996). However, Zwarts, Anne-Marie, and Roelof (1990) have demonstrated that they rarely feed at night. Rohweder and Baverstock (1996) observed that some birds leave the daylight sandy mudflat habitat at night, but where the birds went was unknown. Dann (1999) have recorded that they tend to change the habitat to feed on the mudflats and supratidal areas at night.

1.2.1.6 Sharp-tailed sandpiper (*Calidris acuminata*)

Sharp-tailed sandpipers breed at tundra in north-eastern Siberia (Hayman, Marchant, & Prater, 1986). After breeding, they migrate to New Guinea, Australia and New Zealand (Hayman, Marchant, & Prater, 1986; Medway, 2000).

The body length of sharp-tailed sandpiper is 17–22 cm, and the body mass is 39–114 g (Medway, 2000). They are medium-sized, brown speckled waders with a short, slightly decurved, dark bill and yellowish-green legs (Hayman, Marchant, & Prater, 1986; Medway, 2000). The wing length of males is average longer than females', but the sexes look similar in the field (Hayman, Marchant, & Prater, 1986; Medway, 2000).

Sharp-tailed sandpipers are usually found foraging on grasslands along the edges of freshwater, brackish lagoons, low-growing saltmarshes and open marsh-turf flats, but sometimes on tidal mudflats (Hayman, Marchant, & Prater, 1986; Powlesland, 1998). Although they are gregarious, they often only forage in small flocks of themselves, but on tidal mudflats tend to associate with other species (Hayman, Marchant, & Prater, 1986; Medway, 2000). They eat worms, molluscs, crustaceans, insects, and seeds (Medway, 2000).

1.2.1.7 Little whimbrel (*Numenius minutus*) (other common name: little curlew)

Little whimbrels breed in open areas in larch woodland along river valleys (Hayman, Marchant, & Prater, 1986). After breeding, they migrate to New Guinea and north Australia in flocks (Hayman, Marchant, & Prater, 1986). They also move within Australia following rainfall, sometimes reach southern Australia, Tasmania, and New Zealand (Hammond, 2013; Hayman, Marchant, & Prater, 1986).

The body length of little whimbrel is 29–32 cm, and the body mass is 118–221 g (Hayman, Marchant, & Prater, 1986). They are the world's smallest curlew with a short, slightly decurved bill (Hayman, Marchant, & Prater, 1986). Females are on average slightly larger than males (Hayman, Marchant, & Prater, 1986).

Little whimbrels are usually found foraging on grassland, marshes, bare cultivation, mown grass, and black soil plains near fresh water (Hammond, 2013; Hayman, Marchant, & Prater, 1986). They eat small terrestrial insects sized from ant to grasshoppers, and they also take seeds (Hammond, 2013). They pick and probe for the food (Hammond, 2013).

1.2.1.8 Whimbrel (*Numenius phaeopus*)

The whimbrel analysed was from Australia, where the most numerus subspecies is *variegatus* (Powlesland, 1998). The Asiatic subspecies *variegatus* breeds in eastern Siberia, and the American subspecies *hudsonicus* (recently considered as separate species) breed in northern North America (Medway, 2000; Melville, 2022; Powlesland, 1998). The non-breeding range for both species extends from tropical and temperate regions in south-eastern Asia to Australia and New Zealand (Hayman, Marchant, & Prater, 1986; Medway, 2000).

The body length of whimbrel is 40–46 cm, and the body mass is 270–493 g (Hayman, Marchant, & Prater, 1986). They are large waders with a long, decurved, black bill with a pink base and bluish-grey legs (Medway, 2000; Powlesland, 1998).

Whimbrels are usually found foraging on open mudflats, sandflats, coastal estuaries, lagoons, salt marshes, and mangroves, but sometimes on rocky shores, reefs, inland wetlands, dry grasslands, and farmlands (Hayman, Marchant, & Prater, 1986; Hockey & Douie, 1995; Powlesland, 1998). They often forage singly or in small groups, although individuals may join a flock of Eastern Curlew (Hayman, Marchant, & Prater, 1986; Medway, 2000). The long bill enables them to probe deeply into mud and sand burrows (Hockey & Douie, 1995). Whimbrels mainly eat fiddler crabs, which they dismember before consumption, and they also take polychaetes (Hockey & Douie, 1995; Medway, 2000). They walk slowly and continuously to look for food (Hockey & Douie, 1995). Although the long bills make them potential competitors to bar-tailed godwits, compared with godwits, whimbrels typically lunge and capture prey from surface and shallow burrows (Hockey & Douie, 1995; Powlesland, 1998). They also use visual cues, especially at night to locate crabs or their burrows (Turpie & Hockey, 1993). Nocturnal feeding in whimbrel has been confirmed (Hockey & Douie, 1995; Zwarts, Anne-Marie, & Roelof, 1990). They feed on the same habitat day and night (Rohweder & Baverstock, 1996). The time they feed at night appears related to lunar phase (Rohweder & Baverstock, 1996; Turpie & Hockey, 1993). Although their night foraging time is not long, they tend to catch larger prey species at that time (Hockey & Douie, 1995; Zwarts, Anne-Marie, & Roelof, 1990).

1.2.1.9 Grey-tailed tattler (*Tringa brevipes*)

Grey-tailed tattlers breed along stony riverbeds in the mountains of northeastern Siberia from late May to early September (Hayman, Marchant, & Prater, 1986; Steed, 2017). After

breeding, they migrate to south-eastern Asia, Australia, some of the Pacific islands including New Guinea, Micronesia, Fiji, and Tuvalu (Steed, 2017). Small numbers reach in Tasmania and New Zealand (Hayman, Marchant, & Prater, 1986).

The grey-tailed tattler was formerly in the genus *Heteroscelus,* but the recent genetic analysis put the grey-tailed tattler in the genus *Tringa* (Banks *et al.*, 2006). The body length of grey-tailed tattler is 24–27 cm, and the body mass is 80–162 g (Hayman, Marchant, & Prater, 1986). They are medium-sized waders with a straight bill and short legs (tarsus shorter than bill) (Hayman, Marchant, & Prater, 1986; Steed, 2017). Females are on average larger than males (Hayman, Marchant, & Prater, 1986).

Grey-tailed tattlers are usually found foraging on coasts and estuaries, including tidal mudflats, sandflats, reefs, and rocky coasts, and sometimes on inland on paddy fields (Hayman, Marchant, & Prater, 1986; Steed, 2017). They feed singly or in loose groups (Hayman, Marchant, & Prater, 1986). The tattlers mainly eat polychaetes, molluscs, crustaceans, and insects, but they also take fish (Steed, 2017). They prefer to eat small crabs and sometimes remove the legs of crabs before consumption (Steed, 2017). They mainly probe around rocks and rubble, or on mudflats for food (Steed, 2017). Nocturnal feeding at low tide in grey-tailed tattlers has been well documented in a recent study (Stuart, Wooding, & Takurou, 2015). They tended to spend the night feeding on the main body of a rock platform, instead of the edge of the rock platforms where they forage in daylight (Stuart, Wooding, & Takurou, 2015). The habitat change may relate to the activity of prey (Stuart, Wooding, & Takurou, 2015).

1.2.1.10 Common greenshank (*Tringa nebularia*)

Common greenshank breed in taiga and forest zones from Scotland and Scandinavia to the Kamchatka Peninsula of Siberia and Japan (Hayman, Marchant, & Prater, 1986; Powlesland, 1998). After breeding, Scottish breeders winter mainly around British Isles, while other greenshanks migrate to Africa, India, China, Malaysia, the Philippines, Australia, and a few arrive in New Zealand (Powlesland, 1998).

The body length of common greenshank is 30–34 cm, and the body mass is 150–280 g (Hayman, Marchant, & Prater, 1986). They are elegant, moderately large waders with a dark, long, slightly upturned bill and long, green-yellow legs (Hayman, Marchant, & Prater, 1986; Powlesland, 1998). Females are slightly larger than females, but the sexes look similar in the field (Hayman, Marchant, & Prater, 1986).

Common greenshanks are usually found foraging on estuaries, salt marshes, and open coastal tidal flats, but sometimes on inland wetlands (Hayman, Marchant, & Prater, 1986; Hockey & Douie, 1995; Powlesland, 1998). They prefer to feed singly (Hayman, Marchant, & Prater, 1986; Hockey & Douie, 1995). Greenshanks eat polychaetes, crabs, insects, insect larvae, amphibians, and sometimes fish (Hockey & Douie, 1995). They walk briskly to peck and probe for food on sand and mud flats (Powlesland, 1998). They also rapidly dash for fish and small prey (Hayman, Marchant, & Prater, 1986; Hockey & Douie, 1995). In addition, they can sweep sideways as a 'mowing' or 'scything' method used by avocets (Hockey & Douie, 1995; Rico-Guevara *et al.*, 2019). They seldom forage while swimming (Hockey & Douie, 1995). Nocturnal feeding in common greenshanks has been confirmed (Hockey & Douie, 1995; Ntiamoa-Baidu *et al.*, 1998). They tend to spend the night feeding on moist sandy mud, which is different from the daylight habitat (Rohweder & Baverstock, 1996).

1.2.1.11 Wood sandpiper (*Tringa glareola*)

Wood sandpipers breed in pine forests, open tundra, marshes or bogs in Northern Europe, Baltic countries, Russia and Asia (Hayman, Marchant, & Prater, 1986). After breeding, they migrate south to Africa, India, New Guinea, Southeast Asia, and scarcely to Australia ("Birdlife Australia," 2022a; Hayman, Marchant, & Prater, 1986).

The body length of wood sandpiper is 19–21 cm, and the body mass is 50–90 g (Hayman, Marchant, & Prater, 1986). They are small slim waders with a short straight bill and long legs (Hayman, Marchant, & Prater, 1986). Females are average slightly larger than males (Hayman, Marchant, & Prater, 1986).

Wood sandpipers are usually found foraging on inland freshwater wetlands and river flood plains, but they also tolerate brackish wetlands ("Birdlife Australia," 2022a; Hayman, Marchant, & Prater, 1986; Hockey & Douie, 1995). They are also found at sewage works, drainage ditches and along lakes and farm dams (Hockey & Douie, 1995). They forage in singly or in small flocks, often with other waders ("Birdlife Australia," 2022a; Hayman, Marchant, & Prater, 1986). Wood sandpipers mainly eat aquatic insects, insect larvae, molluscs, crustaceans, and seeds, but they also take small fish, frogs and snails (Hockey & Douie, 1995). They mostly forage by pecking from the water or mud surface (Hayman, Marchant, & Prater, 1986; Hockey & Douie, 1995; Powlesland, 1998). In addition, they can swim well, submerge the head rapidly to the muddy bottom, probe into soft mud burrows, or sweep sideways as a 'mowing' or 'scything' method used by avocets (Hockey & Douie,

1995; Rico-Guevara *et al.*, 2019). Nocturnal feeding in a few wood sandpipers has been recorded at tropical wintering sites (Ntiamoa-Baidu *et al.*, 1998). However, it has been suggested that wood sandpipers do not often feed at night unless prey numbers during the day are low (Krupa *et al.*, 2009)

1.2.1.12 Marsh sandpiper (*Tringa stagnatilis*)

Marsh sandpipers mainly breed on freshwater marshland with lush grassy vegetation in eastern Europe, central Asia and Mongolia from April to September (Hayman, Marchant, & Prater, 1986; Powlesland, 1998). After breeding, they migrate to Africa, southern Asia, and Australasia (Powlesland, 1998).

The body length of marsh sandpiper is 22–25 cm, and the body mass is 45–120 g (Hayman, Marchant, & Prater, 1986). They are medium-sized, slim waders with long, black, needle-like bill and long legs (Hayman, Marchant, & Prater, 1986; Hockey & Douie, 1995; Powlesland, 1998). Females are average slightly larger than males, but the sexes look similar in the field (Hayman, Marchant, & Prater, 1986).

Marsh sandpipers are usually found foraging on fresh or brackish wetlands, but sometime on estuaries and coastal lagoons (Hayman, Marchant, & Prater, 1986; Hockey & Douie, 1995; Powlesland, 1998). They are gregarious, often foraging in mixed-species flocks (Hayman, Marchant, & Prater, 1986; Hockey & Douie, 1995; Powlesland, 1998). The active stirring behaviour of greenshanks in shallow water may let marsh sandpipers catch their prey more easily (Hockey & Douie, 1995). The long legs enable them to wade through shallow water (Hockey & Douie, 1995). They mostly forage by pecking from the water or mud surface (Hayman, Marchant, & Prater, 1986; Hockey & Douie, 1995; Powlesland, 1998). In addition, they can submerge the head rapidly to the muddy bottom, probe into soft mud burrows, or sweep sideways as a ‘mowing’ or ‘scything’ method used by avocets (Hockey & Douie, 1995; Rico-Guevara *et al.*, 2019). Marsh sandpipers mainly eat larvae of the order Coleoptera and the family Chironomidae, but they also take crustaceans, molluscs and polychaetes (Hockey & Douie, 1995). Nocturnal feeding in a few marsh sandpipers has been recorded at tropical wintering sites (Ntiamoa-Baidu *et al.*, 1998).

1.2.1.13 Terek sandpiper (*Xenus cinereus*)

Terek sandpiper breed along rivers and freshwater lakes in Eastern Europe and Finland (Hayman, Marchant, & Prater, 1986). After breeding, they migrate to tropical coasts in Western Europe, Africa, Arabia, Southern and Southeast Asia, the Philippines and Australasia (Hayman, Marchant, & Prater, 1986; Powlesland, 1998).

The body length of terek sandpiper is 22–25 cm, and the body mass is 50–126 g (Hayman, Marchant, & Prater, 1986). They are small waders with a long, slightly upcurved bill and short legs (Hayman, Marchant, & Prater, 1986; Powlesland, 1998). Females are on average slightly larger than males (Hayman, Marchant, & Prater, 1986).

Terek sandpipers are usually found foraging on mudflats, sandflats, reefs, and brackish coastal lagoons (Hayman, Marchant, & Prater, 1986; Hockey & Douie, 1995). They mainly eat small crabs, but they also take shrimp and insects (Hockey & Douie, 1995). They usually forage actively by chasing and pecking prey on the surface (Hayman, Marchant, & Prater, 1986; Hockey & Douie, 1995; Powlesland, 1998). In addition, they can probe deeply into soft mud burrows or sweep sideways as a 'mowing' or 'scything' method used by avocets (Hayman, Marchant, & Prater, 1986; Hockey & Douie, 1995; Powlesland, 1998; Rico-Guevara *et al.*, 2019). They forage in scattered flocks mixing with other waders (Hayman, Marchant, & Prater, 1986; Hockey & Douie, 1995). There is a lack of record of nocturnal feeding in terek sandpipers. Some birds leave the daylight habitat at night, but there is no information of what those birds do overnight yet (Rohweder & Baverstock, 1996).

1.2.1.14 Ruddy turnstone (*Arenaria interpres*)

Ruddy turnstones breed on the coastal plain or lowlands throughout the Arctic from late May to early August (Hayman, Marchant, & Prater, 1986; Medway, 2000; Powlesland, 1998). After breeding, they migrate to tropical and temperate coasts worldwide (Hayman, Marchant, & Prater, 1986; Medway, 2000; Powlesland, 1998).

The body length of ruddy turnstone is 21–25.5 cm, and the body mass is 84–190 g (Hayman, Marchant, & Prater, 1986). They are distinctively stocky, medium-sized waders with black, white, and brown plumage, a short, slightly upturned, wedge-shaped bill, and short legs (Hayman, Marchant, & Prater, 1986; Medway, 2000; Powlesland, 1998). Females are on average slightly larger than males (Hayman, Marchant, & Prater, 1986).

Ruddy turnstones prefer to feed on especially rocky and coasts and exposed reefs (Hayman, Marchant, & Prater, 1986; Medway, 2000). They are usually found on wave platforms, coastal lagoons, some estuaries, and sometimes on rough farmland (Medway, 2000; Powlesland, 1998). They tend to feed along the tideline as soon as the ebb starts (Powlesland, 1998). They are gregarious, often forming flocks in various sizes (Medway, 2000). Sometimes a single bird joins the group of other waders (Medway, 2000). Ruddy turnstones use their wedge-shape bill in unique ways that enable them to search for food in many ways (Hayman, Marchant, & Prater, 1986; Hockey & Douie, 1995; Medway, 2000). They mainly eat gastropod, isopod, polychaete, and insect larvae, but they also take amphipods, bivalves and terrestrial arthropods (Hockey & Douie, 1995). In addition, they sometimes scavenge on left food or carcasses (Hayman, Marchant, & Prater, 1986; Hockey & Douie, 1995). The prey they can take are fairly large for their size (Hockey & Douie, 1995). Turnstones can flick over and push aside seaweed and small stones, probe and peck under debris to look for prey (van de Kam *et al.*, 2004; Whitfield, 1990). They can dig the small mud crab burrows and chase the crabs (Hayman, Marchant, & Prater, 1986; Medway, 2000; Powlesland, 1998; Whitfield, 1990). They can smash barnacles and probe to cut the adductor muscle of gastropods (Hockey & Douie, 1995; Whitfield, 1990). They can peck for prey on or just below the surface (Whitfield, 1990). Moreover, they sometimes steal food from other waders (Hockey & Douie, 1995). Systematic observations show that the turnstones do feed at night, but the time is much less than other waders (Hockey & Douie, 1995; Ntiamoa-Baidu *et al.*, 1998; Zwarts, Anne-Marie, & Roelof, 1990).

1.2.2 Glareolidae

1.2.2.1 Australian pratincole (*Stiltia isabella*)

Australian Pratincole only breed in semi-arid areas in Australia (Hayman, Marchant, & Prater, 1986). They breed after suitable rainfall, which does not have to be any certain month ("Birdlife Australia," 2022b). They regularly migrate between north and south and can reach Java, Borneo, Sulawesi, New Guinea, Lord Howe Island and Christmas Island ("Birdlife Australia," 2022b; Hayman, Marchant, & Prater, 1986).

The body length of Australian pratincole is 22–24 cm, and the body mass is 55–75 g (Hayman, Marchant, & Prater, 1986). They are slim sandy-olive birds with long legs and very long and attenuated wings ("Birdlife Australia," 2022b).

Australian Pratincoles are usually found close to water ("Birdlife Australia," 2022b). The habitat includes open inland plains, sparsely wooded plains, tussock grasslands, stony plains, claypans, stock-tanks, stock routes and airfields ("Birdlife Australia," 2022b). They are insectivores and mainly eat insects, spiders and centipedes ("Birdlife Australia," 2022b). They can not only search prey on the grounds but also hawk flying insects in the air (Hayman, Marchant, & Prater, 1986). When foraging on the grounds, they forage by using the typical plover 'stop-run-peck' strategy; when hawking in the air, they dash more like terns or swallows ("Birdlife Australia," 2022b; Hayman, Marchant, & Prater, 1986). Pratincoles are mostly crepuscular (Colwell, 2010). They also have been recorded feeding at night by runway lighting (van, Vestjens, & Slater, 1969).

1.2.3 Charadriidae

1.2.3.1 Red-capped plover (*Charadrius ruficapillus*) (other common name: red-capped dotterel)

Red-capped plovers breed in south-eastern Australia and Tasmania (Powlesland, 1998). They are sedentary with some post-breeding dispersal (Hayman, Marchant, & Prater, 1986).

The body length of red-capped plover is 14–16 cm, and the body mass is 35–40 g (Hayman, Marchant, & Prater, 1986).

Red-capped plovers are usually found foraging on a variety of coastal habitats, including shell beaches, mudflats, sandflats, and inland salt lakes (Hayman, Marchant, & Prater, 1986). They are gregarious, often foraging in huge flocks (Hayman, Marchant, & Prater, 1986). The red-capped plovers mainly eat small invertebrates, molluscs, crustaceans, annelids, and some plant material (Griffin, 2013). They forage by using the typical plover 'stop-run-peck' strategy (Griffin, 2013; Hayman, Marchant, & Prater, 1986).

1.2.3.2 Black-fronted dotterel (*Elseyornis melanops*) (other common name: black-fronted plover)

Black-fronted dotterel are common in Australia and New Zealand, and rare in Tasmania (Hayman, Marchant, & Prater, 1986). They breed on open grounds, fields, gravel pits, riverbeds, and shingle lands near to fresh water (Armitage, 2017; Hayman, Marchant, & Prater, 1986). Although they can fly for long distance, most birds stay on the breeding

grounds all year, and the others move to non-breeding grounds for foraging (Armitage, 2017; Hayman, Marchant, & Prater, 1986).

The body length of black-fronted dotterel is 16–18 cm, and the body mass is 26–35 g (Hayman, Marchant, & Prater, 1986).

Black-fronted dotterel are usually found foraging on stony riverbeds lagoons, lakes, estuaries and sewage ponds, but not on coastlines (Armitage, 2017; Hayman, Marchant, & Prater, 1986). They usually feed singly, but small groups form sometimes (Armitage, 2017; Hayman, Marchant, & Prater, 1986). They eat insects, small earthworms, snails, crustaceans, spiders and mites (Armitage, 2017). In addition, small seeds of clover and grasses are parts of their diet (Armitage, 2017). They forage by using the typical plover 'stop-run-peck' strategy (Armitage, 2017). Sometimes probing and foot-trembling methods are also used for feeding (Hayman, Marchant, & Prater, 1986).

1.2.3.3 Red-kneed dotterel (*Erythrogonys cinctus*)

Red-kneed dotterels are native to Australia and New Guinea (Robertson, 2017). They move to inland for breeding after heavy rains, and then return to the coast as non-breeding grounds when the breeding grounds dry out (Hayman, Marchant, & Prater, 1986; Robertson, 2017).

The body length of red-kneed dotterel is 17.5–19.5 cm, and the body mass is 40–55 g (Hayman, Marchant, & Prater, 1986). They are small, distinctively-coloured plover with fairly long and thin bill, and long legs (Hayman, Marchant, & Prater, 1986; Robertson, 2017).

Red-kneed dotterels are usually found foraging on shores of freshwater lakes and swamps, and brackish coastal lakes and lagoons (Robertson, 2017). They are solitary or form small loose flocks (Hayman, Marchant, & Prater, 1986; Robertson, 2017). They mainly eat aquatic invertebrates and their larvae (Robertson, 2017). The dotterels are littoral and they forage through wading and sometimes swimming into the water (Hayman, Marchant, & Prater, 1986; Robertson, 2017).

1.2.4 Recurvirostridae

1.2.4.1 Pied stilt (*Himantopus himantopus*) (other common name: black-winged stilt)

Pied stilt analysed were from Australia and New Zealand, where the most numerous subspecies is *leucocephalus* (Hayman, Marchant, & Prater, 1986; Medway, 2000). They breed in a variety wetland in tropical and subtropical regions, including inland lakes, swamps, lagoons, damp fields, gravel riverbeds, estuaries, saltmarshes, and commercial salt pans (Hayman, Marchant, & Prater, 1986; Medway, 2000). They regularly migrate between north and south or between inlands and coasts (Hayman, Marchant, & Prater, 1986). In New Zealand, the inland and southern breeders migrate to coastal and northern areas after breeding, however the coastal and northern breeders usually don't have post-breeding dispersal (Medway, 2000).

The body length of pied stilt is 33–37 cm, and the body mass is 136–220 g (Medway, 2000). They are distinctive black and white waders with a thin, black, straight bill and very long pink legs (Hayman, Marchant, & Prater, 1986; Medway, 2000). Males are slightly larger than females, but the sexes look similar in the field (Hayman, Marchant, & Prater, 1986; Medway, 2000).

Pied stilts are usually found foraging on a variety of habitats, including estuaries, lagoons, ponds, tidal flats, swamps, lake edge, river flood plains, wet pasture, and even highly saline pans (Hockey & Douie, 1995; Medway, 2000). They feed mainly in the early morning and late afternoon, but sometimes also at night (Hockey & Douie, 1995; Medway, 2000). They are gregarious, often foraging in huge flocks with gulls and other waders. (Medway, 2000). The needle-like bill enables them to catch small fast-moving prey with quick jabs (Hockey & Douie, 1995). Pied stilts mainly eat aquatic insects and the larvae, earthworms, and crustaceans, but they also take small molluscs, gastropods, polychaetes, amphibians, and the eggs of fish (Hockey & Douie, 1995; Medway, 2000). They walk through shallow water with their long legs to pick at the surface or plunge their head underneath water to search for food (Hayman, Marchant, & Prater, 1986; Hockey & Douie, 1995; Medway, 2000). They also pick, probe and scythe when foraging on the soft mud (Hayman, Marchant, & Prater, 1986; Hockey & Douie, 1995). Pierce (1985) observed that the pied stilts at Lake Wainono usually peck for amphipods with visual cues during good weather, but they changed to scything with tactile cues in rainy and windy days. Nocturnal feeding in pied stilts has been confirmed (Ntiamoa-Baidu *et al.*, 1998; Rojas *et al.*, 1999). The vision of pied stilts was suggested to be physiologically well adapted for nocturnal feeding (Rojas *et al.*, 1999).

1.2.5 Haematopodidae

1.2.5.1 South Island pied oystercatcher (SIPO) (*Haematopus finschi*)

SIPO is endemic to New Zealand (Sagar, 2022). They mainly breed inland on riverbeds and farmland east of the Southern Alps in South Island (Medway, 2000). After breeding, they migrate to coastal areas of both the North and South Islands (Sagar, 2022).

The body length of SIPO is 47–49 cm, and the body mass is average 550 g (Medway, 2000). They are striking black-and-white wader with long, robust bill and short legs (Medway, 2000). Females are slightly larger than males but the sexes look similar in the field (Medway, 2000).

SIPOs are usually found foraging in estuaries and harbours from December to July, but they also feed in pastures, ploughed paddocks and riverbeds (Medway, 2000; Sagar, 2022). They are gregarious, often foraging and roosting in huge flocks (Medway, 2000). They mainly eat bivalve molluscs, but they also take estuarine worms, crustaceans, cnidarians, and fish (Medway, 2000; Sagar, 2022). In addition, terrestrial invertebrates, beetle larvae and earthworms have been recorded in their diets when they feed on wet pasture (Medway, 2000; Sagar, 2022). There are no published studies with details of SIPO's foraging behaviour, but the behaviour of their closely related species the variable oystercatcher (*Haematopus unicolor*) has been well described. The bill shape and diet of variable oystercatcher are similar to SIPO's (Dowding, 2022; Sagar, 2022). The long, robust bill enables variable oystercatchers to break apart the shells (Dowding, 2022). They can also pick from the surface or probe deeply with their bill (Medway, 2000). In addition, in Eurasian Oystercatchers (*Haematopus ostralegus*), another species closely related to SIPOs, their highly keratinised bill tips enabled them to open the bivalves but limited the capability to detect deeply buried prey (Choi *et al.*, 2017). Although there is a lack of record of nocturnal feeding in SIPO, there were records of the close relative species Eurasian oystercatcher spent long time feeding at night when the daytime was getting shorter (Zwarts, Anne-Marie, & Roelof, 1990).

1.3 Materials and Methods

1.3.1 Specimen information

Only preserved dead specimens were used in this study. The specimens were collected from New Zealand and Australia and preserved in the freezer at Massey University (Palmerston North, New Zealand). The collecting year ranged between 2004 and 2014. The total mass, head length, maxilla length, mandible length, and tarsus lengths, and the maturity of birds were recorded before further processing (Table 1.1).

Table 1.1: Information of the samples.

Species name & Sample amount	Location	Collecting date	Mass (g)	Head length (mm)	Straight maxilla length (mm)	Major foraging behaviour	Nocturnal foraging	Major sensory cues for foraging in daytime
Bar-tailed godwit (*Limosa lapponica*) n=6	NZ	13/12/2004	329	150.5	111.4	Probing 'Sewing machine' jabbing	Confirmed, Showed habitat selection	Tactile & Visual
	NZ		371	134.5	93.7			
	Aus		314	127.5	87			
	NZ	29/01/2014	337	152.5	112.8			
	Aus		299	150	112.5			
	Aus	1/7/2006	287	138	99			
Red knot (*Calidris canutus*) n=5	NZ	2/10/2004	128	59.5	31.8	Probing, Surface pecking, 'Sewing machine' jabbing	Confirmed, Showed habitat selection	Tactile
	NZ	12/2/2008	141	62.8	33			
	NZ	2/10/2004	143	61.8	34.3			
	NZ	28/03/2008	132	62.2	32.2			
	Aus	12/10/2008	141	59.5	31.6			
Great knot (*Calidris tenuirostris*) n=1	Aus	17/11/2008	169	73.7	42.4	Probing	Suggested	Tactile & Visual
Red-necked stint (*Calidris ruficollis*) n= 3 (The dentary of the 3rd sample was broken)	Aus		21	38.2	18	Probing, Surface pecking, 'Sewing machine' jabbing	Confirmed, Showed habitat selection	Tactile (with visual aid)
	Aus		29	39.8	19.6			
	Aus		17	37.8	16.4			
Curlew sandpiper (*Calidris ferruginea*) n=2	Aus	30/08/2008	50	57.3	37.5	Probing, Surface pecking	Suggested, Showed habitat selection	Tactile
	Aus	2/8/2008	66	63.9	39.9			
Sharp-tailed sandpiper (*Calidris acuminata*) n=1	Aus	26/09/2006	54	50.5	26.4	Probing	N/A	Tactile
Little whimbrel (*Numenius minutus*) n=2 (The maxilla of the 1st sample was broken)	Aus	13/11/2006	125	78.8	44.1	Probing	N/A	Tactile (with visual aid)
	Aus	28/11/2008	162	85.3	50.1			
Whimbrel (*Numenius phaeopus*) n=1	Aus	28/11/2008	393	121	83.3	Probing	Confirmed, Showed prey selection	Tactile & Visual
Grey-tailed tattler (*Tringa brevipes*) n=2	Aus		85	68.8	40.2	Probing	Confirmed, Showed habitat selection	Tactile & Visual
	Aus		107	67.7	38.4			

Table 1.1 continued.

Species name & Sample amount	Location	Collecting date	Mass (g)	Head length (mm)	Straight maxilla length (mm)	Major foraging behaviour	Nocturnal foraging	Major sensory cues for foraging in daytime
Common greenshank (*Tringa nebularia*) n=1	Aus	2/11/2006	158	90.4	52.9	Probing, Surface pecking, Scything, Ploughing	Confirmed, Showed habitat selection	Tactile & Visual
Wood sandpiper (*Tringa glareola*) n=1	Aus		43	55.6	28.4	Probing, Surface pecking, Scything	Less record	Tactile (with visual aid)
Marsh sandpiper (*Tringa stagnatilis*) n=1	Aus		54	67.1	38.8	Probing, Surface pecking, Scything, Ploughing	Less record	Visual (with tactile aid)
Terek sandpiper (*Xenus cinereus*) n=2	Aus Aus	 21/11/2006	92 79	78.1 75.3	51.5 48	Probing, Surface pecking, Scything	N/A	Visual (with tactile aid)
Ruddy turnstone (*Arenaria interpres*) n=1	Aus		75	50.6	21.5	Flicking, Probing, Pecking, Surface pecking, Smashing	Less time	Visual (with tactile aid)
Australian pratincole (*Stiltia isabella*) n=2	Aus Aus	25/11/2005	40 55	46.7 44.8	15.9 15.4	Hawking, 'Stop-run-peck'	Need light source	Visual
Red-capped plover (*Charadrius ruficapillus*) n=2	Aus Aus	30/08/2008 19/11/2008	34 33	40.2 40	15.5 14.9	Probing, Surface pecking, 'Stop-run-peck'	N/A	Visual
Black-fronted dotterel (*Elseyornis melanops*) n=3	Aus Aus Aus	 	22 23 16	37.2 34.4 36.4	16.4 14.7 16.3	Probing, Surface pecking, 'Stop-run-peck'	N/A	Visual
Red-kneed dotterel (*Erythrogonys cinct*us) n=1	Aus		45	47.6	20.5	Probing	N/A	Visual
Pied stilt (*Himantopus himanto*pus) n=2	NZ Aus	12/1/2020 	175 178	100.7 100.5	61 62.4	Probing, Surface pecking, Scything	Confirmed	Visual
South Island pied oystercatcher (SIPO) (*Haematopus finschi*) n=1	NZ	10/10/2012	458	140	92.7	Probing	N/A	Visual

1.3.2 Geometric morphometrics

Geometric morphometrics is a suite of statistical analyses used to quantify biological shape and is often based on landmark configurations (Mitteroecker & Gunz, 2009; Webster & Sheets, 2010). Geometric morphometrics analyses often involve digitising biological shape and visualising a reduced dimensional dataset (Mitteroecker & Gunz, 2009). Compared to traditional morphometrics, which requires measuring numerous variables directly on specimens, geometric morphometrics can analyse landmarks placed on homologous points across a sample set (Mitteroecker & Gunz, 2009; Sun *et al.*, 2018). Geometric morphometric analysis often begin with Procrustes superimposition, which translates, scales and rotates landmark configurations to make them share the same centroid (the coordinate-wise average of the landmarks of one form), centroid size (the square root of the summed squared deviations of the coordinates from their centroid) and orientation (through the iterative algorithm of rotating around its centroid until getting the least sum of the squared Euclidian distances between the homologous landmarks), so that different specimens can be compared with each other purely for their shapes (Mitteroecker & Gunz, 2009; Sun *et al.*, 2018; Webster & Sheets, 2010).

Principal component analysis (PCA) is often applied to superimposed landmark configurations. PCA is a linear dimensionality reduction technique used to extract and project the major variance from the dataset into new scores in a few dimensions (Mitteroecker & Gunz, 2009; Webster & Sheets, 2010). PCA is computed by an eigendecomposition of the sample covariance matrix and it shows how the shape is deformed by the landmarks in each specimen (Mitteroecker & Gunz, 2009). In addition, geometric morphometrics can provide clear visualization using thin-plate spline (TPS) to compute deformation grids of the shape differences between two geometries (Mitteroecker & Gunz, 2009; Webster & Sheets, 2010). TPS computes the map of landmark configurations and smooth the space by minimising the bending energy of the deformation (Mitteroecker & Gunz, 2009).

The variation in foraging structures of the shorebird skull morphology such as bill length and shape, and orbit sizes have been highlighted in previous studies (Baker, 1979; Barbosa & Moreno, 1999; Dann, 1987; Nebel, Jackson, & Elner, 2005; R. J. Thomas *et al.*, 2006). Therefore, geometric morphometrics analyses were used to describe the shape of shorebird skulls in this study.

1.3.3 Scanning electron microscope (SEM) of the tongue tip

A SEM is a type of electron microscope that forms images by scanning the surface with a focused beam of electrons to produce signals with surface information (Dunlap & Adaskaveg, 1997). The dry samples have to be observed in high vacuum (Dunlap & Adaskaveg, 1997). The SEM can be used to examine micro-three-dimensional features (Iwasaki, Asami, & Chiba, 1997). Although the morphological features of bird tongues have been widely recorded and analysed, the studies on the microstructure of tongue surfaces have just recently garnered focus (Erdoğan & Iwasaki, 2014; Iwasaki, 2002; Iwasaki, Asami, & Chiba, 1997; Johnston, 2014). There were some findings of keratinised micro spines on the tongue tips in some shorebirds (Elner *et al.*, 2005; Kuwae *et al.*, 2012). It has been suggested that these micro spines enable the birds to feed on biofilm as a new potential feeding method (Beninger & Elner, 2020; Kuwae *et al.*, 2012). However, there is a lack of wider examination of these micro tongue tip spines in different shorebird species. In this study I use SEM to describe the tongue tip structure of shorebirds.

1.3.4 Specimen processing

After a specimen was taken out from the freezer and defrosted in a fridge for one day, the basic information was recorded, and the bird's head was removed for dissection.

First, the right lateral view of the head with the bill was imaged via digital photography. Then, the mandible with the tongue was separated from its maxilla for imaging the tongue and palate. The tongue was further separated from the mandible for detailed images. At the end of the dissection, the tongue tip was removed and soaked in the primary fixative (Modified Karnovsky's fixative (3% glutaraldehyde, 2% formaldehyde in 0.1M phosphate buffer, pH 7.2)) for fixation overnight at room temperature for the SEM. The remainder of the head was processed to reveal the skull.

To clean the bird skull after the dissection of the oropharyngeal cavity, the head was macerated in warm water of less than 50 °C for approximately one week. Then the flesh was removed by flushing. Warm-water maceration is a traditional decomposition technique to let the soft tissues be consumed by bacteria in a controlled condition (Ajayi, Edjomariegwe, & Iselaiye, 2016). The time of maceration depends on the number of bacteria present, the

size of specimen and the temperature of the environment (Ajayi, Edjomariegwe, & Iselaiye, 2016). Once the bone became clean, it was used for imaging the skull and the bill-tip organ.

For the SEM process, the fixative was removed on the following day. Then the sample was rinsed three times (10–15 minutes each) in phosphate buffer (0.1 M, pH 7.2) and dehydrated in ascending ethanol series (25%, 50%, 75%, 95%, 100%) for 10–15 minutes each and a final 100% ethanol wash for 1 hour. The sample was further critical point dried using liquid CO_2 as the CP fluid and 100% ethanol as the intermediary (Polaron E3000 series II critical point drying apparatus). To be ready for observation, the samples was mounted on to aluminium stubs using double sided tape and sputter coated with approximately 100 nm of gold (Baltec SCD 050 sputter coater). The mounted sample was observed under an FEI Quanta 200 Environmental Scanning Electron Microscope at an accelerating voltage of 20kV at the Manawatū Microscopy and Imaging Centre, Massey University.

1.3.5 Photography protocol

All the images of the bills, the oropharyngeal cavities, and the skulls were taken with a Canon EOS Kiss X5 with 50 mm or 100 mm lens on a vertical adjustable mount. Most images were taken on the same height except for large birds beyond the border of the image. The images were taken with a scale on the same horizontal plane. For the bills, the images of the right lateral view were taken with the bill tip raised to make the sagittal plane horizontal. For the oropharyngeal cavities, the images of the dorsal view of the tongue within the mandible were taken with the mandible tip raised to make the mandible margin horizontal; the images of the left lateral view of the tongue were taken with the tongue tip raised to make the sagittal plane horizontal; the images of the ventral view of the palate were taken with the maxilla tip raised to make the maxilla margin horizontal. For the skulls, the images of the dorsal view were taken with the bill tip on the same horizontal plane as basioccipital; the images of the right lateral view were taken with the bill tip raised to make the sagittal plane horizontal; the images of the ventral view were taken with the bill tip raised to the same horizontal plane as basioccipital.

The images of the bill-tip organs were taken using a dissection microscope with an inbuilt camera (Olympus SC100). Images of eight angles (dorsal, left-dorsal lateral-45-degree, left lateral, left-ventral lateral-45-degree, ventral, right-ventral lateral-45-degree, right lateral

and right-dorsal lateral-45-degree) of the premaxilla (the tip bone of the maxilla; see Fig. 3.2) and the dentary (the tip bone of the mandible) were taken for 360° panoramic images.

The images of the tongue tip were taken using the FEI Quanta 200 Environmental Scanning Electron Microscope. The samples were set in right-dorsal lateral-45-degree and zoomed in 50 x, 100 x and 200 x.

1.4 Thesis Outline and Structure

The main target of this thesis is to answer the question: “How do phylogeny and foraging methods shape the morphology of the feeding apparatus in charadriiform shorebirds?” This is evaluated through a series of independent analyses of specific components of the foraging structures, which are then evaluated in relation to phylogeny, as follows.

Chapter 2 uses geometric morphometric analyses to study interspecific variation of skull shape among different species to address how bill and cranium shapes covary in consistent ways and/or vary phylogenetically, and whether the orbit of primarily visual foragers is comparatively larger than in tactile foragers.

Chapter 3 uses digital imagery of bill structure and sensory pits to address whether a certain maxilla length is related to bird sizes, phylogeny or foraging behaviours, whether the numbers and densities of sensory pits are related to phylogeny, bill length, bill-tip organ lengths, and foraging behaviours, and whether there is any association between the bill-tip organ and distal rhynchokinesis of bills.

Chapter 4 uses digital imagery of the organs within oropharyngeal cavity and the SEM imagery of the microstructure on the tongue tip to address how tongue length varies with bill length and phylogeny, whether the presence of micro tongue spine is related to phylogeny, bird size, bill morphology or specific foraging behaviours, and if the presence of distal rhynchokinesis is associated with the presence of micro tongue spines.

Chapter 5 uses phylogenetic tools to test whether the Brownian motion model or the Pagel’s lambda model better explains the trait evolution of total sensory pit numbers, and whether the equal-rates (ER) model or the all-rates-different (ARD) model better explains the evolution of presence of micro tongue spines, and presence of distal rhynchokinesis among shorebirds. The evidence of phylogenetic signal in the taxonomic distribution of trait was tested with the lambda transformation.

Chapter 6 is a General Discussion in which I combine the findings of each chapter above to discuss particular morphological traits, the association between different traits, and the foraging strategies of specific clades or species.

2 The analysis of the skull shape of shorebirds using landmark-based geometric morphometrics

2.1 Abstract

The birds in the order Charadriiformes have developed diverse morphological traits to adapt to different diets. Their skull shapes are highly related to their foraging strategies, such as prey types, behaviours and foraging time. Two major parts that vary in the skull shapes are the structures of bills and orbits. Bills vary in length, width and curvature, and orbits vary in size. I used landmark-based geometric morphometrics to analyse the skull shapes of 20 charadriiform shorebird species. Every skull specimen was recorded and digitised from dorsal (14 landmarks), right lateral (15 landmarks), and ventral (18 landmarks) views. Along with geometric morphometrics, principal component analysis (PCA) was used to extract and display the major variances of the shapes, and thin-plate spline (TPS) was used to visualise and compare the shapes in deformation grids. I used these methods to test if bill and cranial shapes covary in consistent ways or if they vary phylogenetically, and if the orbit of primarily visual foragers is comparatively larger than in tactile foragers. The results of the dorsal view showed the effects of the bill length, head length, and skull width on the shape variation; the right lateral view showed the effects of the distance from the rostral end of the external nares to the proximal-most point of the bill, the distance from the tip of premaxilla to the rostral end of the external nares, head length, and orbit; the ventral view showed the effects of the bill length, head length, and structure of the rear part of the cranium. The results showed that some tactile foragers, such as the little whimbrel (*Numenius minutus*) and wood sandpiper (*Tringa glareola*), had bulging orbits, whereas some visual foragers, such as the red-kneed dotterel (*Erythrogonys cinctus*) and South Island oystercatcher (SIPO) (*Haematopus finschi*), did not have obvious orbital deformation. Thus, it is not suggested that visual foragers have larger eyes than tactile foragers. The application of visual and tactile cues in a species is complicated with the changing habitats and feeding time. The PCA and TPS results demonstrate that landmark-based geometric morphometrics did provide useful information for studying the skull shape variation. The selection of landmarks is important for answering specific questions.

2.2 Introduction

Birds have diverse foraging strategies and corresponding morphological adaptations for different diets (Rico-Guevara *et al.*, 2019), including within the order Charadriiformes (Baker, 1979; Barbosa & Moreno, 1999; Dann, 1987; Hayman, Marchant, & Prater, 1986; Hockey & Douie, 1995; Nebel, Jackson, & Elner, 2005). Mosaic evolution is the concept that the evolutionary rates of some traits are not simultaneous with those of other body parts (Felice & Goswami, 2018). The different traits of avian skulls have evolved at different evolutionary rates showing mosaic evolution, reflecting rapid adaptations to diverse ecological selection pressures (Felice & Goswami, 2018; Pecsics *et al.*, 2020). Previous studies have demonstrated that morphological variation in the avian skull, which is where most jaw muscles attach, related to dietary preferences (Pecsics *et al.*, 2020; Sun *et al.*, 2018). Hence, the analysis of skull shape variation should provide information for better understanding the foraging strategies of each bird.

The bill is a part of the skull (Schäfer & Schmitz, 2016). The length and shape of the bill of charadriiform shorebirds are highly related to their particular diets and foraging strategies (Baker, 1979; Barbosa & Moreno, 1999; Dann, 1987; Nebel, Jackson, & Elner, 2005). For example, bar-tailed godwits (*Limosa lapponica*) with long bills can probe deeply to reach polychaetes, whereas plovers with short bills usually peck the surface for food (Hayman, Marchant, & Prater, 1986; Hockey & Douie, 1995). Whimbrels (*N. phaeopus*) have curved bills that fit in crab holes (Hockey & Douie, 1995). Ruddy turnstones (*Arenaria interpres*) with wedge-shape bill can flip objects to search for food (Hockey & Douie, 1995).

This interspecific variation in bill morphology is effectively 'fixed' rather than plastic within the lifetime of the individual, and it is considered to be the result of heritable change (Barbosa & Moreno, 1999). An exception to this rule is the rhamphotheca of oystercatchers, in which diet choice shapes the foraging structure. Eurasian oystercatchers (*Haematopus ostralegus*) have robust bills with three different forms of the bill tips: pointed, chisel-shaped and blunt (Dowding, 2022; Swennen *et al.*, 1983). Pointed bills are sharp at the tip and are suitable for probing to catch worms (Swennen *et al.*, 1983). Chisel-shaped bills are sharp from the dorsal view but truncated from the lateral view, and they are suitable for stabbing through the gap between valves of bivalves to cut their adductor muscles (Dit Durell & Goss-Custard, 1984; Swennen *et al.*, 1983). Blunt bills are both truncated from dorsal and lateral view, and they are suitable for stabbing and hammering through shells (Dit Durell & Goss-Custard, 1984; Swennen *et al.*, 1983). Bill form can change in individual birds and may be

caused by the wear on the rhamphotheca when foraging on different kinds of habitats and prey (Swennen *et al.*, 1983).

In addition to bill length, the vision of birds is considered to be an important tool for certain foraging strategies (Martin & Piersma, 2009; R. J. Thomas *et al.*, 2006). Nocturnal feeding has been recorded in many shorebirds (Rohweder & Baverstock, 1996; Sitters *et al.*, 2001; Stuart, Wooding, & Takurou, 2015; Zwarts, Anne-Marie, & Roelof, 1990). Visual foragers with better vision than the average tactile foragers enable them to see in the dark with little light (van de Kam *et al.*, 2004). It has been suggested that shorebirds that often feed at night have large eyes (Martin & Piersma, 2009; R. J. Thomas *et al.*, 2006). The large eyes are anchored in the orbits of the skull by *Os supraorbitale aliforme,* the supraorbital aliform bone named by Martin and Piersma (2009), extending on the edge of orbits in European golden plovers (*Pluvialis apricaria*) (Hughes, 2015).

Geometric morphometrics analysis techniques have been used widely in research on the ecomorphological evolution of avian skulls for foraging (Bright *et al.*, 2019; Felice *et al.*, 2019; Kass, Montalti, & Acosta Hospitaleche, 2018; Kulemeyer *et al.*, 2009; Pecsics *et al.*, 2020; Profico *et al.*, 2019; Sun *et al.*, 2018). However, detailed studies have been focused on the order Psittaciformes, and the families Accipitridae and Corvidae, but not yet in the order Charadriiformes (Kulemeyer *et al.*, 2009; Pecsics *et al.*, 2020; Sun *et al.*, 2018).

In this study, 20 charadriiform species native to New Zealand or Australia were investigated using geometric morphometrics to identify patterns of variation in skull shape. The aim is to test the relationships between foraging strategies and the features of skull structures that have been proposed in previous studies, and if the difference in skull shape is related to phylogeny. Specifically, I address how bill and cranium shapes covary in consistent ways and vary phylogenetically, and whether the orbit of primarily visual foragers is comparatively larger than in tactile foragers.

2.3 Methods

The bill of a little whimbrel was broken during the preparation, so only 39 individuals of 20 species were used in this experiment (Table 1.1).

The variation of skull morphology was analysed using landmark-based geometric morphometry. Landmarks were selected from obvious structures on the edges and joints of the skull to represent the shape and length of the skull, focusing on bill length, head length and orbital size. The selection of landmarks referred to the instruction following Webster and Sheets (2010), referring to previous studies (Pecsics *et al.*, 2020; Sun *et al.*, 2018) to outline the shape of skulls. The anatomical terms of the skull were from Burton (1974). To gain and compare more information from different views, the landmarks were collected in three views of each skull: dorsal (14 landmarks), right lateral (15 landmarks), and ventral (18 landmarks) (Fig. 2.1) (Table 2.1). First, a mounted camera was used to take images of the skulls with a scale on the same plane, and then the landmarks were marked and digitised using the software tpsDig2 with tpsUtil (Rohlf, 2018a, 2018b). The coordinates of the landmarks were translated, scaled and rotated using Procrustes superimposition method in the geomorph R package (version 4.0.2) before further statistical analysis (Adams *et al.*, 2016). The geomorph package was also used to produce principal component analysis (PCA) results (loadings and scores) and deformation grids drawn with thin-plate spline (TPS) for assessing the variances among landmark coordinates (Adams *et al.*, 2016; Webster & Sheets, 2010).

PCA analysis reveals the outliers and the clusters of specimens with similar morphology (Webster & Sheets, 2010). The eigenvalues represent the linear transformed variance of the associated PC (principal component) (Abdi & Williams, 2010). Principal components are ordered in decreasing explained variance contributions (PC1 explains the highest variance, PC2 the second highest, and so on) (Abdi & Williams, 2010; Savriama, 2018).

TPS shows no data, but the expansion or contraction of the deformation grids expresses the obvious differences in enlarged or reduced regions between the specimen and others (Webster & Sheets, 2010).

The landmarks of distal bill parts (No. 1 of the dorsal view, Nos. 1 and 2 of the right lateral view, and No. 1 of the ventral view) were later removed. However, the results were not affected by removing those landmarks. These results (the principal component one and two

scores plots, and the first three principal components of the principal component analysis) are given in Appendix 2 for comparison.

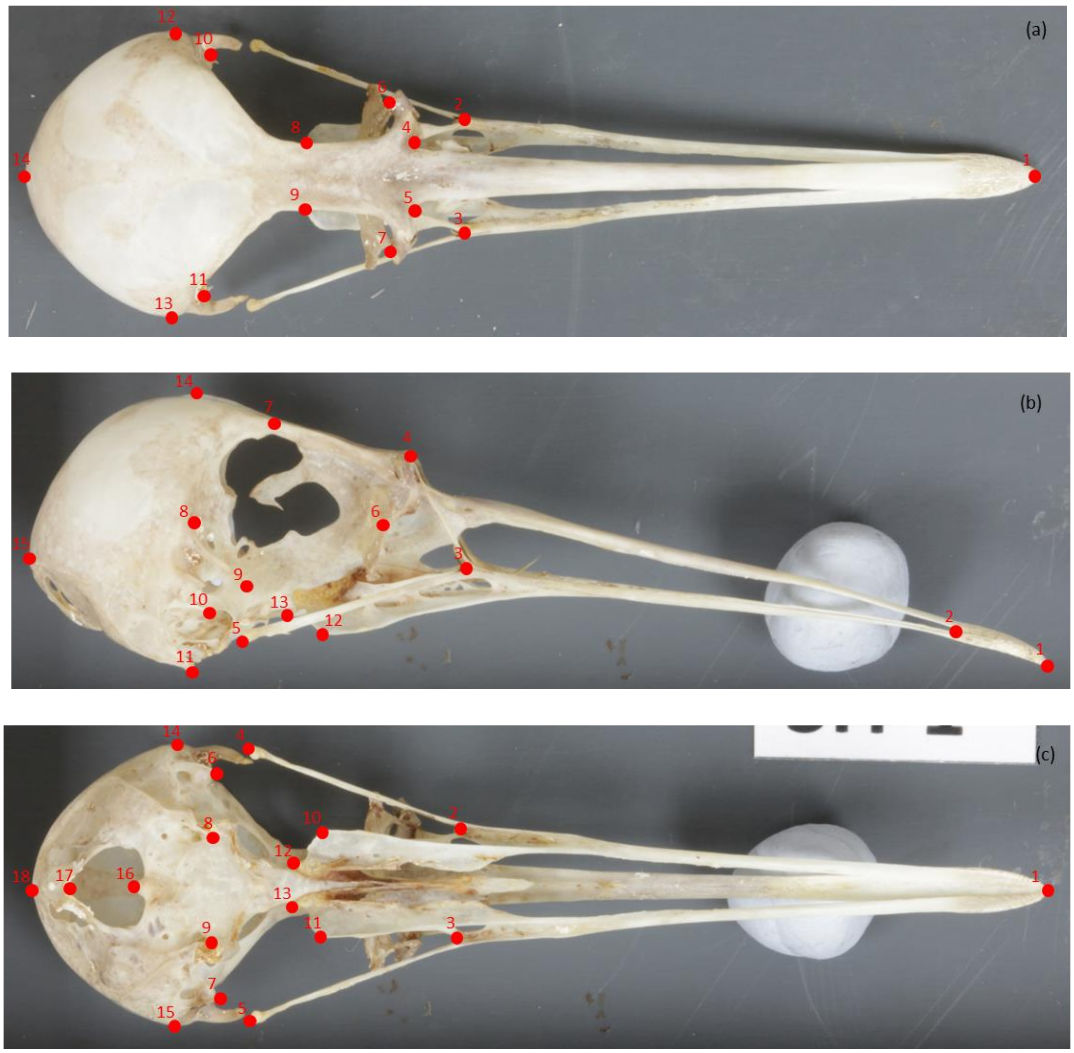

Fig. 2.1: Landmarks of the skull in the (a) dorsal, (b) right lateral and (c) ventral views.

Table 2.1: List of landmarks of the dorsal, right lateral and ventral views and their anatomical descriptions.

No.	Description of landmark
Dorsal view	
1	The tip of premaxilla
2,3	The left and right junctions of nasal and jugal bar
4,5	The left and right inner junctions of nasal and frontal
6,7	The leftmost and rightmost anterior lateral edges of orbit in the dorsal view
8,9	The leftmost and rightmost proximal points of orbit in the dorsal view
10,11	The leftmost and rightmost caudal points of orbit in the dorsal view
12,13	The leftmost and rightmost lateral points of squamosal
14	The caudal-most point of prominentia cerebellaris
Right lateral view	
1	The tip of premaxilla
2	Maximum of the curvature at the rostral end of the external nares
3	The junction of nasal and jugal bar
4	The junction of nasal and frontal
5	The junction of jugal bar and quadrate
6	The anterior-most point of orbit
7	The highest point of orbit
8	The caudal-most lateral point of orbit
9	The tip of postorbital process
10	The tip of suprameatic process
11	The tip of opisthotic process
12	Maximum of the curvature at the caudal lateral end of palatine
13	The caudal-most point of palatine in the lateral view
14	The dorsal-most point of frontal
15	The caudal-most point of prominentia cerebellaris
Ventral view	
1	The tip of premaxilla
2,3	The left and right junctions of nasal and jugal bar
4,5	The left and right junctions of jugal bars and quadrate
6,7	The left and right tips of suprameatic process
8,9	The left and right tips of opisthotic process
10,11	The right and left maximum of the curvature at the caudal lateral end of palatine
12,13	The right and left junctions of the lateral-caudal end of palatine and basitemporal plate
14,15	The leftmost and rightmost lateral points of squamosal
16	The caudal-most point of occipital condyle
17	The caudal-most point of foramen magnum
18	The caudal-most point of prominentia cerebellaris

2.4 Results

2.4.1 The dorsal view of skulls

The first three principal components (PCs) explained 92.7% (PC1), 2.8% (PC2) and 2.1% (PC3) of the variation in skull shape (Fig. 2.2). Here the X and Y with numbers meant the relative position of the nth landmark. For example, 1.X refers to the x axis variable of the first landmark. Along PC1 1.X and 14.X contributed the largest variance; these two measurements effectively describe the skull length. In PC2, 2.X, 3.X and 14.X had the largest loadings. These points describe the distance from the proximal-most point of the bill to the

caudal-most point of the skull. 12.Y and 13.Y, which describe the skull width, also contributed large variances to PC2 (Fig. 2.3). In PC3, 9.X and 8.X had the largest loadings.

The TPS deformation grids displayed that the elongation of the bill had great effect on the skull shape; this difference was obvious between *L. lapponica* with the long bill and *S. isabella* with the short bill. Another obvious deformation effect was caused by the skull width that seemed to bulge in some species, including *N. minutus*, *T. glareola*, *Ch. ruficapillus, El. melanops,* and *Hi. himantopus*. The other deformation was the contraction of the bill base, which was obvious in *L. lapponica, Ca. ruficollis, Ca. ferruginea, Ca. acuminata, X. cinereus,* and *A. interpres* (Fig. 2.4).

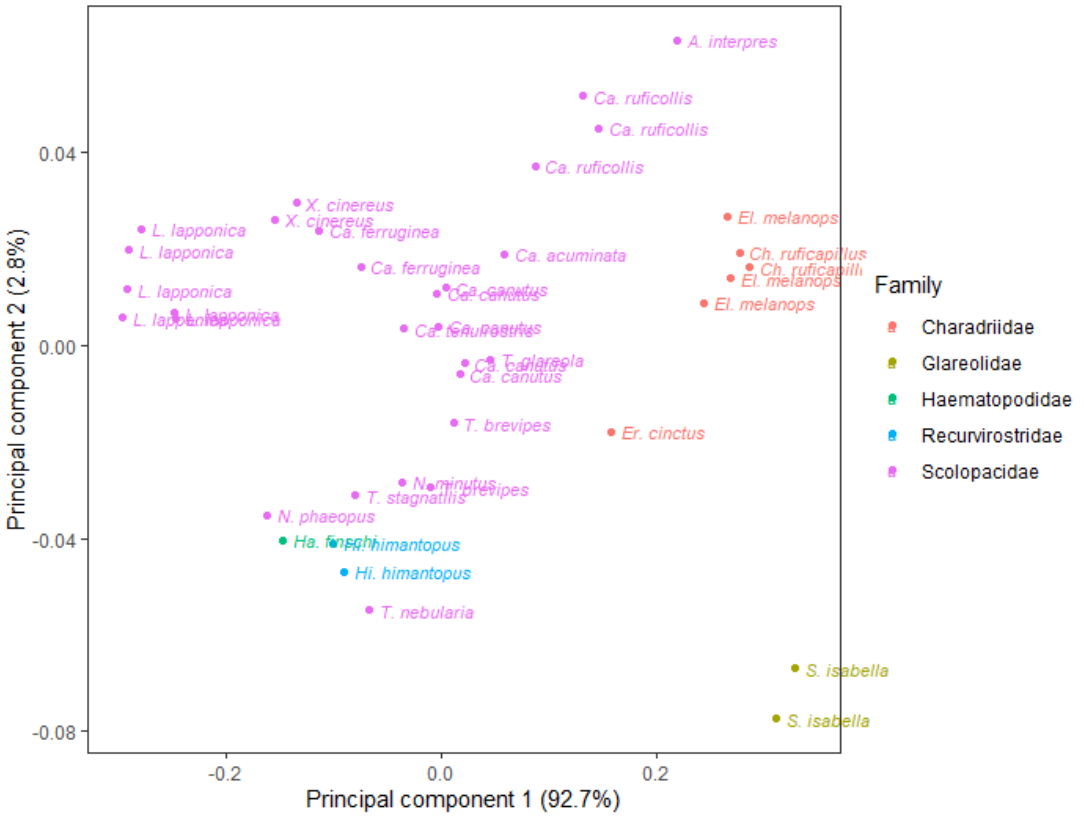

Fig. 2.2: Principal component one and two scores plot. The first two principal components explain more than 95% of the variation in the dataset, with most of this variation explained along PC1. The dots are labelled with species and coloured with family.

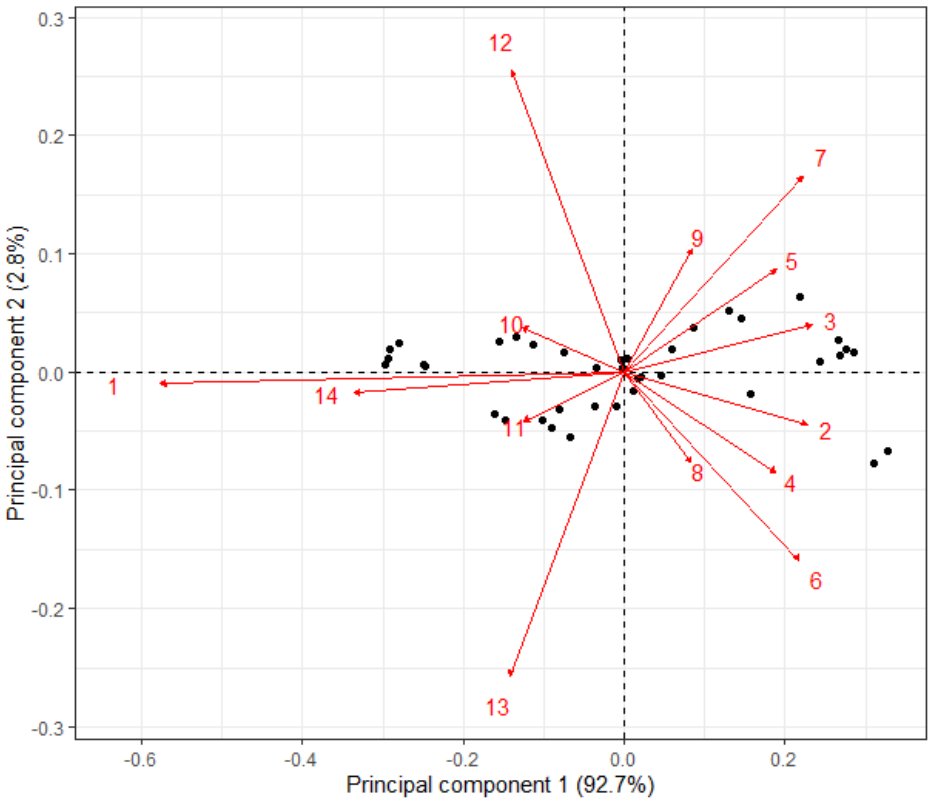

Fig. 2.3: The principal component analysis (PCA) biplot of the dorsal view with PC1 (92.7%) as x-axis and PC2 (2.8%) as y-axis on the two-dimensional biplot. The black dots are the projected PCA results same as Fig. 2.2. The red arrows describe the loading strength of each landmark on the shapes.

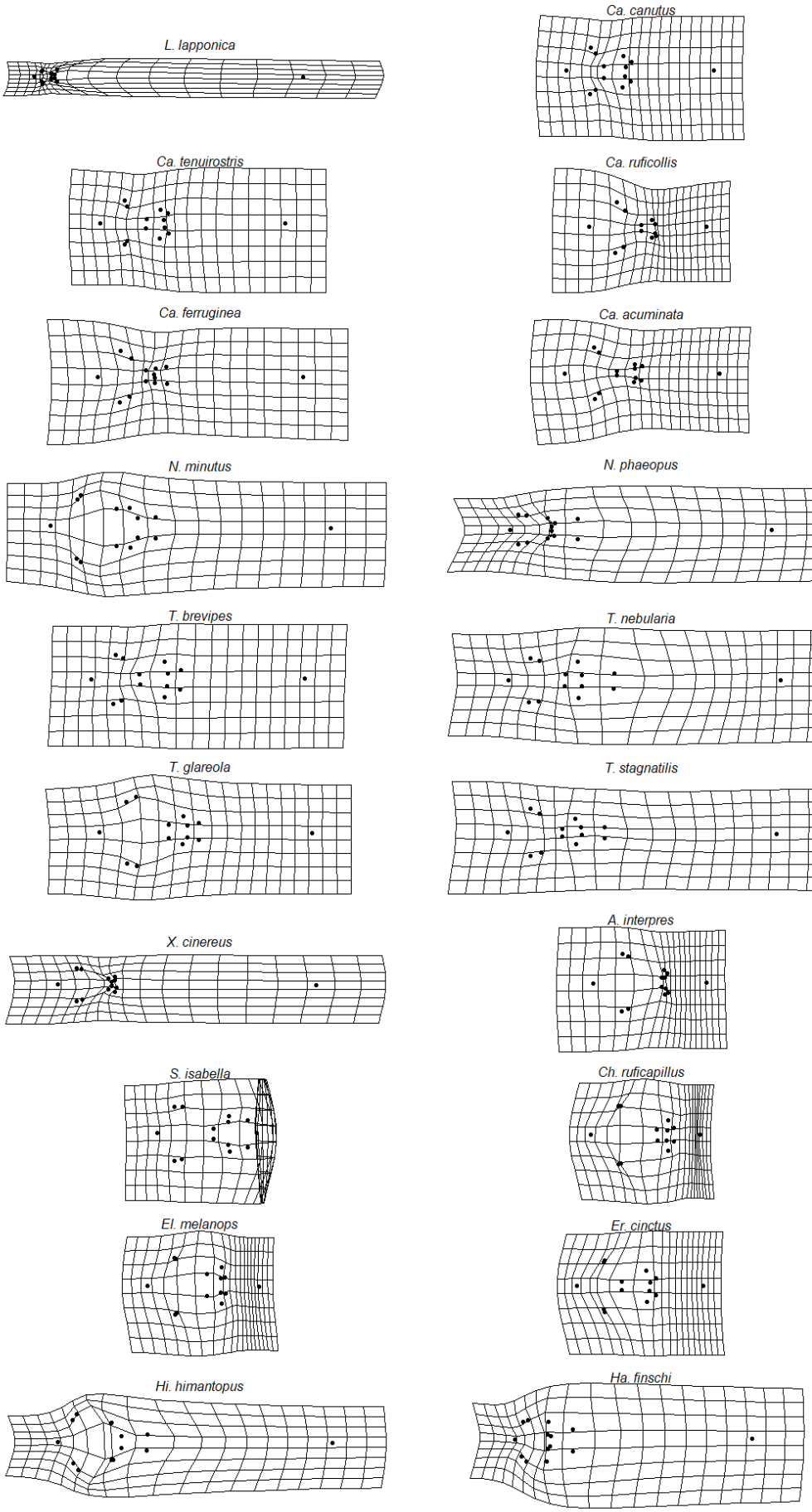
L. lapponica
Ca. canutus
Ca. tenuirostris
Ca. ruficollis
Ca. ferruginea
Ca. acuminata
N. minutus
N. phaeopus
T. brevipes
T. nebularia
T. glareola
T. stagnatilis
X. cinereus
A. interpres
S. isabella
Ch. ruficapillus
El. melanops
Er. cinctus
Hi. himantopus
Ha. finschi

Fig. 2.4: Previous page. Thin plate spine (TPS) deformation grids of the dorsal view of each species for comparison. The direction of the landmarks was the same as in Fig. 2.1a with the caudal-most point of the skull on the left and the tip of the bill on the right. Bar-tailed godwit (*L. lapponica*), red knot (*Ca. canutus*), great knot (*Ca. tenuirostris*), red-necked stint (*Ca. ruficollis*), curlew sandpiper (*Ca. ferruginea*), sharp-tailed sandpiper (*Ca. acuminata*), little whimbrel (*N. minutus*), whimbrel (*N. phaeopus*), grey-tailed tattler (*T. brevipes*), common greenshank (*T. nebularia*), wood sandpiper (*T. glareola*), marsh sandpiper (*T. stagnatilis*), terek sandpiper (*X. cinereus*), ruddy turnstone (*A. interpres*), Australian pratincole (*S. isabella*), red-capped plover (*Ch. ruficapillus*), black-fronted dotterel (*El. melanops*), red-kneed dotterel (*Er. cinctus*), pied stilt (*Hi. himantopus*), and SIPO (*Ha. finsch*).

2.4.2 The right lateral view of skulls

The first three principal components (PCs) explained 74.2% (PC1), 16.3% (PC2) and 3.0% (PC3) of the variation in skull shape (Fig. 2.5). Along PC1 13.X, 2.X, 15.X, and 4.X contributed the largest variance. 3.X and 2.X effectively describe the distance from the rostral end of the external nares to the proximal-most point of the bill. 15.X, and 4.X describe the head length (the distance from the proximal-most point of the bill to the caudal-most point of the cranium). In PC2, 2.X and 1.X had the largest loadings; these two measurements effectively describe the distance from the tip of premaxilla to the rostral end of the external nares. In PC3, 3.X, 10.X and 5.X had the largest loadings; these three measurements describe the distance from the proximal-most point of the bill to the suprameatic process.

The TPS deformation grids displayed that the elongation of the bill had great effect on the skull shape (Fig. 2.7). Another obvious deformation effect was caused by the distance between the maximum of the curvature at the rostral end of the external nares (landmark No. 2) and the junction of nasal and jugal bar (landmark No. 3); the distance was elongated in *L. lapponica* and *N. phaeopus,* whereas it was compressed in *Tringa* spp. and *S. isabella.* The other deformation was the curvature of the bill; it was slightly upcurved in *L. lapponica* and *X. cinereus,* and decurved in *Ca. ferruginea, N. minutus, N. phaeopus,* and *S. isabella.* In addition, it seemed that the landmarks around the orbit (Nos. 6, 7, 8, and 9) bulge slightly in *Ch. ruficapillus*, *El. melanops*, and *Hi. himantopus.*

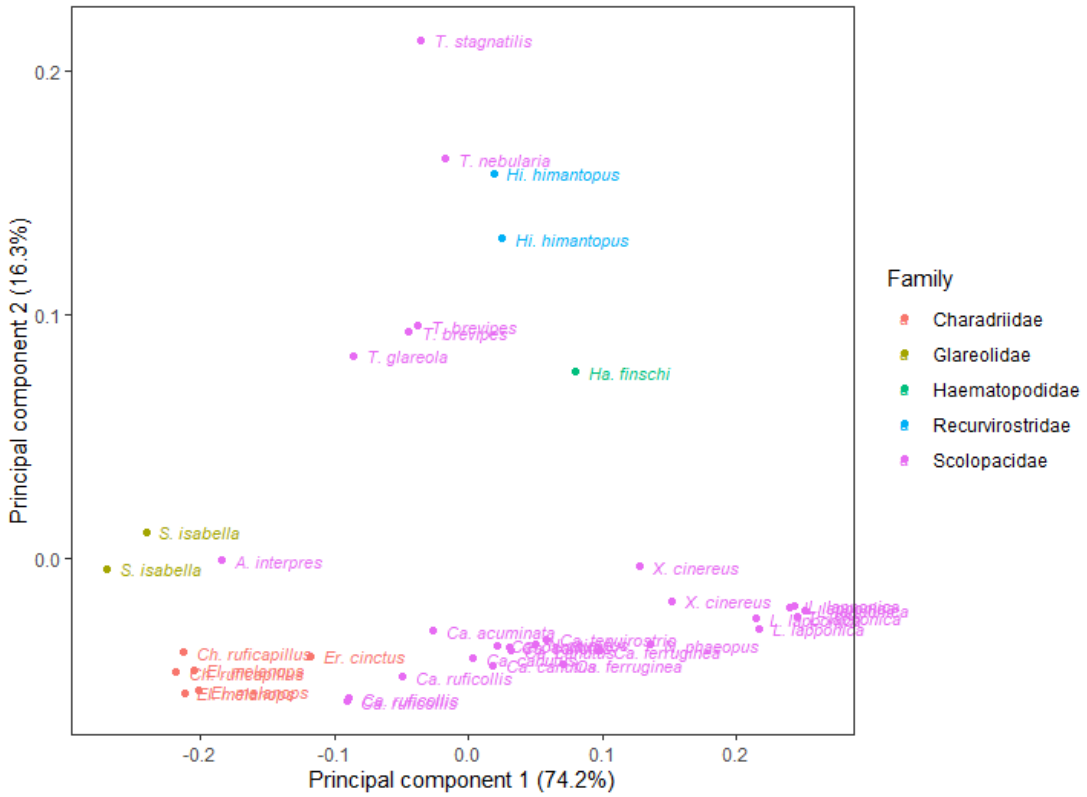

Fig. 2.5: Principal component one and two scores plot. The first two principal components explain more than 90% of the variation in the dataset, with most of this variation explained along PC1. The dots are labelled with species and coloured with family.

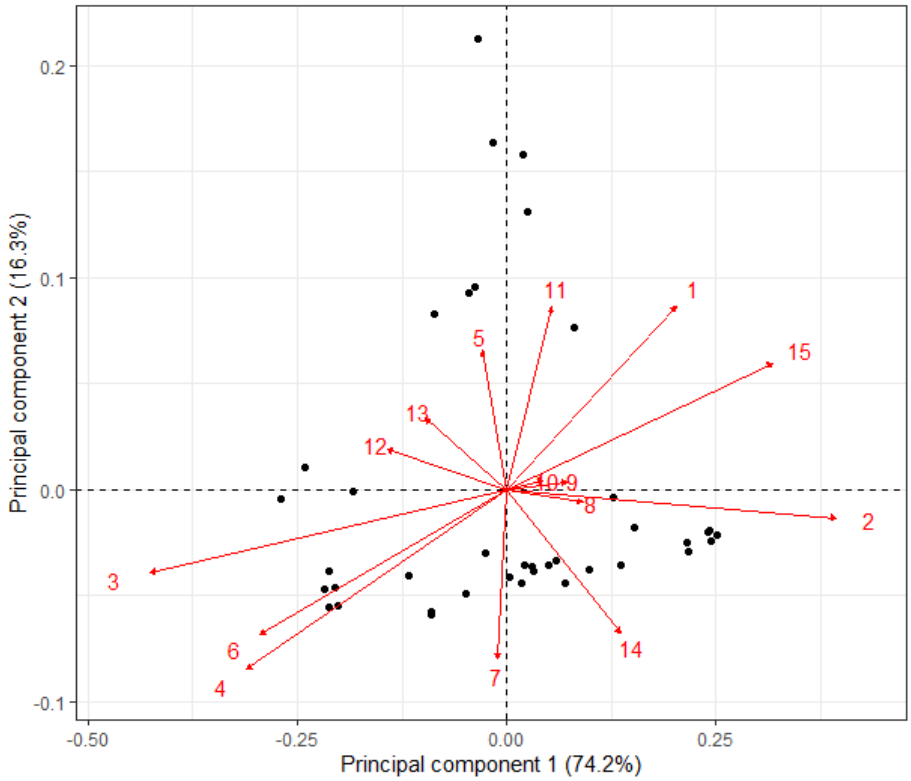

Fig. 2.6: The principal component analysis (PCA) biplot of the right lateral view with PC1 (74.2%) as x-axis and PC2 (16.3%) as y-axis on the two-dimensional biplot. The black dots are the projected PCA results same as Fig. 2.5. The red arrows describe the loading strength of each landmark on the shapes.

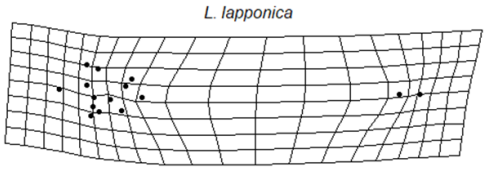
L. lapponica

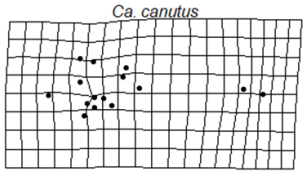
Ca. canutus

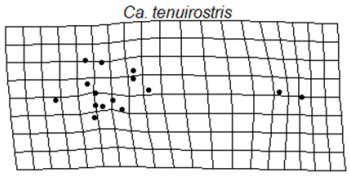
Ca. tenuirostris

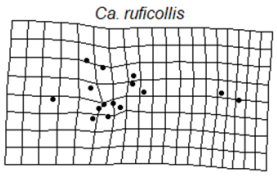
Ca. ruficollis

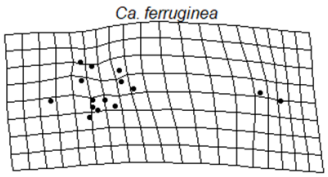
Ca. ferruginea

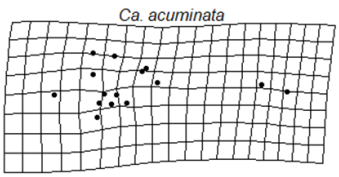
Ca. acuminata

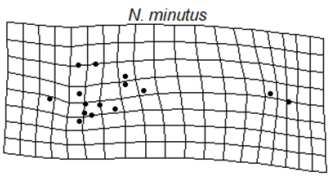
N. minutus

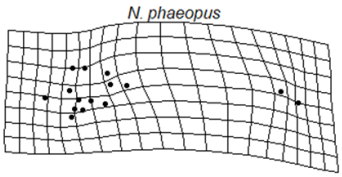
N. phaeopus

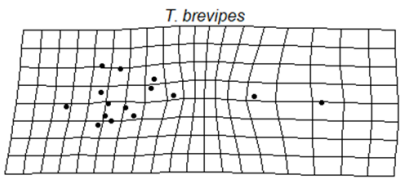
T. brevipes

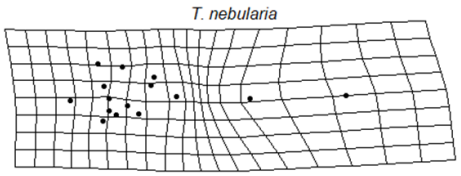
T. nebularia

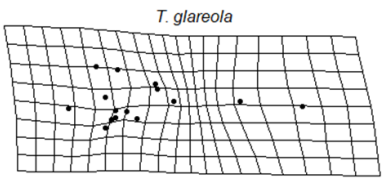
T. glareola

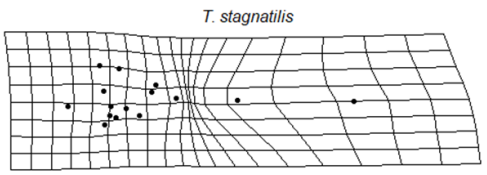
T. stagnatilis

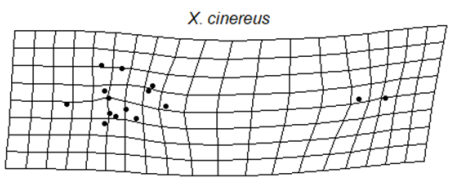
X. cinereus

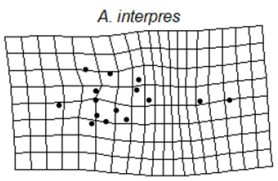
A. interpres

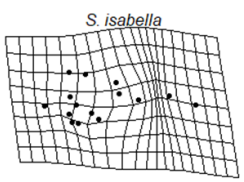
S. isabella

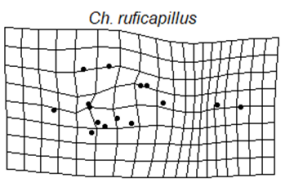
Ch. ruficapillus

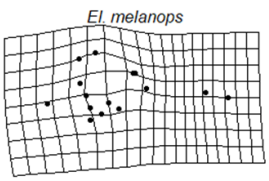
El. melanops

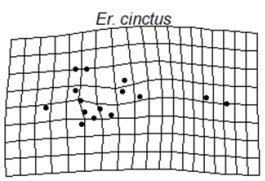
Er. cinctus

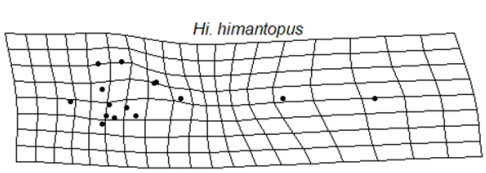
Hi. himantopus

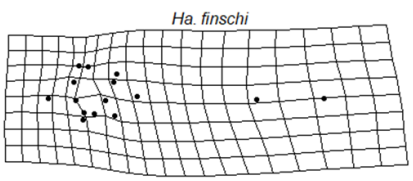
Ha. finschi

Fig. 2.7: Previous page. Thin plate spine (TPS) deformation grids of the right lateral view of each species for visualising comparison. The direction of the landmarks was the same as in Fig. 2.1b with the caudal-most point of the skull on the left and the tip of the bill on the right.

2.4.3 The ventral view of skulls

The first three principal components (PCs) explained 87.6% (PC1), 6.3% (PC2) and 1.9% (PC3) of the variation in skull shape (Fig. 2.8). Along PC1 1.X, 2.X and 3.X contributed the largest variance; these three measurements effectively describe the bill length. In PC2, 3.X, 2.X and 18.X had the largest loadings. These points describe the head length. 14.Y and 15.Y, which describe the skull width, also contributed large variances to PC2 (Fig. 2.9). In PC3, 5.Y and 4.Y had the largest loadings.

The TPS deformation grids displayed that the elongation of the bill had great effect on the skull shape (Fig. 2.10). Another obvious deformation effect was caused by the shape and direction of the rear part of the skull; the rear landmarks were close to a curved line to form the expansion of the skull in *N. minutus, T. brevipes, T. nebularia, T. glareola, A. interpres,* and *Hi. himantopus.* The other deformation was the contraction of the bill base, which was obvious in *N. phaeopus, T. brevipes, T. stagnatilis, Ch. ruficapillus, El. melanops,* and *Er. cinctus.*

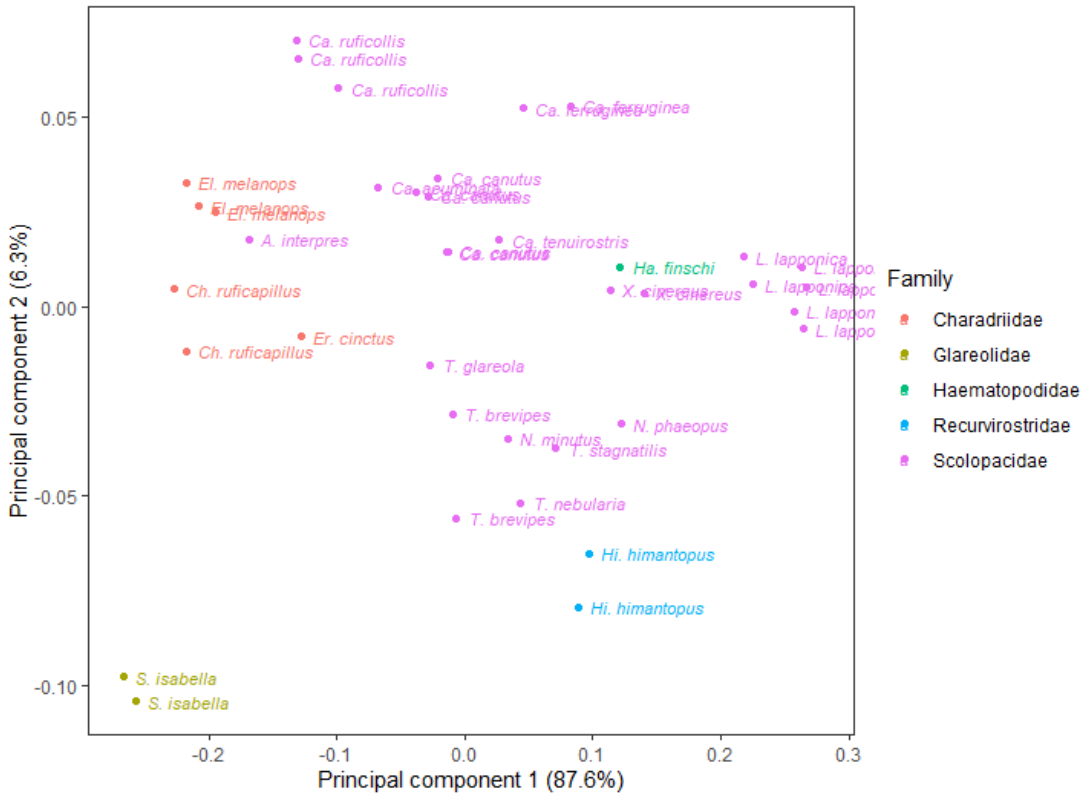

Fig. 2.8: Principal component one and two scores plot. The first two principal components explain more than 90% of the variation in the dataset, with most of this variation explained along PC1. The dots are labelled with species and coloured with family.

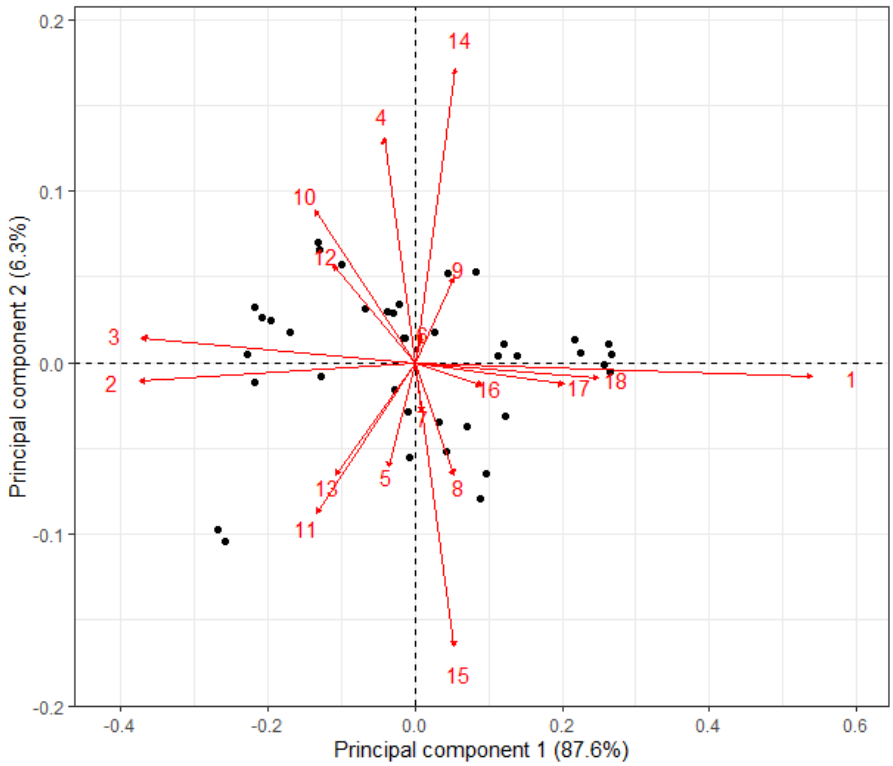

Fig. 2.9: The principal component analysis (PCA) biplot of the ventral view with PC1 (87.6%) as x-axis and PC2 (6.3%) as y-axis on the two-dimensional biplot. The black dots are the projected PCA results same as Fig. 2.8. The red arrows describe the loading strength of each landmark on the shapes.

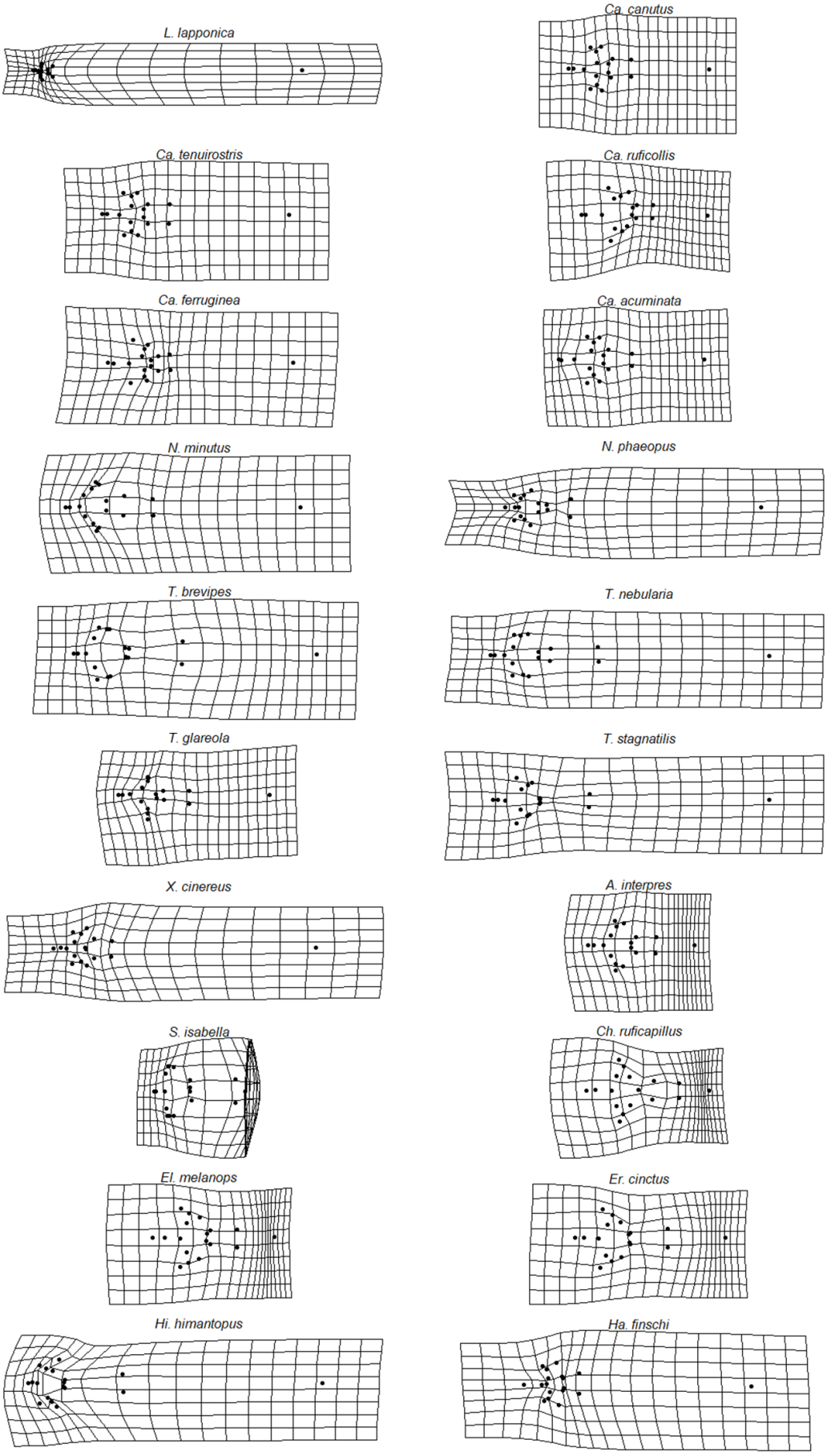
L. lapponica
Ca. canutus
Ca. tenuirostris
Ca. ruficollis
Ca. ferruginea
Ca. acuminata
N. minutus
N. phaeopus
T. brevipes
T. nebularia
T. glareola
T. stagnatilis
X. cinereus
A. interpres
S. isabella
Ch. ruficapillus
El. melanops
Er. cinctus
Hi. himantopus
Ha. finschi

Fig. 2.10: Previous page. Thin plate spine (TPS) deformation grids of the ventral view of each species for visualising comparison. The direction of the landmarks was the same as in Fig. 2.1c with the caudal-most point of the skull on the left and the tip of the bill on the right.

The first three principal components (PC1, PC2, and PC3) of the principal component analysis are displayed in Appendix 1.

2.5 Discussion

Shape variation in the dataset studied here is largely due to skull length, with PC1 explaining 92.7% of the variation in the study of skulls in dorsal view. In addition, the head length has a great effect in PC2, which explains a much lower percentage (2.8%) of the variation. The skull length consists of the bill length and the head length. Therefore, the bill length relative to the head length is considered a major element among the shape variation. The distortion effect of the bill and head length can be detected in the TPS deformation grids (Fig. 2.4), in which grids with long bills and heads are greatly elongated. Moreover, the great effect upon the shape variation caused by the skull width in PC2 is also evident on the deformation grids.

Compared with the dorsal and ventral view, the variation in the right lateral view is less concentrated in PC1; however, still more than 90% of the variation is explained by the sum of PC1 and PC2. Shape variation is largely due to the distance from the rostral end of the external nares to the proximal-most point of the bill, and the head length, with PC1 explaining 74.2% of the variation in right lateral view. In addition, the distance from the tip of premaxilla to the rostral end of the external nares has a great effect in PC2, which explains 16.3% of the variation. Therefore, the length and structure of bills, and the bill length relative to the head length are considered major elements among the shape variation. The distortion effect of the bill length and structure can be detected in the TPS deformation grids (Fig. 2.7). The landmarks around the orbit also have an effect upon the shape variation in PC1 and PC3, which slightly reflects on the deformation grids.

Shape variation in ventral view is largely due to skull length bill length, with PC1 explaining 87.6% of the variation. In addition, the head length has a great effect in PC2. However, this explains a much lower percentage (6.3%) of the variation. Therefore, it is similar to the results of the dorsal view in that the bill length relative to the head length is considered a major element among the shape variation. The distortion effect of the bill and head length can be detected in the TPS deformation grids (Fig. 2.10), where the grids with long bills and heads were greatly elongated. Moreover, the landmarks of the rear part of the cranium gathered in different directions.

After removing the landmarks of the distal bill parts, the sum of PC1 and PC2 of the dorsal, right lateral and ventral views explains 62.8%, 46.2% and 62.6% of the variations respectively (Appendix 2), which are lower than 65% and lower than the results with the distal bill parts.

Besides the bill length, the other landmarks that contribute large variance are the same in the analysis with and without the distal bill parts.

The results indicate the great effect on shape variation caused by the bill length, curvature, and its length relative to the head. This is an expected result as the bill variation is well-known in shorebirds (Baker, 1979; Barbosa & Moreno, 1999; Dann, 1987; Nebel, Jackson, & Elner, 2005). As for the orbit, the TPS deformation grids show that the spaces around the orbits of the little whimbrel and wood sandpiper in the dorsal view, and of the red-capped plover (*Charadrius ruficapillus*), black-fronted dotterel (*Elseyornis melanops*), pied stilt (*Himantopus himantopus*) in both the dorsal and right lateral views seem to bulge out. However, the little whimbrel and wood sandpiper are considered to be tactile foragers with the bill-tip organs full of sensory pits (Piersma *et al.*, 1998). The red-capped plover, black-fronted dotterel, and pied stilt are considered to be visual foragers, but some other potential visual foragers like the red-kneed dotterel and the SIPO do not show obvious orbital shape deformation in the TPS grids.

R. J. Thomas *et al.* (2006) suggested that the visual foragers did not have larger eyes than the tactile foragers. According to the records by Schäfer and Schmitz (2016), the diameter of orbita (OD) of the whimbrel was long and similar to the OD of oystercatchers (*Haematopus* spp.); the OD of the whimbrel and the oystercatcher were longer than of the pied stilt; the OD of the pied stilt was longer than of the bar-tailed godwit. The whimbrel and bar-tailed godwit are regarded as tactile foragers, but they also use visual cues to locate prey, especially for nocturnal feeding in the whimbrel (Hockey & Douie, 1995; Piersma *et al.*, 1998; Turpie & Hockey, 1993); on the other hand, the pied stilt and oystercatcher are mainly regarded as visual foragers, but they also use direct tactile cues, especially for nocturnal feeding in pied stilts (Heppleston, 1970; Rojas *et al.*, 1999). As for small birds, the records showed that plovers (family Charadriidae), ruddy turnstone, and red knot (*Calidris canutus*) had similar OD (Schäfer & Schmitz, 2016). Plovers are regarded as visual foragers, whereas the red knot is regarded as a tactile forager with particular organs for remote touch (Piersma *et al.*, 1998; R. J. Thomas *et al.*, 2006). The ruddy turnstone may use both visual and tactile senses (Piersma *et al.*, 1998; Powlesland, 1998). Therefore, the hypothesis that the orbit of primarily visual foragers is comparatively larger than in tactile foragers is not suggested by the combination of the previous studies and my results. In addition, the bulging eyes in plovers may reduce the blind area extending in front of their short bills (Martin, 2017). More studies about visual fields will be needed for further discussion.

Because of the physical properties of light, there are trade-offs associated with the visual capabilities of eyes. The eye capable of high resolution of details is unable to detect objects well in low light conditions, and vice versa (Martin, 2017). Most predominantly nocturnal owls have large eyes for collecting more light in the dark, but such large eyes are considered too large and heavy for birds making long-distance flights (Martin, 2017). Martin and Piersma (2009), and R. J. Thomas *et al.* (2006) suggested that the shorebirds that feed at night possess relatively large eyes. According to the records by Schäfer and Schmitz (2016), the OD of the whimbrel was longer than of the pied stilt, the OD of the pied stilt was longer than of the bar-tailed godwit, and the OD of the bar-tailed godwit was longer than the red knot. These differences broadly follow the body size differences in the species: the whimbrel is slightly larger than the bar-tailed godwit; the bar-tailed godwit is larger than the pied stilt; the pied stilt is larger than the red knot (Hayman, Marchant, & Prater, 1986; Medway, 2000). The TPS deformation grids show that the space around the orbit of the pied stilt is expanded, whereas that space is shrunk in the bar-tailed godwit; there is no obvious deformation of that space in the whimbrel and red knot. Besides the above interspecific variation, nocturnal feeding has been recorded in those four species (Rohweder & Baverstock, 1996; Rojas *et al.*, 1999; Scheiffarth *et al.*, 2002; Sitters *et al.*, 2001; Zwarts, Anne-Marie, & Roelof, 1990). Therefore, the results do not suggest that the big eyes are only present in nocturnal foragers. Furthermore, the capability of night vision is not absolutely limited to eye sizes. A comparison between the eyes of Rock doves (*Columba livia*) and Manx shearwaters (*Puffinus puffinus*) revealed that it is possible for the eyes of Manx shearwaters to produce brighter images by their different optical structures than the doves even though they have the same eye size (Martin & Brooke, 1991).

In summary, the bill length is the major element that causes the skull shape variation among shorebirds. Some visual foragers do have big eyes. However, tactile foragers can also have large eyes. The shape deformation of the eyes is only evident in some cases. Most birds seem to apply multiple sensory cues to feed at night (Heppleston, 1970; Turpie & Hockey, 1993). Although some studies did not get a better result from geometric morphometrics analysis compared to traditional morphometrics (Kass, Montalti, & Acosta Hospitaleche, 2018), the result of this study does provide us useful information. It is also worth noting that the selection of the angles and landmarks of the samples is quite important, and it depends on what questions we want to answer. For example, in this study more landmarks were selected for the ventral view, but the results of the dorsal and right lateral views provided the most useful information in the end.

3 The morphological analysis of the bill and the bill-tip organs in shorebirds

3.1 Abstract

Charadriiform shorebirds possess remarkable bill forms, which reflect their diets and foraging behaviours. The length and curvature are the major variations in bill shape, but mechanoreceptors under the rhamphotheca allow birds to detect prey by pressure and may be concentrated into a bill-tip organ. In this study, I compared the bill morphology among 20 charadriiform shorebird species, focusing on sensory pit numbers, bill-tip organ lengths, and the presence of distal rhynchokinesis (the ability to bend the tip of the upper mandible). Bill lengths generally increased with body masses and head lengths, but there were species variations. Five species had especially long bills relative to head length (South Island oystercatcher (SIPO) (*Haematopus finschi*), bar-tailed godwit (*Limosa lapponica*), whimbrel (*Numenius phaeopus*), terek sandpiper (*Xenus cinereus*), and curlew sandpiper (*Calidris ferruginea*), whereas proportionately short bills were found in the ruddy turnstone (*Arenaria interpres*), Australian pratincole (*Stiltia isabella*) and small plovers**.** Sensory pits were present on both the premaxilla and the dentary and were found in all species, but clusters of pits in bill-tip organs were found only in the Scolopacidae, with largest numbers and highest densities of pits in the genus *Calidris*. The bill-tip organs were generally short (3-13 mm) and did not vary systematically with size except for in the shanks (*Tringa* spp.), which had low-density bill-tip organs that covered up to almost half the bill length. Species that used scything when feeding tended to have lower densities of sensory pits than those that used mostly pecking or probing. The bill-tip organ likely functions differently in the shanks than in the other groups studied. Shanks are known to feed actively in the water column for fish, including by ploughing and sometimes in social flocks, and the large but sparsely-pitted organs may enable the submerged portion of the bill to function as a tactile prey sensor. In contrast, the higher-density concentrated organs in other sandpipers may enable sewing or probing birds to detect buried prey more efficiently. Distal rhynchokinesis was present in ten species, in both long-billed and short-billed birds. There was a (non-significant) tendency for species with rhynchokinesis to have more sensory pits than those without, but species with rhynchokinesis had significant shorter bill-tip organs. This suggests that prey capture in species with flexible bills may be enhanced by the presence of a sensory bill-tip organ.

3.2 Introduction

Charadriiform shorebirds possess diverse bill forms, which are closely related to their feeding habits (Barbosa & Moreno, 1999; Burton, 1974; Colwell, 2010). Probing and pecking are considered two main feeding methods in shorebirds (Johnston, 2014). Scything is a tactile feeding method used by some *Tringa* spp. and terek sandpipers (Hockey & Douie, 1995; Pierce, 1985; Rico-Guevara *et al.*, 2019). The bird scythes by lowering its head and sweeping its bill horizontally in soft muddy substrates from one side to the other (Pierce, 1985). Stilts (*Himantopus* spp.) in New Zealand can do single scything with the head raised every time or multiple scything with the bill sweeping from side to side (Pierce, 1985).

While bills vary in many ways, an obvious one is in the curvature (Burton, 1974; Nebel, Jackson, & Elner, 2005). Straight bills are suitable for direct pecking in plovers, *Tringa* species and *Himantopus* species, and for specialized probing with inserting force (Burton, 1974; van de Kam *et al.*, 2004). Slight decurved bills are present in many species, possibly for facilitating a gripping mechanism, whereas the clearly decurved bills in curlews (*Numenius* spp.) enable them to effectively explore and capture crabs in complex three-dimensional burrows (Davidson *et al.*, 1986; Ferns & Siman, 1994). Slight upcurved bills are suitable for pursuing prey horizontally in shallow water or on the surface in some *Tringa* spp. and occasionally in godwits (Burton, 1974; Colwell, 2010). Another feature is the bill length (Barbosa & Moreno, 1999; Burton, 1974). Birds with long bills can probe for prey hiding in deep burrows, whereas birds with short bills probe shallow small invertebrates (Colwell, 2010; Hockey & Douie, 1995). In some species, such as the bar-tailed godwit, the bill length is different between the males and females as sexual dimorphism; Ross (2018) suggested that this difference reduced the competition within the species due to resource partitioning of the prey in different depths.

Another feature of the bill is the keratinous rhamphotheca that covers the bony parts of it (Burton, 1974; Rico-Guevara *et al.*, 2019). The rhamphotheca outlines the beak shape and contributes in part to the stiffness of bills (Rico-Guevara *et al.*, 2019). For instance, oystercatchers (*Haematopus* spp.) possess sturdy chisel-like rhamphotheca for smashing and opening molluscs (Burton, 1974; Dowding, 2022). Turnstones (*Arenaria* spp.) possess a stout and broad-based bill for lifting and flipping small rocks to catch prey (Colwell, 2010; Hockey & Douie, 1995).

Under the rhamphotheca, the mechanoreceptors such as Herbst and Grandry corpuscles are embedded in the bill tip to provide another tool for detecting prey (Berkhoudt, 1979; Rico-Guevara *et al.*, 2019). The sensory pits are small cavities with a high density of Herbst corpuscles, which function as pressure detectors (Cunningham *et al.*, 2013; Nebel, Jackson, & Elner, 2005). A cluster of sensory pits on distal bill portions is called the bill-tip organ (Cunningham *et al.*, 2010). Many birds use those organs to detect the vibrations made by the prey in the sediment (van de Kam *et al.*, 2004). Piersma *et al.* (1998) reported a novel feeding method of "remote touch" foraging in red knots (*Calidris canutus*). The method suggested was that with bill insertion, the birds use Herbst corpuscles at the bill-tip organs to detect pressure gradients generated by bill probing and reflected by infaunal prey in wet substrates (Cunningham *et al.*, 2010; Piersma *et al.*, 1998; van de Kam *et al.*, 2004). Remote touch foraging allows the birds to search for hidden prey more efficiently than just by direct touch (Cunningham *et al.*, 2010; Piersma *et al.*, 1998; van de Kam *et al.*, 2004). This foraging method is supported by other subsequent evidence. Bill-tip organs have been found on the elongated bills of other probing feeding birds from effectively unrelated families, including certain shorebirds (Scolopacidae), kiwi (Apterygidae) and ibises (Threskiornithidae) (Colwell, 2010; Cunningham *et al.*, 2010; Cunningham *et al.*, 2013; Nebel, Jackson, & Elner, 2005). It is interesting that these three families are not closely related (Kuhl *et al.*, 2021). Therefore, it is suggested that the bill-tip organ has evolved independently in these groups. This independent adaptation was also suggested by the fact that not all species in the order Charadriiformes possess the bill-tip organ (Martin & Piersma, 2009). Studies of the association between bill-tip organs and brain regions indicated that the probing feeding birds have developed the strategy under similar ecological selective pressures (Cunningham *et al.*, 2010; Cunningham *et al.*, 2013).

In the Scolopacidae, studies of bill-tip organs have been focused on the genus *Calidris* (Cunningham *et al.*, 2013; Nebel, Jackson, & Elner, 2005; Piersma *et al.*, 1998). The discovery of bill-tip organs in most calidrid sandpipers implied that remote touch foraging is a major detecting tool for them (Nebel, Jackson, & Elner, 2005). In addition, the bill-tip organs in the probing feeding birds of other genera, bar-tailed godwits and Eurasian woodcock (*Scolopax rusticola*), have been described and compared (Cunningham *et al.*, 2013). The number and distribution of sensory pits varied among species, with Eurasian woodcock having more pits than godwits (Cunningham *et al.*, 2013). Eurasian woodcock might have evolved dense pits because they more often rely on probing feeding, whereas godwits also use visual cues to locate and increase the catch rate of the actively retreating worms and crabs (Cunningham

et al., 2013; Hockey & Douie, 1995; Ross, 2018). The interspecific variation of the bill-tip organs may reflect niche differentiation among shorebirds. For example, Cunningham *et al.* (2010) reported that in ibises the number and density of the sensory pits were associated with the substrate types they probed in. The birds that spent more time in aquatic habitats seemed to possess more pits (Cunningham *et al.*, 2010). Different species of Scolopacidae feed in diverse habitats (Baker, 1979; Hayman, Marchant, & Prater, 1986; Hockey & Douie, 1995). However, comparative study of the bill-tip organs among different shorebirds is lacking, especially the birds other than *Calidris* in the Scolopacidae, and how the organ forms reflect their foraging strategies (Cunningham *et al.*, 2013). The number of sensory pits in many species are still uncertain (Nebel, Jackson, & Elner, 2005). Also, not all shorebirds rely on bill-tip organs to find food (Colwell, 2010; Martin & Piersma, 2009; R. J. Thomas *et al.*, 2006). In this study, I documented sensory pit numbers and distribution in shorebird bills and tested whether the interspecific variation of the bill-tip organs is related to phylogeny or other factors.

Cranial kinesis is another skeletal feature of shorebirds (Burton, 1974). It means the movement of the upper jaw relative to the braincase (Burton, 1974; Zusi, 1984). There are many different types of cranial kinesis, but in my study I focus only on distal rhynchokinesis, which is present in kiwi (*Apteryx* spp.) and certain charadriiform birds (Zusi, 1984). Distal rhynchokinesis means that the bending occurs only in the distal part of the upper jaw (Estrella & Masero, 2007; Zusi, 1984). Despite the rigid upper jaw, the mechanism of the flexible distal part provides powerful gaping and grasping capabilities (Fig. 3.1) (Zusi, 1984). It was commonly suggested that the function of distal rhynchokinesis was to grab prey with long bill when the bird use the deep probing feeding method (van de Kam *et al.*, 2004; Zusi, 1984). However, Estrella and Masero (2007) have reported that the shorebirds use distal rhynchokinesis to enhance feeding efficiency on small surface prey when they use the surface tension transport (STT) feeding method (Colwell, 2010; Johnston, 2014; Rubega & Obst, 1993). It is unclear if distal rhynchokinesis is also associated with other feeding functions yet.

Here I test if the traits of bills and sensory pits are associated with specific body sizes and foraging behaviours. Specifically, I address whether a certain maxilla length is related to bird sizes, phylogeny or foraging behaviours, whether the numbers and densities of sensory pits are related to phylogeny, bill length, bill-tip organ lengths, and foraging behaviours, and whether there is any association between the bill-tip organ and distal rhynchokinesis of bills.

Fig. 3.1: The outward (upper) and inward (lower) bending of distal rhynchokinesis in the bar-tailed godwit. The bill shows gaping and grasping capabilities with distal rhynchokinesis. Images: P. Battley; Manawatū Estuary.

3.3 Methods

All 40 individuals in this thesis were used in this investigation. However, the maxilla of a little whimbrel (*N. minutus*) and the dentary of a red-necked stint (*Ca. ruficollis*) were broken during the preparation. The software ImageJ was used, with the scale of the images as a length reference, to measure all the lengths including the bill-tip organ lengths, and to count the sensory pit numbers (Rasband, 2020).

The images of the right lateral view of the head with the bill were used to measure the straight maxilla and mandible lengths with rhamphotheca. After cleaning the skulls, the images of the dorsal view of the skull were used to measure the skull length, the images of the right lateral view of the skull were used to measure the length between maxilla tip and the junction of nasal and jugal bars, and the images of the dorsal view of the mandible were used to measure the mandible length. The distance from the proximal-most point of the bill to the caudal-most point of the cranium was defined as head length.

The images of the eight different angles (dorsal, left-dorsal lateral-45-degree, left lateral, left-ventral lateral-45-degree, ventral, right-ventral lateral-45-degree, right lateral and right-dorsal lateral-45-degree) of the premaxilla and the dentary were used to measure the bill-tip organ lengths and to count the sensory pit numbers (Fig. 3.2). The density of pits in the organ was calculated as the pit number divided by the organ length.

The position of the hinge for the rotation of distal rhynchokinesis accorded with the description by Gussekloo, Vosselman, and Bout (2001), and Zusi (1984). Zusi (1984) defined distal rhynchokinesis as only the distal restricted or extended portion of the upper jaw bending beyond the symphysis, whereas the rest of the upper jaw was fused and stiffened. The movement of distal rhynchokinesis was checked by manually bending the distal portion of the bill relative to the braincase, and recorded as yes/no.

I used the Shapiro-Wilk test for the normality of the data and Tukey's Ladder of Powers to transform non-normal data where normality could be achieved (Royston, 1995; Tukey, 1977).

To test for relationships between the maxilla length and the bird mass, and between the maxilla length and the head length, I used linear mixed-effects models in the R package lmer (Kuznetsova, Brockhoff, & Christensen, 2017), with Species as a random factor to account for multiple individuals in some species. The ANOVA F-test in fitting linear mixed-effects models tells us which of the fixed effects mainly interact with the factor (Kuznetsova, Brockhoff, & Christensen, 2017).

To test for differences in maxilla length between groups of presence of surface pecking or scything behaviour, in premaxilla and dentary sensory pit density between groups of presence of scything behaviour, and in total sensory pit number or premaxilla bill-tip organ length between groups of presence of distal rhynchokinesis, I used t-tests on untransformed (total sensory pit numbers) or transformed (maxilla lengths, premaxilla and dentary sensory pit densities, and premaxilla bill-tip organ lengths) species averages.

For comparisons involving non-normal data (the correlation between the bill-tip organ length and the bill length of both maxilla and mandible, between the sensory pit numbers and the bill-tip organ length of both premaxilla and dentary, and between the sensory pit density and the bill-tip organ length of both premaxilla and dentary), Spearman's rank correlation was used to test the relationships.

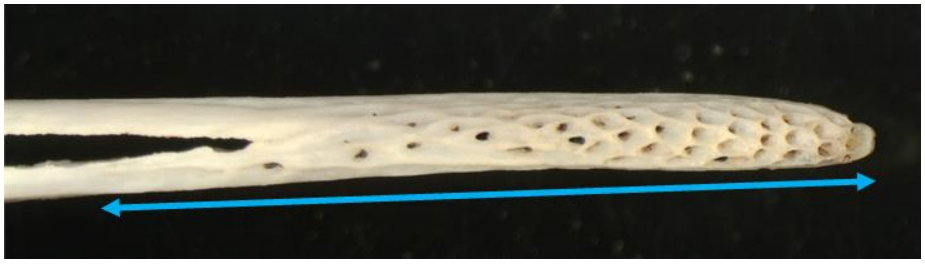

Fig. 3.2: The right lateral view of the premaxilla bill-tip organ of a bar-tailed godwit. The blue double-headed arrow shows the bill-tip organ length that covers all the sensory pits.

3.4 Results

3.4.1 Bill length

In general, larger (and hence heavier) species had longer bills (maxilla length in relation to bird mass; Fig. 3.3; ANOVA F-test in lmer model on species averages, $F_{30} = 20.73$, $P < 0.001$). On the other hand, there was substantial variation between species in the relative bill length (maxilla length in relation to head length; Fig. 3.4; ANOVA F-test in lmer model on species averages, $F_{29} = 0.12$, $P = 0.74$). The ruddy turnstone, Australian pratincole and the plovers all had similarly short bills in spite of some variation in head length, while the scolopacid shorebirds had considerable variation between species in the maxilla length (Fig. 3.4). Species with comparatively long bills for their head size were SIPO, bar-tailed godwit, whimbrel, terek sandpiper, and curlew sandpiper. For species with multiple individuals, bill length variation was generally small apart from in bar-tailed godwits.

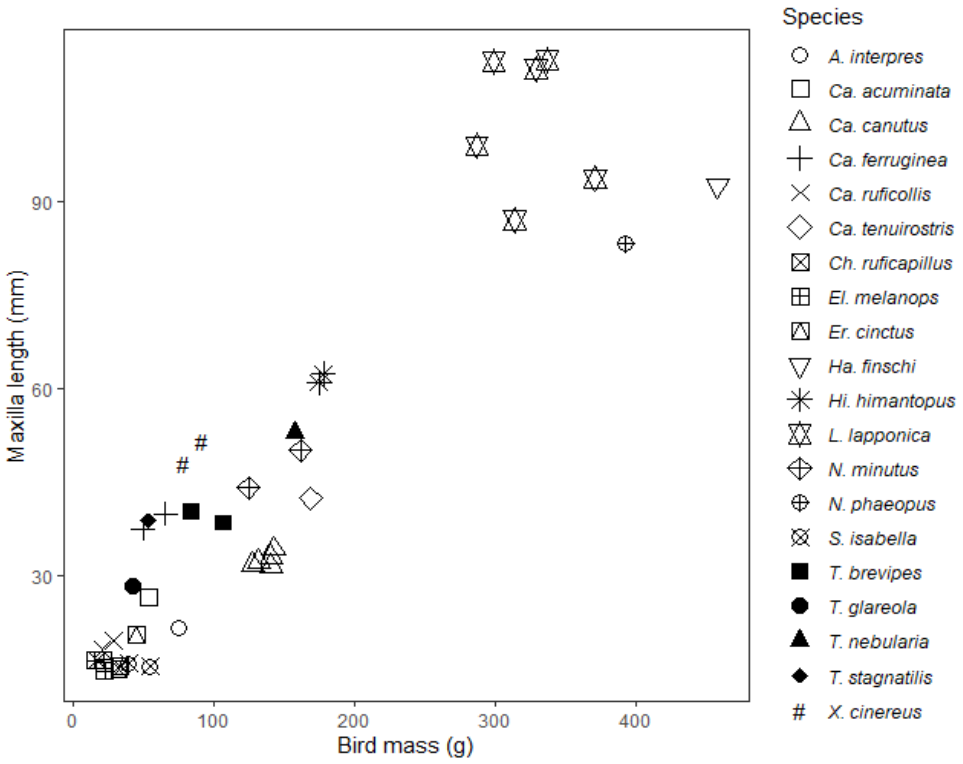

Fig. 3.3: Maxilla length vs. bird body mass.

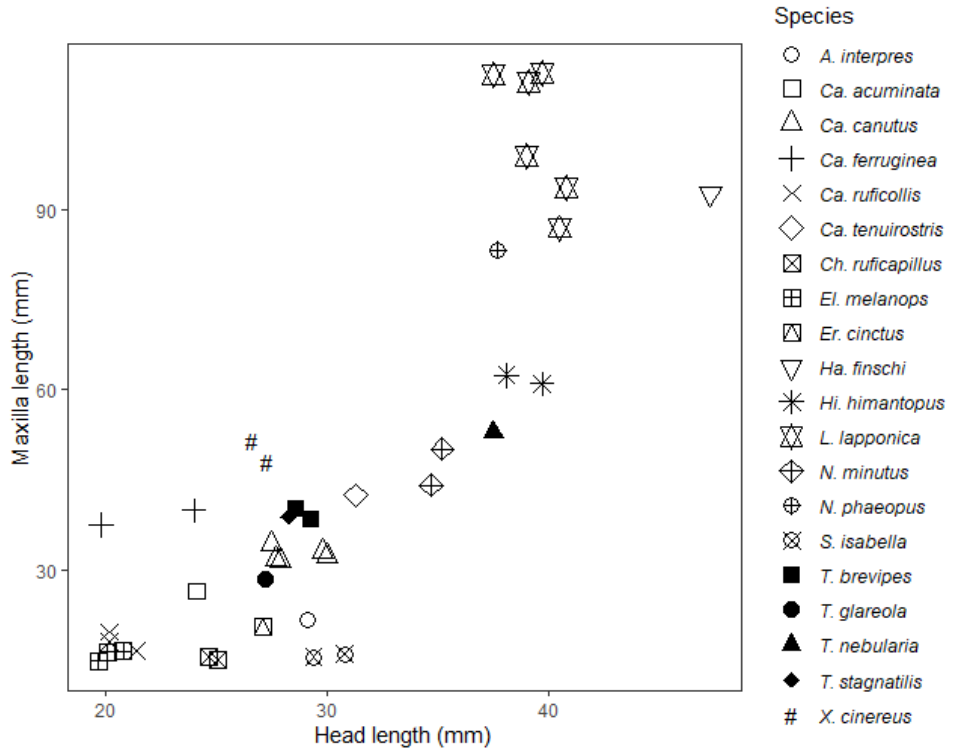

Fig. 3.4: Maxilla length vs. head length.

There was no significant difference between the average maxilla length of each species and the presence of surface pecking behaviour (t-test on transformed species averages, $t_{15} = -1.28$, $P = 0.22$) (Fig. 3.5, left panel), and between the maxilla length and the presence of scything behaviour (t-test on transformed species averages, $t_{15} = 1.45$, $P = 0.17$) (Fig. 3.5, right panel). However, it seemed that shorter bills were suitable for pecking and medium-length bills (28.4–62.4 mm) were suitable for scything.

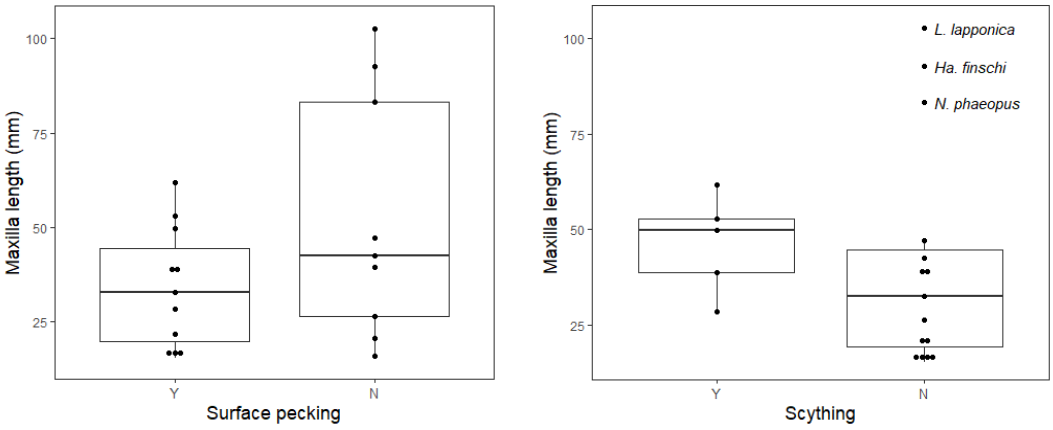

Fig. 3.5: Average maxilla length of each species vs. foraging behaviours.

3.4.2 Sensory pits

Sensory pits of some form were found in all species, but the birds of the families Glareolidae, Charadriidae, Recurvirostridae, and Haematopodidae had only a few tiny pits on their bill bones, and they did not have the bill-tip organs with clusters of sensory pits like those found in the Scolopacidae (Fig. 3.6). *Calidris* generally had the largest number of sensory pits (376–549 pits) among Scolopacidae. *Tringa* had the second largest number of pits (241–375 pits), but the number of the grey-tailed tattler (*T. brevipes*) (241–244 pits) is close to the number of the bar-tailed godwit (201–250 pits). The ruddy turnstone had the smaller number of pits (149 pits). The sensory pits of the ruddy turnstone were shallow, and their form looked quite different from other species (Fig. 3.7).

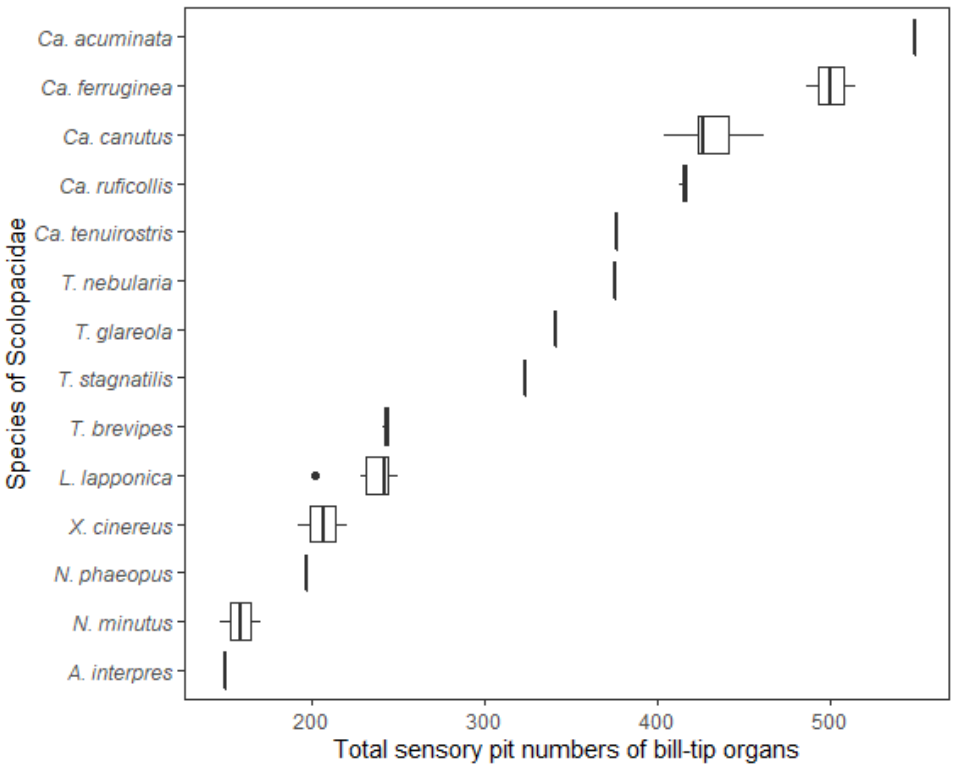

Fig. 3.6: Total sensory pit numbers (premaxilla + dentary) of each species of Scolopacidae (Specimen numbers from top to bottom, n = 1, 2, 5, 2, 1, 1, 1, 1, 2, 6, 2, 1, 2, 1).

Fig. 3.7: The premaxilla bill-tip organs. Upper: Dorsal view of red-necked stint (the blue double-headed arrow was approximately 4.1 mm); the red-necked stint had the highest density of the sensory pits over the organ length in this study. Middle: Right lateral view of common greenshank (the blue arrow was approximately 31 mm); the *Tringa* species had elongated organs. Lower: Dorsal view of the premaxilla bill-tip organ of ruddy turnstone (the blue arrow was approximately 8.3 mm); the rhamphotheca was sturdy and closely attached to the bone.

Only the birds in the family Scolopacidae had bill-tip organs that could be measured for the organ length. There was a moderate positive correlation between the premaxilla bill-tip organ length and the maxilla straight length (Spearman's, ρ = 0.46) (Fig. 3.8a), and a strong positive correlation between the dentary bill-tip organ length and the mandible straight length (Spearman's, ρ = 0.51) (Fig. 3.8b). The bar-tailed godwit had the bill-tip organ length close to the length of the terek sandpiper, little whimbrel and *Calidris*, but their bills were much longer. On the other hand, the lengths between the bill and bill-tip organ in *Tringa* displayed a positive correlation.

There was a moderate negative correlation between the sensory pit numbers on the premaxilla length and the premaxilla bill-tip organ length (Spearman's, ρ = -0.31) (Fig. 3.8c), and a weak negative correlation between the sensory pit numbers on the dentary and the dentary bill-tip organ length (Spearman's, ρ = -0.18) (Fig. 3.8d). The bar-tailed godwit, terek sandpiper, little whimbrel and ruddy turnstone had the organ lengths slightly longer but the pit numbers fewer than *Calidris.* The dentary bill-tip organ length of the whimbrel was relatively long as the sensory pits were aligned along the elongated curved mandible (Appendix 3). Note that *Tringa* generally had long bill-tip organs.

There were strong negative correlations between the sensory pit density and the bill-tip organ length in both the premaxilla (Spearman's, ρ = -0.89) (Fig. 3.8e) and the dentary (Spearman's, ρ = -0.80) (Fig. 3.8f). The bar-tailed godwit, terek sandpiper, little whimbrel and ruddy turnstone had short bill-tip organ lengths with low sensory pit densities. *Calidris* generally had short organ lengths with high pit densities, whereas *Tringa* had long organ lengths with low pit densities. Note that the red-necked stints had the highest pit densities, although they did not have the largest total pit numbers. The curlew sandpipers also had high pit densities over the premaxilla. On the other hand, the common greenshank (*T. nebularia*) had the largest total pit numbers among shanks, but it had low pit densities. The whimbrel had a relatively long dentary bill-tip organ, though the pit density was low.

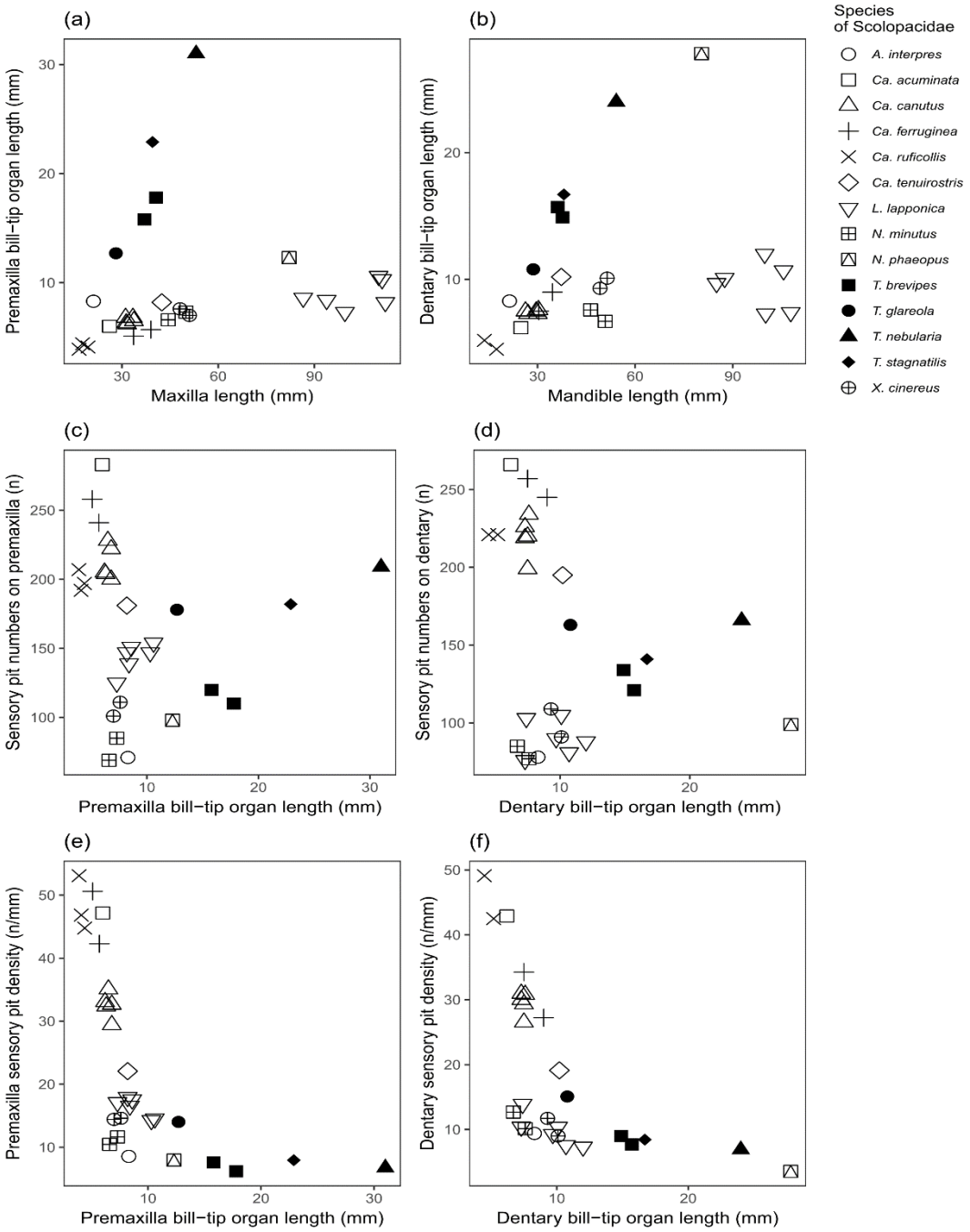

Fig. 3.8: (a) Premaxilla bill-tip organ length vs. maxilla length. (b) Dentary bill-tip organ length vs. mandible length. (c) Sensory pit numbers on premaxilla vs. premaxilla bill-tip organ length. (d) Sensory pit numbers on dentary vs. dentary bill-tip organ length. (e) Premaxilla sensory pit density vs. premaxilla bill-tip organ length. (f) Dentary sensory pit density vs. dentary bill-tip organ length.

There was no significant difference between the average premaxilla sensory pit density and the presence of scything behaviour (t-test on transformed species averages, $t_8 = -1.56$, $P = 0.16$) (Fig. 3.9, left panel), and between the average dentary sensory pit density and the presence of scything behaviour (t-test on transformed species averages, $t_{12} = -1.39$, $P = 0.19$)

(Fig. 3.9, right panel). However, it seemed that the birds using scything foraging behaviour tended to have low sensory pit densities.

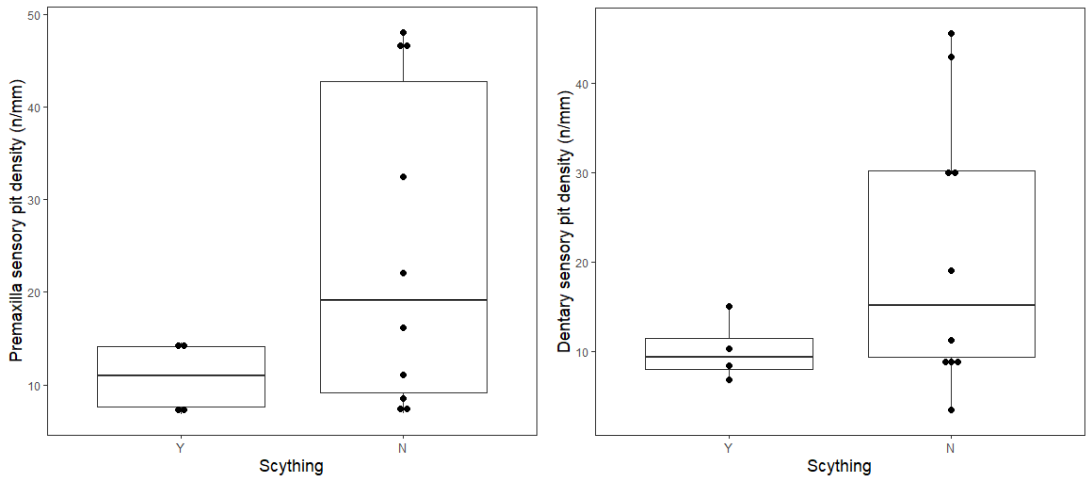

Fig. 3.9: Average premaxilla and dentary sensory pit densities of each scolopacid species vs. the presence of scything behaviour.

Distal rhynchokinesis was present in ten charadriiform species in my study. These species include the bar-tailed godwit, red knot, great knot (*Ca. tenuirostris*), red-necked stint, curlew sandpiper, sharp-tailed sandpiper (*Ca. acuminata*), little whimbrel, and terek sandpiper in the Scolopacidae family, and the red-capped plover (*Charadrius ruficapillus*) and black-fronted dotterel (*Elseyornis melanops*) in the Charadriidae family. Some species with distal rhynchokinesis had long bills (the maxilla straight length was 86.5–112.1 mm in bar-tailed godwit; 44.4–49.9 mm in little whimbrel; 48.1–51.0 mm in terek sandpiper), whereas rhynchokinesis was also present in some short-billed birds (16.6–17.7 mm in red-necked-stint; 14.9–15.4 mm in red-capped plover; 14.6–15.8 mm in black-fronted dotterel).

There was no significant difference between the average total sensory pit numbers of each species and the presence of distal rhynchokinesis (t-test, $t_{16} = 1.56$, $P = 0.14$) (Fig. 3.10). Although it seemed that the birds with large sensory pit numbers tended to possess distal rhynchokinesis, the kinesis was also found in the birds with small pit numbers. Since distal rhynchokinesis depicted the movement of the distal part of the upper jaw, here only the premaxilla bill-tip organ was used for the relevant analysis. Scolopacid species with distal rhynchokinesis had significantly shorter premaxilla bill-tip organs than others (t-test on transformed species averages, $t_{11} = -4.60$, $P < 0.005$) (Fig. 3.11).

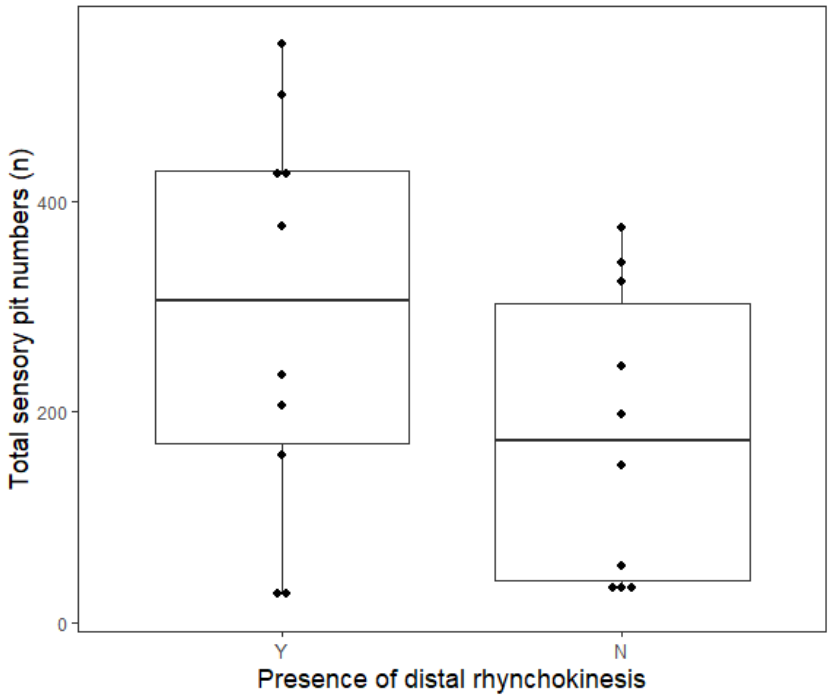

Fig. 3.10: Average total sensory pit numbers of each species vs. presence of distal rhynchokinesis.

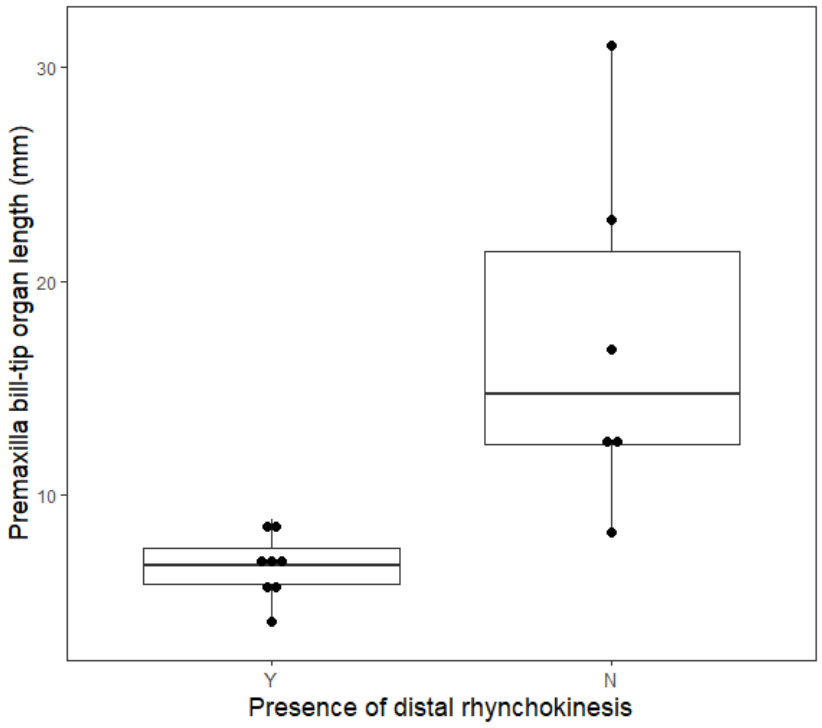

Fig. 3.11: Average premaxilla bill-tip organ length of each scolopacid species vs. presence of distal rhynchokinesis.

3.5 Discussion

The specimens used in this study had been frozen for varying periods and could have undergone some post-mortem changes. In general, changes in structural length measurements between pre-mortem and post-mortem are small compared to changes in body mass measurements (McCormack *et al.*, 2016). Despite variation in the freshness of some specimens after freezing, post-mortem assessment still provides useful information for this comparative study. The results indicate that bill lengths generally increase with body masses and head lengths, though the effect of body mass is more significant. Also, there are deviations caused by species effects. Both the terek sandpiper and the SIPO have proportionately long bills, but the terek sandpiper's is quite light while the oystercatcher is heavy. The red knot is slightly robust in terms of its bill length. Note that in the comparison between maxilla length and body mass (Fig. 3.3), and between maxilla length and head length (Fig. 3.4), there are size gaps between the large birds such as the bar-tailed godwit, SIPO and whimbrel, and the other medium to small birds. The gaps might be filled with intermediate-sized birds such as grey plovers (*Pluvialis squatarola*) and Pacific golden plovers (*Pluvialis fulva*) in future research.

The independent variation of the bill length in relation to head length in different species has been suggested to relate to their feeding habits (Barbosa & Moreno, 1999; Burton, 1974; Colwell, 2010). Note that the relative long head length in the SIPO may provide a rigid base for using its powerful bill with sturdy and closely attached rhamphotheca (Hulscher, 1982; Johnson, 1984). Two other species with hard bills, the ruddy turnstone and Australian pratincole, also have relative long head lengths, but their bills are very short. On the other hand, the birds with relative long bills, the bar-tailed godwit, curlew sandpiper and terek sandpiper have flexible bills. Although the results show no significant relationship between any bill length and any foraging behaviour (Fig. 3.5), it seems that the short bill is suitable for but not limited to the pecking behaviour. The shanks and the stilts that use the scything behaviour have bill length ranging from 28.4–62.4 mm.

There is a variety of sensory pit numbers among the shorebirds. In this study, only the birds of the family Scolopacidae had obvious bill-tip organs with large numbers of sensory pits in them. In addition, there was considerable variation in pit numbers between genera in the Scolopacidae, which rarely overlapped (Fig. 3.6). Hence, the sensory pit numbers are suggested to relate to phylogeny.

There were positive correlations between the bill length and the bill-tip organ length in scolopacid birds (Fig. 3.8a,b). However, most species had bill-tip organ less than 13 mm in length. The exceptions were the shanks (*Tringa* spp.), whose organs took up much more of their bill length. Also note that the whimbrel had a long bill-tip organ on the lower jaw.

Most *Calidris* spp. had short bills with large numbers of pits. On the other hand, the bar-tailed godwit and whimbrel had long bills but not many pits. Despite the similarly small numbers of pits among *Numenius,* the whimbrel had a much longer bill than the little whimbrel. The shanks formed a group with the bills slightly longer but the pit numbers slightly smaller than *Calidris.* There was considerable variation in the numbers of pits in the shanks that the pit numbers obviously increased with longer bill-tip organs (Fig. 3.8c,d). The sensory pit density and the bill-tip organ length demonstrated strong negative non-linear relationships. Generally, the pit density decreased with longer organ length. However, the major variation was the elongated bill-tip organ length among the shanks, whereas in other scolopacid species the major variation was the pit density. In *Calidris*, pit densities decreased with body size: they were highest in the smallest species (red-necked stint, sharp-tailed sandpiper and curlew sandpiper) and declined in the red knot and great knot; the largest great knots had the lowest pit density. Therefore, the diverse sensory pit density in shorebirds may be associated with different foraging strategies for different prey size. This clarification will require further research.

It seems that the sensory pit densities tend to be low in the shanks that use scything when foraging. Scything was used by some *Tringa* spp. and recurvirostrids (avocets and stilts). However, the avocets and stilts do not have the bill-tip organs (Schäfer & Schmitz, 2016). Therefore, the prey capture mechanism and diets of shanks and recurvirostrids using scything may be different, or the shank's bills may have multiple functions. Shanks like greenshank and marsh sandpiper (*T. stagnatilis*) are piscivorous (feed on small fish), and one of their foraging strategies is to 'plough', running forwards fast in a line (Battley *et al.*, 2003). Ploughing may temporarily increase prey availability through social foraging, with flocks concentrating fish together (Battley *et al.*, 2003). A long sensory organ along the distal part of the bill may enable birds to detect the movement of fish from any direction and aid herding and blocking fish from escaping.

As for probing, although it has been suggested that the bill-tip organ was used for detecting prey through probing (Cunningham *et al.*, 2013; Piersma *et al.*, 1998), most shorebirds in my study (except Australian pratincole) can probe for food with or without the bill-tip organ

(Hayman, Marchant, & Prater, 1986; Hockey & Douie, 1995; Powlesland, 1998). Without the bill-tip organ, the birds can still use the Herbst corpuscles within the bony premaxilla for direct touch to detect prey (Cunningham *et al.*, 2013; Heppleston, 1970). Detecting cockles and Baltic tellins with specialised sensory organs in knots, however, was suggested to be more efficient than oystercatchers using direct touch (van de Kam *et al.*, 2004). It is worth noting that grey-tailed tattlers (*T. brevipes*) have the smallest total pit number among *Tringa*, which is close to the number for bar-tailed godwits. Terek sandpipers have the pit number between bar-tailed godwits and whimbrels. Grey-tailed tattlers, terek sandpipers, bar-tailed godwits, and whimbrels all prefer to feed on crabs or polychaetes by probing (Duijns, Hidayati, & Piersma, 2013; Hockey & Douie, 1995; Steed, 2017). Therefore, it is possible that there is an association between deep probing and small sensory pit numbers.

The sensory pit numbers may be related to the substrates of the habitat that the birds often forage on. In ibises, it has been suggested that the birds that preferred aquatic habitats had larger number of sensory pits (Cunningham *et al.*, 2010). In my study, the scolopacids that prefer terrestrial areas (ruddy turnstone and little whimbrel) do have small sensory pit numbers, whereas other shorebirds that spend most time on sandflats or mudflats have various pit numbers. van de Kam *et al.* (2004) explained that the knots preferred to forage on the flats neither too dry nor too wet because the moderately wet sediments provided the best medium of pressure field for remote touch foraging. However, the sensory pit numbers (251) of the North Island brown kiwi (*Apteryx mantelli*), a terrestrial species, were slightly more than of the bar-tailed godwit (Cunningham *et al.*, 2013). Therefore, the variation of the sensory pit numbers between and within genera cannot be completely explained by the habitat differences of the birds. It is also important to note that the number of the mechanoreceptors embedded in each sensory pit is not fixed (Cunningham *et al.*, 2013). There were more mechanoreceptors per pit in the bar-tailed godwit than in the North Island brown kiwi (*Apteryx mantelli*) (Cunningham *et al.*, 2013). Apart from this, there are birds like the Eurasian oystercatcher (*Haematopus ostralegus*) with numerous Herbst corpuscles close to the tip within the bony core of the bill (Heppleston, 1970). The forms of the mechanoreceptors within sensory pits in different species will need further research.

In this study I made a manual assessment of the rhynchokinesis present in the bills of the specimens. It is possible that the properties of the bone of the bill are different after freezing and preparation than in life, but Gussekloo, Vosselman, and Bout (2001) have also used specimens that were frozen and defrosted for studying cranial kinesis. Regardless, distal rhynchokinesis was defined as the flexibility of the distal part of the upper jaw (Estrella &

Masero, 2007; Zusi, 1984). The flexibility measurement can be affected by the length of the bill, the condition of the sample, person carrying the assessment out and environmental conditions. It is beyond the scope of this work, but a more objective standardized technique for assessing the presence or absence of rhynchokinesis will be required in the future. Distal rhynchokinesis was present in the birds with a wide range of sensory pit numbers. This implies that the kinesis can be applied for the same or different tasks in those birds. The birds with large numbers of sensory pits tended to possess distal rhynchokinesis. In addition, there was a significant relationship between the short bill-tip organ and distal rhynchokinesis as assessed by manual bending of a dried specimen. The flexible distal premaxilla may allow the concentrated sensory receptors within the bill-tip organ at the tip to touch things sensitively.

It has been suggested that nocturnal feeding shorebirds were mostly visual foragers with great night vision (van de Kam *et al.*, 2004). The physiological structure of the eyes enables some birds to feed at night (Rojas *et al.*, 1999; R. J. Thomas *et al.*, 2006). R. J. Thomas *et al.* (2006) suggested that nocturnal foragers might not rely more on tactile sense than visual sense to search for prey. In fact, the species with fewer pits such as the pied stilt and Eurasian oystercatcher have been recorded foraging at night (Rojas *et al.*, 1999; Zwarts, Anne-Marie, & Roelof, 1990). Therefore, nocturnal feeding may not be the cause of different sensory pit numbers in different species. However, some studies suggested that the long-billed shorebirds seemed to use more tactile cues than visual cues at night (van de Kam *et al.*, 2004)—for example, shanks use more tactile ploughing than visual pecking at night (Battley *et al.*, 2003).

In summary, as in the conclusion of Chapter 2, the bill length is a major variation among different species. In addition, long head lengths seem to relate to rigid bills for powerful foraging behaviour such as breaking apart shells by oystercatchers. The variation of the sensory pit numbers is suggested to relate to phylogeny, and this idea is tested with evolutionary models in Chapter 5. Besides numbers, the distribution of the sensory pits in bill-tip organs varies with species, which may be related to their different foraging behaviours. Distal rhynchokinesis is commonly present in birds with short bill-tip organs with large numbers of sensory pits in the premaxilla. Visual cues may be critical for nocturnal foraging, while some species may feed well at night with not only visual cues but also the assistance of tactile cues. On top of that, intermediate-sized birds must be added to the species list of future study.

4 The morphological analysis of the tongues and palates, and the SEM images of the tongue tip microstructure in shorebirds

4.1 Abstract

Charadriiform shorebirds possess diverse tongue and palate forms for collecting, manipulating and swallowing food such as marine invertebrates, seeds or fish. The diversity includes macrostructures (the gross anatomy of oropharyngeal cavities) and microstructures (such as micro tongue tip spines, which have been suggested to facilitate grazing of biofilms in small shorebirds). In this study, I compared the tongue and palate morphology among 20 charadriiform shorebird species, focusing on the length of the tongue parts and the presence of micro tongue spines. Gross anatomy demonstrated that the elongated tongue body majorly contributed to the length of tongue. Tongue lengths generally increased with mandible lengths, except for the short tongue in the South Island pied oystercatcher (SIPO) (*Haematopus finschi*) and whimbrel species (*Numenius* spp.). The distances between the tongue tip and the mandible tip were short (within 1 cm) in the *Calidris* and the terek sandpiper (*Xenus cinereus*). Micro tongue tip spines were documented by scanning electron microscopy in the terek sandpiper, wood sandpiper (*Tringa glareola*), black-fronted dotterel (*Elseyornis melanops*), red-necked stint (*Ca. ruficollis*), curlew sandpiper (*Ca. ferruginea*), red knot (*Ca. canutus*) and ruddy turnstone (*Arenaria interpres*). There was a significant tendency for spines to be present in small (light) birds and species with a short distance between the tongue tip and the mandible tip. However, there was no significant association of the presence of tongue spines with the foraging behaviours of surface pecking or scything, or the presence of distal rhynchokinesis. The distribution of spines in shanks (terek sandpiper and wood sandpiper), however, was not only concentrated at the tongue tips but also spread along their long tongue bodies. This could be related to a filter feeding function associated with scything behaviour. At the same time, we cannot exclude the possibility that the micro tongue spines can be used for other functions more than just for biofilm feeding.

4.2 Introduction

Since birds do not have teeth, tongues and palates play important roles in the oropharyngeal cavity to collect, manipulate and swallow food (Erdoğan & Iwasaki, 2014; Erdoğan & Perez, 2015). The various diets among birds are highly associated with the diverse morphological features of their tongues within the floor of the mandibles (Erdoğan & Iwasaki, 2014; Erdoğan & Perez, 2015; Johnston, 2014). The adaptations of avian tongues are reflected in different lifestyles, environmental conditions, and evolutionary events (Erdoğan & Perez, 2015; Iwasaki, 2002; Iwasaki, Asami, & Chiba, 1997). The morphological variation in bird tongues include gross and microstructures among different species (Emura, 2016; Erdoğan & Iwasaki, 2014; Iwasaki, 1992).

From rostral to caudal, avian tongues generally comprise several parts: tongue tip, or *apex linguae,* which usually is composed of connective tissue and epidermal epithelium, the external keratinised (hardened) layer sometimes developing as *cuticula cornificata linguae* (lingual nail); tongue body, or *corpus linguae*, which usually is wedge-shaped, sometimes elongated, with the dorsal surface (*dorsum linguae*) of the tongue body usually having thick keratinised layer, sometimes with a median sulcus; the papillary crest at the tongue base, or *papillae linguae caudales*, which is composed of one or more transverse rows of hair-like, barb-like, or conical papillae pointing backwards for holding and transporting food; tongue wings, or *alae linguae*, giant conical papillae on each side at the tongue base, forming an inverted "V" shape, but which may be absent (Erdoğan & Perez, 2015; Iwasaki, 2002; Johnston, 2014; Rico-Guevara *et al.*, 2019). In addition, the papillae have been found on other locations such as around the choanae and near the root in the oropharyngeal cavity (Johnston, 2014; Rico-Guevara *et al.*, 2019). The function of those papillae is assumed to help with swallowing food and to prevent regurgitation (Erdoğan & Iwasaki, 2014; Erdoğan & Perez, 2015; Johnston, 2014). Gross anatomy is a general method to examine the macroscopic structure of tissues and organs, and this method has been used to describe the oropharyngeal cavity of the southern lapwing (*Vanellus chilensis*), a shorebird species within the order Charadriiformes (Erdoğan & Perez, 2015).

The shorebirds of the order Charadriiformes mainly feed on marine invertebrates on the non-breeding grounds, but some species have their own preference for other types of food such as terrestrial invertebrates, seeds or fish (Hayman, Marchant, & Prater, 1986; Hockey & Douie, 1995). Sutherland, Shepherd, and Elner (2000) indicated that western sandpiper (*Ca. mauri*) feed on epibenthic copepods and cumaceans by either pecking and/or using surface-

tension transport. Furthermore, recent studies show several functional and mechanistic evidence that western sandpiper and dunlin (*Ca. alpina*) graze biofilms as a trophic source (Beninger & Elner, 2020; Elner *et al.*, 2005; Kuwae *et al.*, 2008; Mathot, Lund, & Elner, 2010). A biofilm is a complex community, which consists of a dense mixture of bacteria and the slimy extracellular matrix secreted by the bacteria themselves (Lopez, Vlamakis, & Kolter, 2010). The extracellular matrix comprises multiple extracellular polymeric substances (EPS) such as polysaccharides, proteins, and DNA (Lopez, Vlamakis, & Kolter, 2010; Passarelli *et al.*, 2015). Biofilms have been found on many surfaces, including the surface of intertidal mudflats and sandflats (Balu *et al.*, 2020; Lopez, Vlamakis, & Kolter, 2010; Passarelli *et al.*, 2015). From a nutritional point of view, it has been suggested that biofilm feeding was a missing trophic link in shorebird food webs, especially for small birds with high metabolic rates that require high energy intake (Kuwae *et al.*, 2008; Kuwae *et al.*, 2012).

Other evidence that suggests superficial intertidal biofilm feeding in some shorebirds is the discovery of micro spines on avian tongue tips by light and scanning electron microscopy (SEM) (Elner *et al.*, 2005). It was proposed that the keratinised lateral spines with mucous around the tongue tips were suitable for adhering to the substances of biofilms (Elner *et al.*, 2005). SEM can be used to visualise the keratinised microstructures on tongues (Elner *et al.*, 2005; Erdoğan & Perez, 2015; Iwasaki, 1992; Iwasaki, Asami, & Chiba, 1997). This potential function of the micro spines at tongue tips was associated with elements from some other research (Beninger & Elner, 2020; Kuwae *et al.*, 2012). It was assumed that larger shorebirds seemed to lack tongue spines because they rely less on taking biofilms as a food source (Kuwae *et al.*, 2012). In addition, although the similar tongue structures could have evolved through convergent evolution in many species, the presence of the tongue spines seemed to be phylogenetically dependent (Johnston, 2014; Kuwae *et al.*, 2012). So far, the tongue tips of only three calidridine sandpipers—western sandpiper, dunlin and red-necked stints (*Ca. ruficollis*)—have been observed using SEM (Beninger & Elner, 2020; Elner *et al.*, 2005).

As for behaviours, surface pecking was considered a way to access to biofilm grazing with the tongue spines (Colwell, 2010; Kuwae *et al.*, 2012). The tiny bristle-like tongue spines are suitable for gathering paste-like substrates (Beninger & Elner, 2020). Besides pecking, surface tension transport feeding (STT) was also considered a way to transport the substances of biofilms along bills (Elner *et al.*, 2005; Rubega & Obst, 1993). Distal rhynchokinesis, a form of cranial kinesis that moves only the distal part of the upper jaw relative to the braincase, was suggested to enhance the efficiency of STT (Burton, 1974; Colwell, 2010; Estrella & Masero, 2007; Rubega & Obst, 1993; Zusi, 1984). It has therefore

been proposed that distal rhynchokinesis is a part of the biofilm-transporting mechanism (Elner *et al.*, 2005). However, it is still unclear whether there is a relationship between the presence of tongue spines and certain foraging strategies. It has been suggested that the scything feeding method used by avocets and some *Tringa* spp. also transports the food through STT and lingual transport (Rico-Guevara *et al.*, 2019).

Here I test if the traits of tongues and micro tongue tip spines are associated with foraging ecology and the potential biofilm feeding method across 20 species of Charadriiform shorebird. Specifically, I address how tongue length varies with bill length and phylogeny, whether the presence of micro tongue spine is related to phylogeny, bird size, bill morphology or specific foraging behaviours, and if the presence of distal rhynchokinesis is associated with the presence of micro tongue spines.

4.3 Methods

All 40 individuals in this thesis were used in this experiment.

After the specimens were taken out from the freezer and defrosted in a fridge for 1 day, the heads of birds were removed. The upper and lower jaw were dissected apart to allow the palate and tongue to be viewed. A mounted camera (Canon EOS Kiss X5 with a 50 mm or 100 mm lens) was used to take digital images of the specimens. Images of the ventral view of palates, the dorsal view of tongues within the mandible, and the dorsal and left lateral view of tongues were taken, with a scale for reference on the same plane in the image. Measurements were made in the software ImageJ, including the scale as a relative length reference (Rasband, 2020). The measurement of the lower jaw included the distance between the tongue tip and the mandible tip, the tongue length, the distance between the tongue tip and the papillary crest, and between the papillary crest and the rear of the tongue, the papillary crest width and thickness (Fig. 4.1) (Appendix 4). The measurement of the upper jaw included the palate length, the distance between the palate tip and the conical papillae, the conical papillae width, and the choanal cleft length (Appendix 4).

For scanning electron microscopy, the tongue tips were removed and soaked in a primary fixative (Modified Karnovsky's fixative (3% glutaraldehyde, 2% formaldehyde in 0.1 M phosphate buffer, pH 7.2)) for fixation overnight at room temperature. The fixative was

removed on the following day. The samples were rinsed three times (10–15 minutes each) in phosphate buffer (0.1 M, pH 7.2) and dehydrated in ascending ethanol series (25%, 50%, 75%, 95%, 100%) for 10–15 minutes each and a final 100% ethanol wash for 1 hour. The samples were further critical point dried using liquid CO_2 as the CP fluid and 100% ethanol as the intermediary (Polaron E3000 series II critical point drying apparatus). To be ready for observation, the samples were mounted on to aluminium stubs using double sided tape and sputter coated with approximately 100nm of gold (Baltec SCD 050 sputter coater). The mounted samples were observed under the FEI Quanta 200 Environmental Scanning Electron Microscope at an accelerating voltage of 20 kV.

The presence of distal rhynchokinesis was determined in Chapter 3.

I used the Shapiro-Wilk test for the normality of the data and Tukey's Ladder of Powers to transform non-normal data where normality could be achieved (Royston, 1995; Tukey, 1977).

For normally distributed data, the Pearson's correlation test was used to test the relationships between measures (distance from the tongue tip to the papillary crest and the tongue length, and between the distance from the tongue tip to the papillary crest and the distance from the papillary crest to the rear of the tongue). For comparisons involving non-normal data (the correlation between the tongue length and the mandible straight length, and between the tongue length and the distance from the tongue tip to the mandible tip), Spearman's rank correlation was used.

To test for differences in bird mass, mandible length, or the gap from the tongue tip to the mandible tip between groups of presence of micro tongue tip spines, I used t-tests on transformed (bird masses, mandible lengths and gaps from the tongue tip to the mandible tip) species averages.

To test the association of the presence of micro tongue tip spines with the presence of specific foraging behaviours (pecking or scything), and with the presence of distal rhynchokinesis, I used Fisher's exact test on two nominal variables.

Fig. 4.1: The dorsal view of the tongue within the mandible of a red knot. The yellow double-headed arrow shows the distance between the tongue tip and the mandible tip. The blue arrow shows the tongue length. The orange arrow shows the distance between the tongue tip and the papillary crest. The green arrow shows the distance between the papillary crest and the rear of tongue.

4.4 Results

4.4.1 Gross anatomy

There was a very strong positive correlation between the distance from the tongue tip to the papillary crest and the tongue length (Pearson, r = 0.99) (Fig. 4.2a), with a length gap between the bar-tailed godwit (*Limosa lapponica*) and terek sandpiper, and the other birds. There was a weaker positive correlation between the distance from the tongue tip to the papillary crest and the distance from the papillary crest to the rear of the tongue (i.e., the distal and proximal parts of the tongue; Pearson, r = 0.68) (Fig. 4.2b), with considerable interspecific variation.

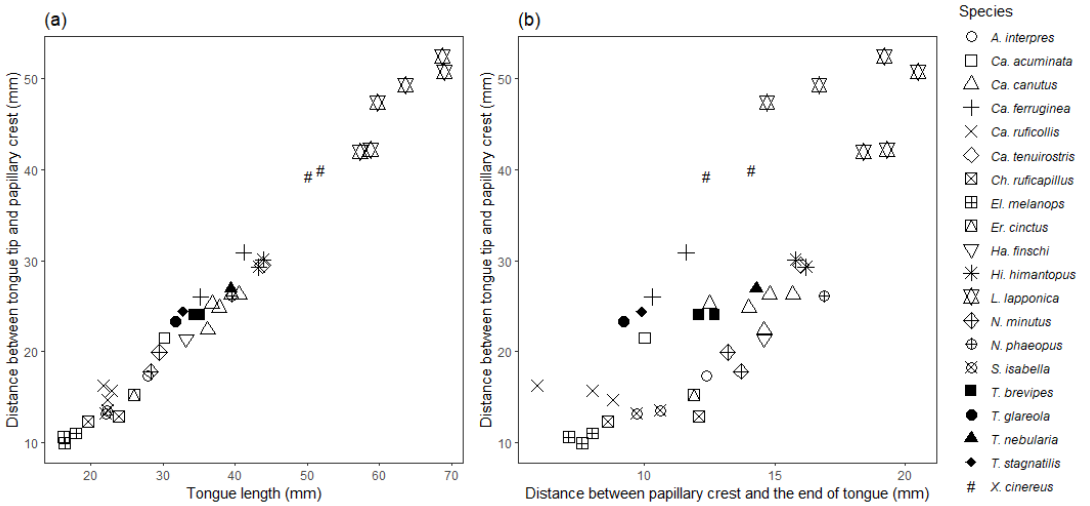

Fig. 4.2: Previous page. (a) Distance between the tongue tip and the papillary crest vs. Tongue length. (b) Distance between the tongue tip and the papillary crest vs. distance between the papillary crest and the rear of the tongue vs.

There was a strong positive correlation between the tongue length and the mandible straight length (Spearman's, ρ = 0.83) (Fig. 4.3a) but with considerable species variation between species. Similarly, there was a moderate positive correlation between the tongue length and the distance from the tongue tip to the mandible tip (Spearman's, ρ = 0.63) (Fig. 4.3b), though again with species differences.

Although the SIPO had a long bill, it had a very short tongue so the distance from the tongue tip to the mandible tip was long. The *Numenius* spp. also had short tongues compared to their bill lengths. In contrast, the *Calidris* sandpipers and the terek sandpiper had a variety of tongue lengths, but all ended within 1 cm of the bill tip.

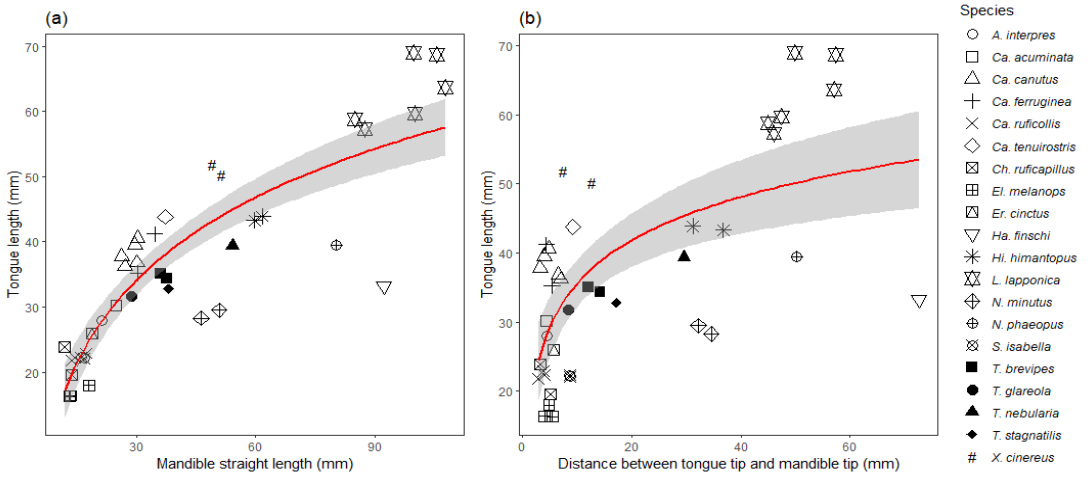

Fig. 4.3: (a) Mandible straight length vs. tongue length. (b) Distance between the tongue tip and the mandible tip vs. tongue length. The red lines are the smoothing curves (formula= y ~ log(x)) with 95% confidence interval.

The gross anatomy data are displayed in more detail in Appendix 4.

4.4.2 Micro tongue tip spines

The specimens analysed had been collected in a wide range of years, from 2004 to 2014, and had been kept frozen since collection. Hence, the tongues were not in perfect condition. Despite the concern about the freshness of the specimens, several micro tongue tip spines were successfully fixed and observed under SEM (Fig. 4.4, 4.6). The spines were present in most *Calidris* samples, including the red-necked stint, curlew sandpiper, and red knot, except the great knot (*Ca. tenuirostris*) and the sharp-tailed sandpiper (*Ca. acuminata*). The spines were also found in the terek sandpiper, wood sandpiper, black-fronted dotterel and ruddy turnstone.

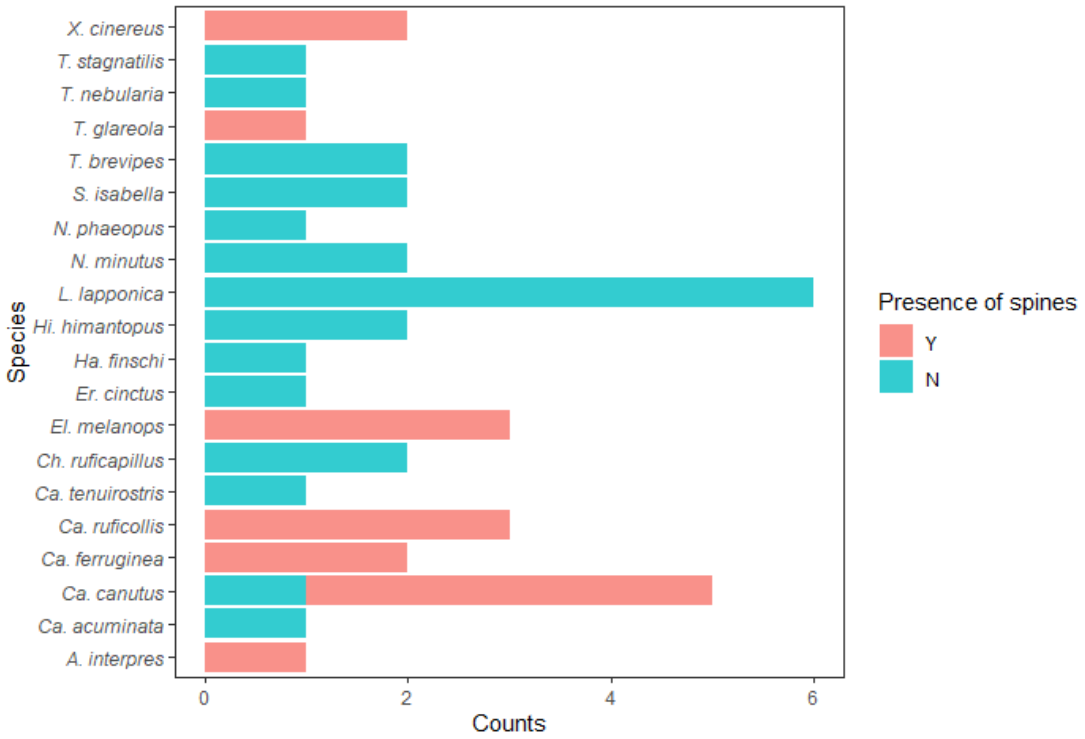

Fig. 4.4: The count (number of individuals) of the presence/absence of the micro tongue tip spines in each species.

There was a significant difference between the average bird mass of each species and the presence of micro tongue tip spines, with spines present in the species with relatively smaller (lighter) bodies (t-test on transformed species averages, $t_{13} = -2.23$, $P < 0.05$) (Fig. 4.5a).

Since the tongue was embedded in the mandible, only the mandible was used for the analysis relevant to the tongue tip spines. There was no significant difference between the average mandible length of each species and the presence of micro tongue tip spines (t-test on transformed species averages, $t_{17} = -1.77$, $P = 0.095$) (Fig. 4.5b), though there was a tendency for spines to be present in species with short bills.

The gap between the tongue tip and the mandible tip was shorter in species with tongue spines (t-test on transformed species averages, $t_{17} = -3.40$, $P < 0.005$) (Fig. 4.5c).

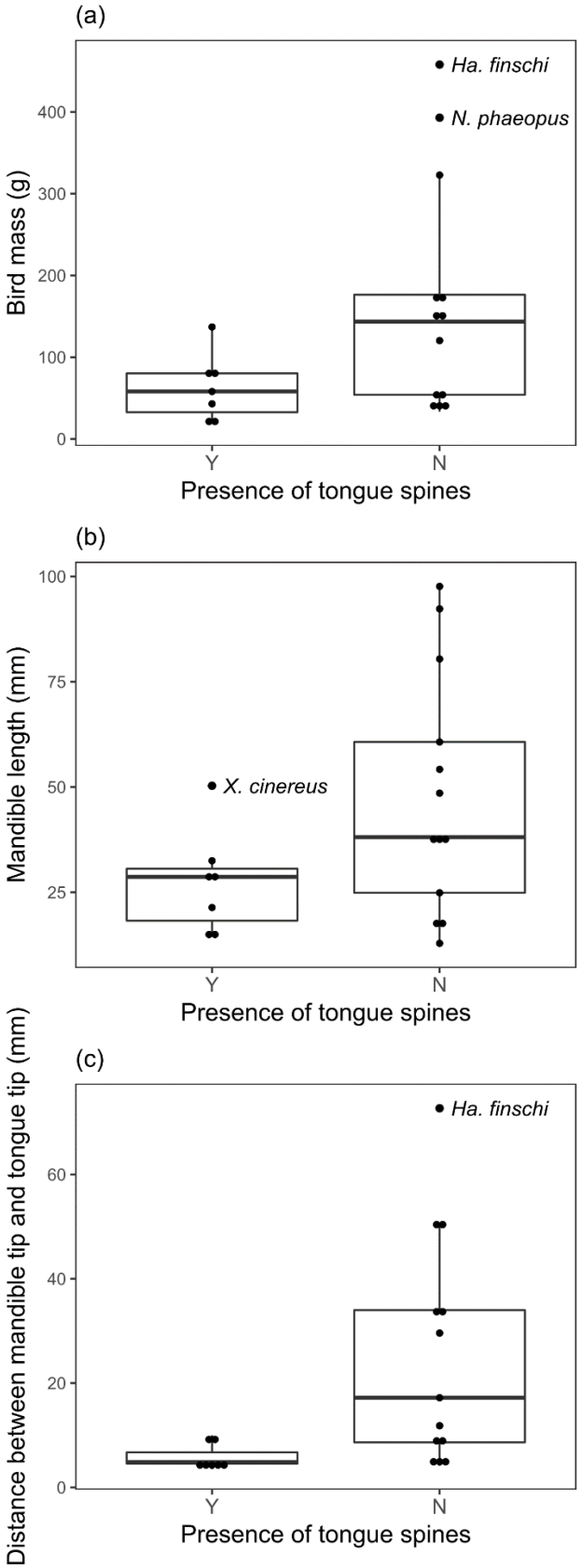

Fig. 4.5: (a) Average bird mass of each species vs. presence of micro tongue tip spines. (b) Average mandible length of each species vs. presence of micro tongue tip spines. (c) Average distance between the tongue tip and the mandible tip of each species vs. presence of micro tongue tip spines.

There was a significant association between the presence of tongue spines and the specific foraging behaviour of surface pecking (Table 4.1). However, there was no significant association between the presence of tongue spines and the foraging behaviour of scything, or the presence of distal rhynchokinesis (Table 4.1). There was no significant association between the presence of rhynchokinesis and pecking or scything foraging behaviour (Table 4.1).

Table 4.1: 2x2 Contingency tables with the Fisher's exact test P-value of the association of the presence of micro tongue tip spines with the presence of the foraging behaviour (pecking or scything), and with the presence of distal rhynchokinesis.

Micro tongue spines	**Pecking**	**No pecking**	Total	**Fisher's exact P-value**
Present	**7**	**0**	7	0.0047
Absent	**4**	**9**	13	
Total	10	10	20	
Micro tongue spines	**Scything**	**No scything**	Total	
Present	**2**	**5**	7	1.00
Absent	**3**	**10**	13	
Total	5	15	20	
Micro tongue spines	**Rhynchokinesis**	**No rhynchokinesis**	Total	
Present	**5**	**2**	7	0.35
Absent	**5**	**8**	13	
Total	10	10	20	
Distal rhynchokinesis	**Pecking**	**No pecking**	Total	
Present	**6**	**4**	10	1.00
Absent	**5**	**5**	10	
Total	10	10	20	
Distal rhynchokinesis	**Scything**	**No scything**	Total	
Present	**1**	**9**	10	0.30
Absent	**4**	**6**	10	
Total	5	15	20	

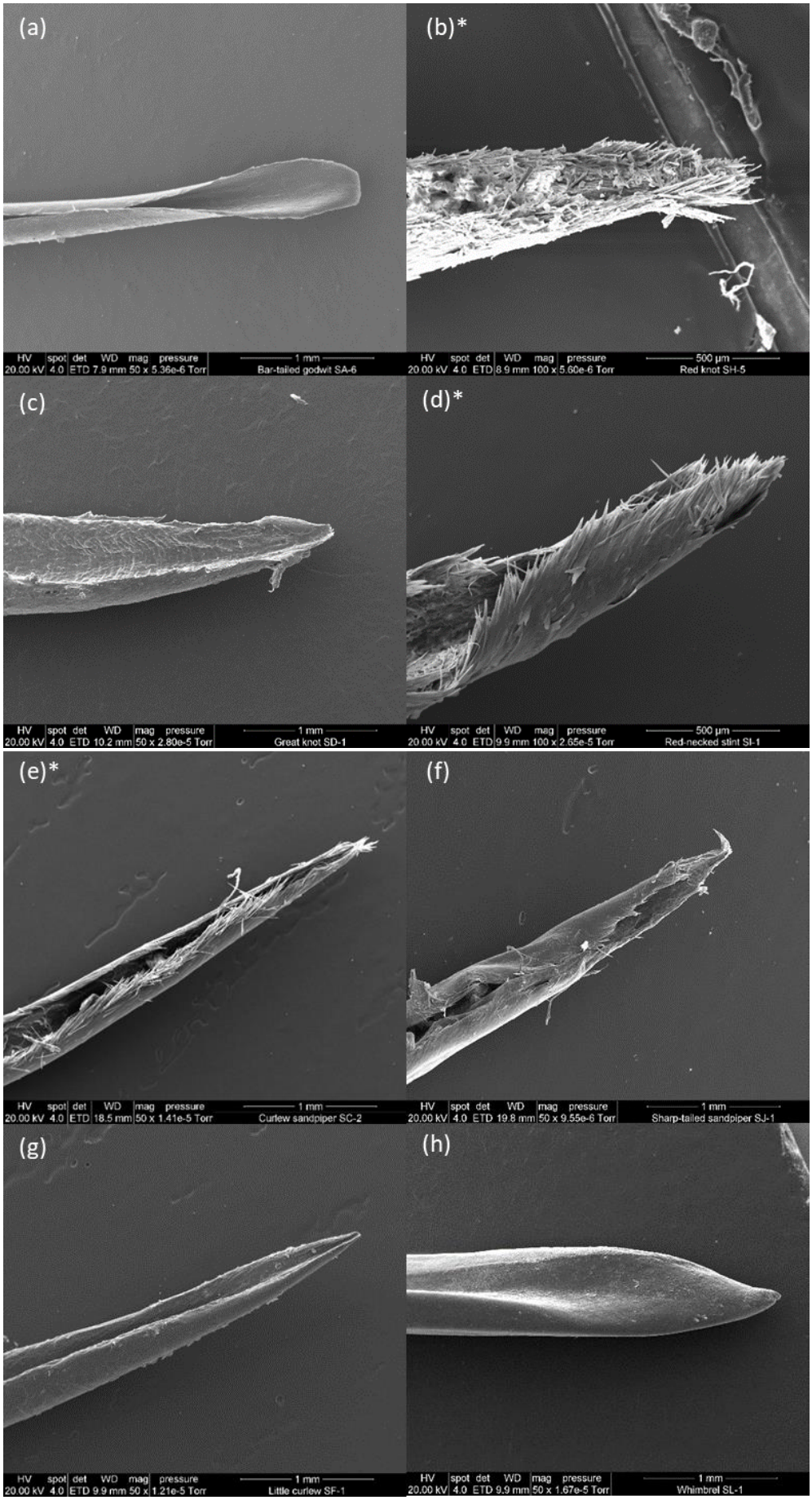
(a)
HV spot det WD mag pressure
20.00 kV 4.0 ETD 7.9 mm 50 x 5.36e-6 Torr
1 mm
Bar-tailed godwit SA-6
(b)*
HV spot det WD mag pressure
20.00 kV 4.0 ETD 8.9 mm 100 x 5.60e-6 Torr
500 µm
Red knot SH-5
(c)
HV spot det WD mag pressure
20.00 kV 4.0 ETD 10.2 mm 50 x 2.80e-5 Torr
1 mm
Great knot SD-1
(d)*
HV spot det WD mag pressure
20.00 kV 4.0 ETD 9.9 mm 100 x 2.65e-5 Torr
500 µm
Red-necked stint SI-1
(e)*
HV spot det WD mag pressure
20.00 kV 4.0 ETD 18.5 mm 50 x 1.41e-5 Torr
1 mm
Curlew sandpiper SC-2
(f)
HV spot det WD mag pressure
20.00 kV 4.0 ETD 19.8 mm 50 x 9.55e-6 Torr
1 mm
Sharp-tailed sandpiper SJ-1
(g)
HV spot det WD mag pressure
20.00 kV 4.0 ETD 9.9 mm 50 x 1.21e-5 Torr
1 mm
Little curlew SF-1
(h)
HV spot det WD mag pressure
20.00 kV 4.0 ETD 9.9 mm 50 x 1.67e-5 Torr
1 mm
Whimbrel SL-1

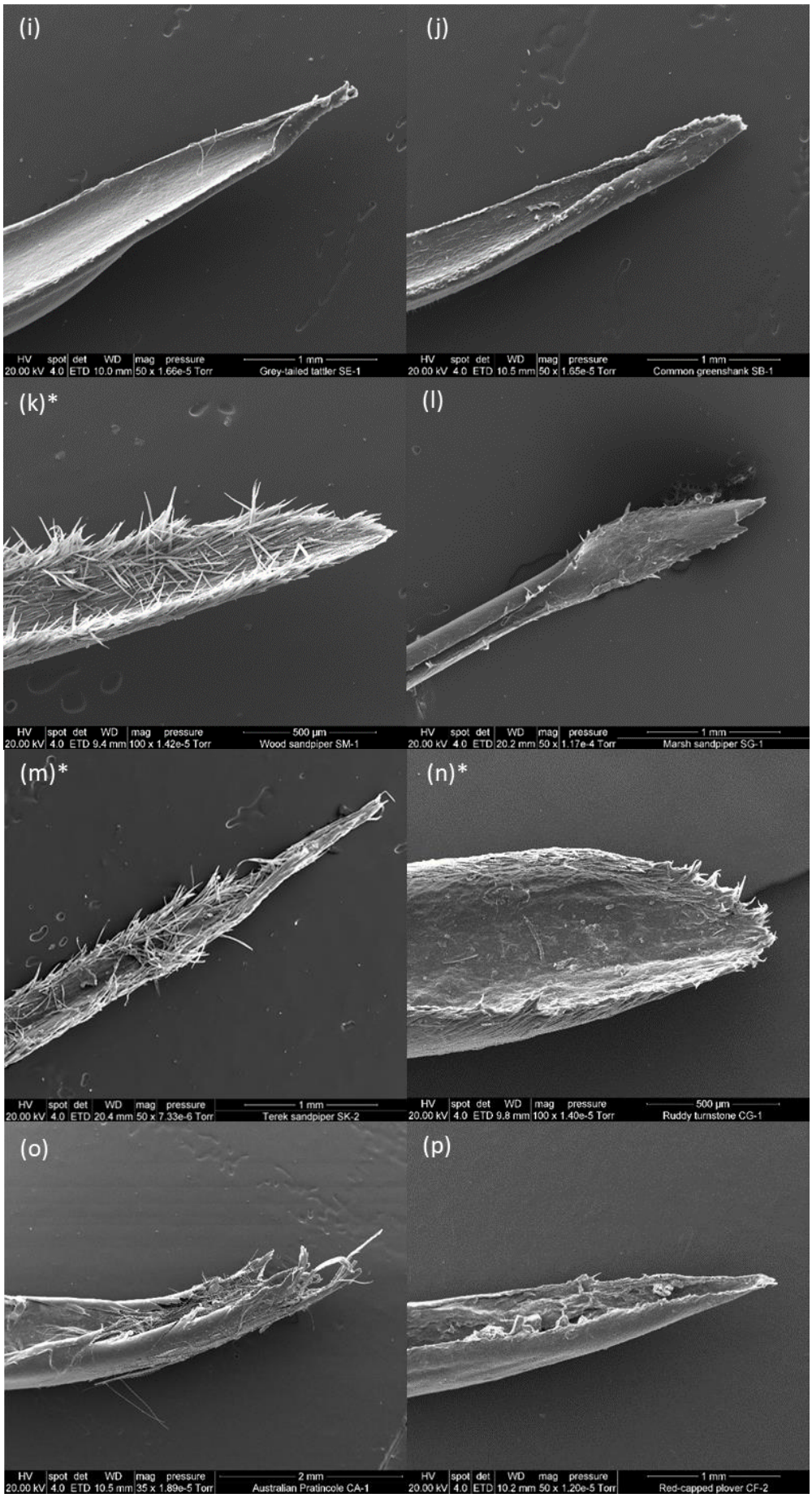
(i)
HV spot det WD mag pressure
20.00 kV 4.0 ETD 10.0 mm 50 x 1.66e-5 Torr
1 mm
Grey-tailed tattler SE-1
(j)
HV spot det WD mag pressure
20.00 kV 4.0 ETD 10.5 mm 50 x 1.65e-5 Torr
1 mm
Common greenshank SB-1
(k)*
HV spot det WD mag pressure
20.00 kV 4.0 ETD 9.4 mm 100 x 1.42e-5 Torr
500 µm
Wood sandpiper SM-1
(l)
HV spot det WD mag pressure
20.00 kV 4.0 ETD 20.2 mm 50 x 1.17e-4 Torr
1 mm
Marsh sandpiper SG-1
(m)*
HV spot det WD mag pressure
20.00 kV 4.0 ETD 20.4 mm 50 x 7.33e-6 Torr
1 mm
Terek sandpiper SK-2
(n)*
HV spot det WD mag pressure
20.00 kV 4.0 ETD 9.8 mm 100 x 1.40e-5 Torr
500 µm
Ruddy turnstone CG-1
(o)
HV spot det WD mag pressure
20.00 kV 4.0 ETD 10.5 mm 35 x 1.89e-5 Torr
2 mm
Australian Pratincole CA-1
(p)
HV spot det WD mag pressure
20.00 kV 4.0 ETD 10.2 mm 50 x 1.20e-5 Torr
1 mm
Red-capped plover CF-2

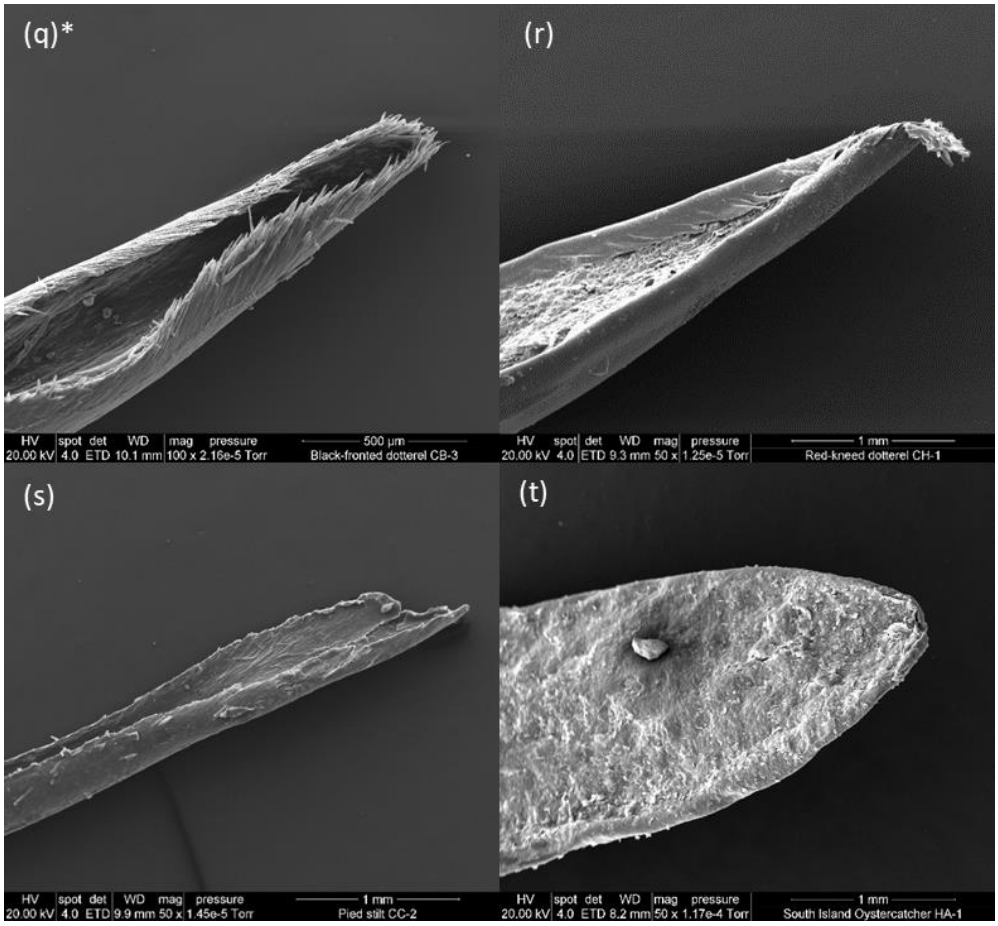

Fig. 4.6: The SEM images of the tongue tip of all the species. The samples with obvious keratinised spines are marked with asterisks. (a) Bar-tailed godwit (*L. lapponica*), (b) Red knot (*Ca. canutus*), (c) Great knot (*Ca. tenuirostris*), (d) Red-necked stint (*Ca. ruficollis*), (e) Curlew sandpiper (*Ca. ferruginea*), (f) Sharp-tailed sandpiper (*Ca. acuminata*), (g) Little whimbrel (*N. minutus*), (h) Whimbrel (*N.phaeopus*), (i) Grey-tailed tattler (*T. brevipes*), (j) Common greenshank (*T. nebularia*), (k) Wood sandpiper (*T. glareola*), (l) Marsh sandpiper (*T. stagnatilis*), (m) Terek sandpiper (*X. cinereus*), (n) Ruddy turnstone (*A. interpres*), (o) Australian pratincole (*S. isabella*), (p) Red-capped plover (*Ch. ruficapillus*), (q) Black-fronted dotterel (*El. melanops*), (r) Red-kneed dotterel (*Er. cinctus*), (s) Pied stilt (*Hi. himantopus*), (t) South Island pied oystercatcher (SIPO) (*Ha. finsch*).

4.5 Discussion

Although there are concerns about post-mortem tissue changes, the change of body length measurements at autopsy is generally considered quite small (McCormack *et al.*, 2016). In my study, the tongues were flexible and not dehydrated when dissected, and no gross post-mortem artefacts were evident. At the micro-scale (tongue tips) some tongues possibly did have some damage, but the SEM images (Fig. 4.6) suggest this was not a widespread problem.

Generally speaking, the gross structures of the shorebird tongues and palates in this study are similar to the descriptions in the previous studies of the black-necked stilt (*Himantopus mexicanus*) (Emura, 2016), southern lapwing (Erdoğan & Perez, 2015), and other charadriiform shorebirds (Johnston, 2014; Rico-Guevara *et al.*, 2019). In most bird species the tongue bodies are elongated with the tongue lengths (Fig. 4.2), and the papillae are distributed behind the tongue body forming an inverted "V" shape at the tongue base and around the choanal cleft, as expected to properly manipulate the food and prevent regurgitation (Erdoğan & Perez, 2015; Johnston, 2014; Rico-Guevara *et al.*, 2019). One interesting finding is the short tongue in the SIPO. The short tongue length has also been mentioned in Eurasian oystercatchers (*Ha. ostralegus*) (Hulscher, 1982). It may be related to the robust bill of oystercatchers for breaking bivalves because a long tongue may limit the hardness of the bill and hence the power of it (Dowding, 2022; Medway, 2000). Similarly, the *Numenius* spp. also had short tongues, which is considered a consequence of their heavily reinforced bills (Davidson *et al.*, 1986). As for the distance between the tongue tip and the mandible tip, the similar short distances in *Calidris* and the terek sandpiper implies a certain foraging strategy among them. The short distance between the bill tip and the tongue tip allows tongues to touch and transport the prey quickly (van de Kam *et al.*, 2004).

Despite concerns about the freshness of the specimens, the SEM results still provide useful information. My study documented the first evidence of tongue spines in the black-fronted dotterel and curlew sandpiper. Compared with the observation of Kuwae *et al.* (2012) using optical microscopes, my result also suggests that the tongue tip spines were commonly present in shanks (*Tringa* spp.) and *Calidris* spp. (especially red knots, four from five samples), but not in godwits or whimbrels (Table 4.2). As for plovers, the spines were common in the study of Kuwae *et al.* (2012) and were documented in the wrybill (*Anarhynchus frontalis*) by Withington (2015), but they were only discovered in one out of

three species in this study (in the black-fronted dotterel, but not in the red-capped plover (*Charadrius ruficapillus*) or red-kneed dotterel (*Erythrogonys cinctus*)) (Table 4.2). Conversely, Kuwae *et al.* (2012) documented spines in the grey-tailed tattler (*T. brevipes*), common greenshank (*T. nebularia*), marsh sandpiper (*T. stagnatilis*), great knot (*Ca. tenuirostris*), and sharp-tailed sandpiper (*Ca. acuminata*), but these were not found in my results. However, the absence of the spines in those species cannot be confirmed because of the deterioration and small samples in my study. Specifically, the common greenshank (none in this study; two from five samples in Kuwae *et al.* (2012)) will need a further check. The size of the tongue spines in the SEM images suggests that they are applied for filtering or sticking to the prey that is much smaller than benthic invertebrates (Fig. 4.6) (Beninger & Elner, 2020; Elner *et al.*, 2005).

Table 4.2: Presence/absence of tongue spines in different shorebirds, summarised from different studies. Numbers represent the number of individuals confirmed with spines / the number checked. Note that my study and Withington (2015) use SEM from specimens, whereas Kuwae *et al.* (2012) is based mostly on digital photography of live birds.

Species		This study	(Withington, 2015)	(Kuwae et al., 2012)
Sandpipers				
Red-necked stint	*Calidris ruficollis*	3/3		19/19
Sharp-tailed sandpiper	*Ca. acuminata*	0/1		4/4
Red knot	*Ca. canutus*	4/5		1/1
Great knot	*Ca. tenuirostris*	0/1		4/4
Curlew sandpiper	*Ca. ferruginea*	2/2		
Ruddy turnstone	*Arenaria interpres*	1/1		7/7
Shanks and Terek sandpiper				
Wood sandpiper	*Tringa glareola*	1/1		1/1
Marsh sandpiper	*T. stagnatilis*	0/1		2/2
Common greenshank	*T. nebularia*	0/1		2/5
Grey-tailed tattler	*T. brevipes*	0/2		5/5
Terek sandpiper	*Xenus cinereus*	2/2		14/14
Godwits and Curlews				
Bar-tailed godwit	*Limosa lapponica*	0/6		0/1
Whimbrel	*Numenius phaeopus*	0/1		0/1
Little whimbrel	*N. minutus*	0/2		
Plovers				
Black-fronted dotterel	*Elseyornis melanops*	3/3		
Red-capped plover	*Charadrius ruficapillus*	0/2		
Red-kneed dotterel	*Erythrogonys cinctus*	0/1		
Wrybill	*Anarhynchus frontalis*		1/1	
Stilts				
Pied stilt	*Himantopus himantopus*	0/2		
Oystercatcher				
South Island oystercatcher	*Haematopus finschi*	0/1		
Pratincole				
Australian pratincole	*Stiltia isabella*	0/2		

Kuwae *et al.* (2008) and Kuwae *et al.* (2012) suggested that biofilm grazing tended to be used by small birds, which needed a high amount of food intake to cope with their high metabolic rates. Thus, it has been suggested that the tongue tip spines for biofilm grazing were present in small birds (Kuwae *et al.*, 2012); my result supports that idea by finding that birds with spines were significantly lighter than those without (Fig. 4.5a). The terek sandpiper is the heaviest bird in my study with the micro tongue spines. If the common greenshank and great knot are presumed to have the micro tongue spines (Kuwae *et al.*, 2012), they would be the heaviest birds with the spines in these studies. However, the size of the common greenshank and great knot are similar to the pied stilt (*Hi. himantopus*) and little whimbrel (*N. minutus*), which do not have the spines. Therefore, there is no clear boundary of the bird mass between the birds with and without the micro tongue spines.

It has been suggested that biofilms were grazed by the surface pecking behaviour with bristle-like tongue spines (Beninger & Elner, 2020; Colwell, 2010; Kuwae *et al.*, 2012). The pecking behaviour is often used by the birds with straight short to medium length bills such as plovers, *Tringa* and *Himantopus* (Burton, 1974). Although my result does not show a significant difference in the mandible length between the birds with and without micro tongue tip spines, Figure 4.5b indicates that the spines were not detected in the birds with longer bills, except for the terek sandpiper with medium length mandibles. While there was a significant association for species with spines to use pecking when foraging (Table 4.1), pecking was also used by species without spines. Pecking is a form of visual foraging that may result from detection of specific prey items on the sediment surface, so the function of pecking behaviour is not just for biofilm grazing. Other foraging behaviour like sewing in red knots and red-necked stints may bring them constant supply of sediment with biofilms. However, with no micro tongue spines, male bar-tailed godwits with bills shorter than females predominantly use sewing to catch mud snails (Ross, 2018).

Biofilm grazing would require birds' tongues to contact the mud surface, so tongues that reach towards the end of the bill may provide greater ability to trap and transport sediment containing biofilm. Therefore, I measured the distance from the tongue tip to the mandible tip. Consistent with this idea, the species that had tongue spines also had smaller gaps between the tongue tip and the bill tip than the species without micro tongue spines (Fig. 4.5c).

There were species differences in the micro tongue spines form and distribution. Spines in the terek sandpiper and wood sandpiper were distributed not only at the tips but also along

their long tongue bodies (Fig. 4.6k,m). This implies that pecking may not be the only behaviour for the birds to access biofilms. In addition to pecking, most shanks use the scything foraging behaviour by swinging their bills from side to side in water or mud (Hockey & Douie, 1995; Rico-Guevara *et al.*, 2019). Therefore, the spines spreading along the tongue body may function as biofilm collectors when scything in sediment. Scything is also known from three species that did not have spines in my dataset (common greenshank, marsh sandpiper and pied stilt), though Kuwae *et al.* (2012) documented spines in two of those species (the shanks, though not in all individual common greenshanks they photographed). The morphology of tongues with tiny spines along the sides is similar to the tongues of certain filter feeding birds (Johnston, 2014), and it has been suggested that the wrybill, a plover known to ingest both sediment and biofilm, may do so via a tongue with a fringe of spines similar to those discussed here (Withington, 2015) (Table 4.2).

Moreover, if the scything behaviour is associated with biofilm feeding, the distance between the mandible pit and the tongue tip may be less important than with pecking behaviour because the bill is submerged for scything. This may reflect my result that *Tringa* have slightly longer distances between the mandible pit and the tongue tip compared to the other species with spines (Fig. 4.3b). There are a couple of different methods for filter feeding, and the scything behaviour is considered one of them (Johnston, 2014). On the other hand, scything may also be applied for different functions because there are birds like the pied stilt that scythe to forage without tongue spines (Hockey & Douie, 1995).

It has been suggested that surface tension transport (STT) increases the feeding efficiency of both pecking and scything (Rico-Guevara *et al.*, 2019; Rubega & Obst, 1993). The smooth lingual apex and the middle groove along the tongue body in many shorebirds also imply the usage of STT (Emura, 2016). In addition, distal rhynchokinesis has been considered a part of biofilm feeding through pecking (Elner *et al.*, 2005). My results show that more species with micro tongue spines show distal rhynchokinesis than with no rhynchokinesis, but also that rhynchokinesis is spread evenly across species with or without tongue spines (Table 4.1). Also, there was no association between surface pecking and distal rhynchokinesis (Table 4.1). On the other hand, only one species, the terek sandpiper, uses both scything and has distal rhynchokinesis. In summary, distal rhynchokinesis may relate to not only pecking but also other functions. However, the scything behaviour seems to rely less on distal rhynchokinesis.

Although my study provides more morphological evidence that supports the presumed role in biofilm feeding in certain shorebirds, it is worth noting that there seem to be different

types of tongue tip spines, and some of them actually look like the ‘acicular projections’ at the lingual nail tip that have been mentioned in the hooded crow (*Corvus cornix*), Galliformes, and some passerines (Elsheikh & Al-Zahaby, 2014; Erdoğan & Perez, 2015; Johnston, 2014). The acicular projections are keratinised processes suggested to better hold insects and worms (Erdoğan & Perez, 2015). It was also mentioned that the function of tongue spines was not limited to biofilm scraping, but for adapting to different niches (Kuwae *et al.*, 2012). For example, the ruddy turnstone does surface pecking, but it also feeds on a variety of food and may apply the micro tongue tip spines in multiple feeding ways (Hayman, Marchant, & Prater, 1986; Hockey & Douie, 1995). More analyses of the keratinised structures and studies from different perspectives will be needed to clearly understand their functions.

5 Phylogenetic tests

5.1 Abstract

Morphological variation in the feeding apparatuses of charadriiform shorebirds may be the evolutionary result of relatively rapid adaptation over short evolutionary timescales. In this study, three traits—total sensory pit numbers, presence of micro tongue tip spines, and presence of distal rhynchokinesis—were tested with a partial phylogeny of charadriiform shorebirds to explore hypotheses about their evolution under different models. The partial phylogeny was tested with the lambda transformation to determine if there was a signal supporting phylogenetic dependency. The results demonstrate that the data of average total sensory pit numbers better fits the Brownian motion model than the Pagel's lambda model. The Scolopacidae clade has increased the number of sensory pits in the bill-tip organ, which could be the result of constant accumulation of random trait variance. The taxonomic distribution of micro tongue tip spines across charadriiform shorebirds was best explained by a model where the spines might be gained or completely lost at equal rates through evolutionary time (i.e. an equal-rates (ER) likelihood model). With significant evidence of phylogenetic signal, the spines could be absent at the root and have evolved twice separately because of the equal transition rates of the trait. The presence of distal rhynchokinesis was best explained by an evolutionary model where the loss of this trait occurred more rapidly that it was gained (i.e. all-rates-different (ARD) model).

5.2 Introduction

It has been suggested that the taxonomic distribution of some morphological traits in Charadriiformes are related to the evolution of particular foraging strategies (Barbosa & Moreno, 1999; Hughes, 2015). For example, Hughes (2015) showed that supraorbital ossification (SO) has evolved at least four or five times in charadriiform shorebirds, and is considered independent adaptation. Barbosa and Moreno (1999) demonstrated the evolutionary relationships between the bill length and the foraging behaviours. Some shorebirds possess specific traits such as sensory pits on bills, micro tongue tip spines, and distal rhynchokinesis of bills (Colwell, 2010; Elner *et al.*, 2005; Estrella & Masero, 2007).

The sensory pits are small cavities with nerve endings, which may be clustered into bill-tip organs (Cunningham *et al.*, 2013; Piersma *et al.*, 1998). Bill-tip organs with various pit numbers have been found in the families Scolopacidae (Charadriiformes), Apterygidae (Apterygiformes), and Threskiornithidae (Pelecaniformes) (Cunningham *et al.*, 2010; Cunningham *et al.*, 2013). Even charadriiform shorebirds have various sensory pit numbers (Cunningham *et al.*, 2013). Hence, the evolution of the sensory pit numbers is considered to have occurred independently in those clades (Cunningham *et al.*, 2013).

Keratinised micro tongue tip spines have been described in some shorebirds recently (Elner *et al.*, 2005) and has been suggested to function as biofilm collectors in small birds (Beninger & Elner, 2020; Elner *et al.*, 2005; Kuwae *et al.*, 2012). Kuwae *et al.* (2012) documented micro tongue spines in different shorebird species based on optical microscope images and a few SEM samples, and their phylogenetic analyses suggested that the evolution of the micro tongue spines was phylogenetically dependent.

Distal rhynchokinesis is a term to describe the relative movement of the distal part of the mandible in some birds, including shorebirds (Zusi, 1984). The function of distal rhynchokinesis is controversial. In some studies, it was regarded as a grabbing tool in long bills, but it was also considered to have a role to enhance surface tension transport feeding (Estrella & Masero, 2007; Zusi, 1984). The evolution of distal rhynchokinesis in shorebirds is unclear (Estrella & Masero, 2007).

There are several conceptual models of trait evolution relevant to these issues. The Brownian motion model describes a process in which the trait value changes randomly with a constant multivariate mean over time (Cavalli-Sforza & Edwards, 1967; G. H. Thomas & Freckleton, 2012). It assumes that the phylogenetic tree displays the evolutionary result of

the constant accumulation of covariances from root to tips (Cavalli-Sforza & Edwards, 1967; G. H. Thomas & Freckleton, 2012). Therefore, the tips share the trait from the same ancestor, and the clade evolves independently (Cavalli-Sforza & Edwards, 1967; G. H. Thomas & Freckleton, 2012).

The Pagel's lambda model measures the phylogenetic signal λ (Pagel, 1999; G. H. Thomas & Freckleton, 2012). Phylogenetic signal is a term to describe the tendency of related species to resemble each other more than random development on a phylogenetic tree (Münkemüller *et al.*, 2012). Low phylogenetic signal indicates low phylogenetic influence on trait evolution, i.e. λ = 0 means that the trait has evolved independently of phylogeny (Kamilar & Cooper, 2013; G. H. Thomas & Freckleton, 2012), whereas high phylogenetic signal means the shared history of clades has driven trait distributions (Münkemüller *et al.*, 2012; G. H. Thomas & Freckleton, 2012). λ = 1 indicates strong phylogenetic signal associated with the Brownian motion model of evolution (Kamilar & Cooper, 2013; Münkemüller *et al.*, 2012; G. H. Thomas & Freckleton, 2012).

The equal-rates (ER) model has a same transition rate parameter across the phylogeny, which means a trait can be gained or lost along a lineage at the same rate, whereas the all-rates-different (ARD) model has different parameter of each transition rate, which means a trait can be lost at a faster rate than they are gained, and vice versa (Pennell *et al.*, 2014).

In this study, I address if the phylogenetic patterns of morphological trait variation within my shorebird samples are consistent with random (Brownian motion) or non-random (Pagel's lambda) variance, and equal (ER) or unequal (ARD) evolution. Specifically, I test whether Brownian motion model or Pagel's lambda model best fits to the trait evolution of total sensory pit numbers, and whether the ER or ARD model best fits to the evolution of presence of micro tongue spines and distal rhynchokinesis among shorebirds.

To test the phylogenetic signal of those traits, the R package "Models of trait macroevolution on trees (MOTMOT)" of G. H. Thomas and Freckleton (2012) was used for the continuous character (total sensory pit numbers), and the R package "geiger" of Pennell *et al.* (2014) was used for the discrete character (presence of micro tongue tip spines and distal rhynchokinesis) to evaluate phylogenetic branch lengths in relation to the evolutionary model (Burnham & Anderson, 2002). The evolutionary models describe and analyse the similarities and differences among phylogenetic trees (Cavalli-Sforza & Edwards, 1967). With this approach I could test my results of the morphological trait from Chapters 2–4 with molecular phylogenetic analyses of the Charadriiformes (Mayr, 2011).

5.3 Methods

The data of three specific traits among the shorebirds—average total sensory pit numbers, presence of micro tongue tip spines, and presence of distal rhynchokinesis—were selected from the previous chapters for the phylogenetic signal test. To compensate for sample deterioration and resultant small sample sizes in the micro tongue tip spine section of this study, I combined my data with the results of presence/absence of tongue spines in different shorebird species under optical microscopes of Kuwae *et al.* (2012) (Table 4.2).

The subsets of species in this study were output from the accompanying website (Jetz *et al.*, 2012, 2014). The phylogenetic tree (consensus of 100 trees) was built using the R package ape (version 5.6-2) to access the operational taxonomic units (OTUs) subsets from Jetz *et al.* (2012) and the package phytools (version 1.0-1) to mark and label the tree (Paradis & Schliep, 2019; Revell, 2012). The tree also referred to the phylogenetic result of multiple gene sequences (Gibson & Baker, 2012) and other taxonomic studies (Christian, Christidis, & Schodde, 1992; Mayr, 2011).

To model the continuous character along the sample of 100 phylogenetic trees, the R package "MOTMOT" (version 2.1.3) was used to test which model better fit the trait evolution of sensory pit numbers (G. H. Thomas & Freckleton, 2012). The Brownian motion model and Pagel's lambda model were tested with the phylogenetic tree by comparing the distribution of the chi-squared of likelihood and the second-order Akaike's Information Criterion (AICc) difference between the two models (Burnham & Anderson, 2002). The Brownian motion model was set as the null hypothesis.

To model the discrete character along the sample of 100 phylogenetic trees, the R package "geiger" (version 2.0.10) was used to test which model better fit the trait evolution of presence of micro tongue tip spines and distal rhynchokinesis (Pennell *et al.*, 2014). The ER and ARD models were tested with the phylogenetic tree by comparing the second-order Akaike's Information Criterion (AICc) difference between the two models (Burnham & Anderson, 2002). The models were also tested by fitting the lambda transformation to determine if there was any strong phylogenetic signal (Pagel, 1999; Pennell *et al.*, 2014). The model with no phylogenetic signal was set as the null hypothesis. The best evolutionary model would be used to estimate probabilities that the trait was present or absent in each ancestor of the phylogeny. The probabilities for the trait being present or absent (as

calculated by the ancestral state reconstruction) were displayed in as pie charts at each node.

5.4 Results

The test result indicated that the pattern of average total sensory pit numbers fits the Brownian motion model better than the Pagel's lambda model (average Chi-square test, P = 0.88). The result of the AICc difference also indicated that the Brownian motion model with smaller AICc better fits the data (average AICc difference = -1.47). The phylogeny shows the largest numbers of sensory pits in the Scolopacidae clade (Fig. 5.1).

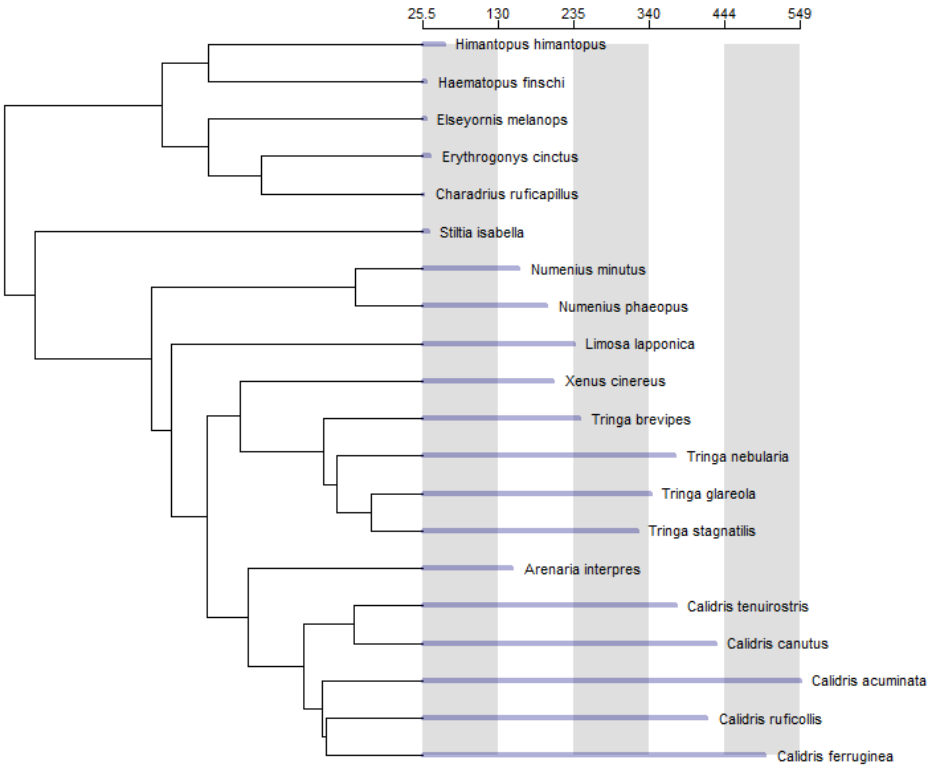

Fig. 5.1: The phylogenetic tree of the charadriiform birds in this study with the distribution of average total sensory pit numbers. This phylogenetic tree was built using the operational taxonomic units (OTUs) from (Jetz *et al.*, 2012) with reference to the phylogenetic result of multiple gene sequences (Gibson & Baker, 2012) and other previous studies (Christian, Christidis, & Schodde, 1992; Mayr, 2011). Bars and the scale show the average total sensory pit numbers of each species.

The test result indicated that the ER model provides the best explanation here for the pattern of presence of micro tongue tip spines. The phylogeny displayed the presence of the tongue spines in the black-fronted dotterel (*Elseyornis melanops*), and the clade containing shanks, terek sandpiper (*Xenus cinereus*), ruddy turnstone (*Arenaria interpres*), and calidrid sandpipers (Fig. 5.2). The lambda test suggested that there was phylogenetic signal in the taxonomic distribution of this trait (average Chi-square test, $P < 0.005$).

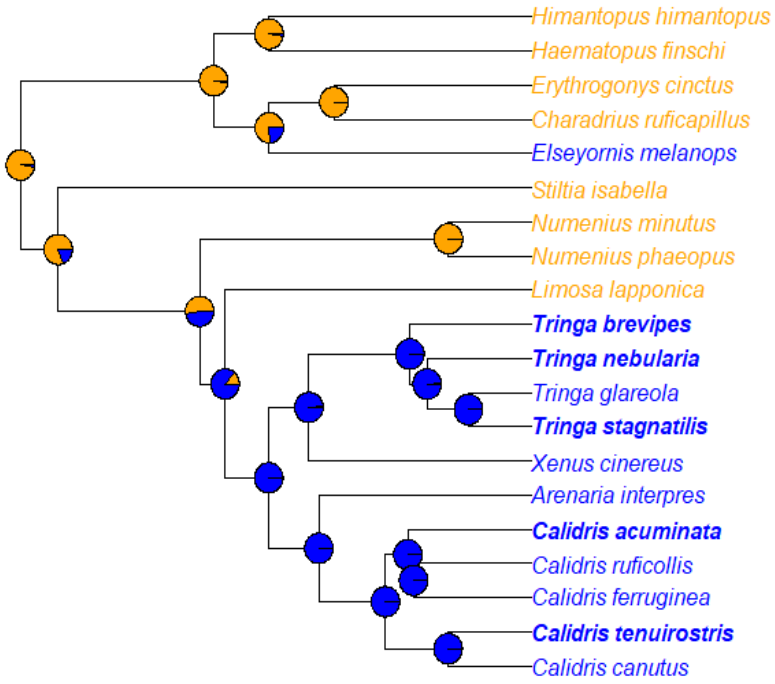

Fig. 5.2: The phylogenetic tree with the distribution of presence of micro tongue tip spines documented by SEM images in each species (blue tips are present and orange tips are absent; blue bold tips combine the document of Kuwae *et al.* (2012)). Pie charts indicate the likely state for those theoretical ancestors on the nodes.

The test result indicated that the ARD model provides the best explanation here for the pattern of presence of distal rhynchokinesis. The phylogeny displayed the presence of the rhynchokinesis in two plover species, little whimbrel (*Numenius minutus*), bar-tailed godwit (*Limosa lapponica*), terek sandpiper, and calidrid sandpipers (Fig. 5.3). The lambda test suggested that the evolutionary pattern here was not dominated by phylogenetic signal (average Chi-square test, P = 0.08).

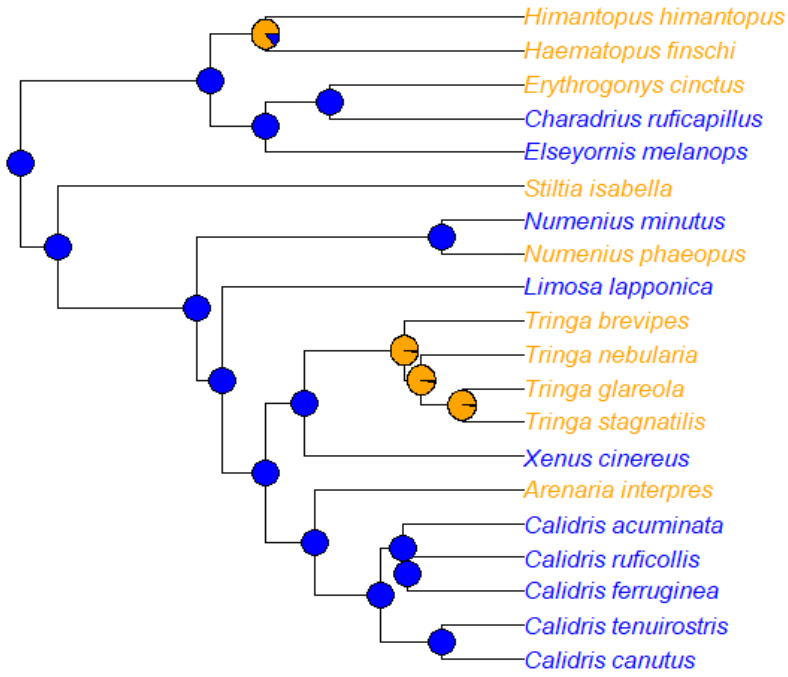

Fig. 5.3: The phylogenetic tree with the distribution of presence of distal rhynchokinesis in each species (blue tips are present and orange tips are absent). Pie charts indicate the likely state for those theoretical ancestors on the nodes.

5.5 Discussion

The presence of sensory pits is likely an ancestral condition for all species studied because all species had them. However, the Brownian motion model suggests that the largest sensory pit numbers of the bill-tip organ have evolved in the most recent common ancestor to Scolopacidae (Fig. 1.1, 5.1) (Cavalli-Sforza & Edwards, 1967). Based on the taxonomic distribution of sensory pit numbers as represented here, the relatively small numbers in *Numenius*, *Limosa,* and *Xenus*, medium number in *Tringa*, and large numbers in *Calidris,* could be the result of constant accumulation of random trait variance suggested by the Brownian motion model (Cavalli-Sforza & Edwards, 1967; G. H. Thomas & Freckleton, 2012) (Fig. 5.1). Descendants of every ancestral node may gain or lose a trait by its variance, and the quantitative trait can be accumulated over time (Cavalli-Sforza & Edwards, 1967). Although the short branches of the Scolopacidae implies recent evolution, the evolutionary rate of the bill morphology in the Scolopacidae has been suggested to be relatively rapid among shorebirds (Barbosa & Moreno, 1999). The relatively small sensory pit numbers in the ruddy turnstone, a species with several special foraging strategies, could be a result of rapid decline (Hayman, Marchant, & Prater, 1986; Hockey & Douie, 1995). The quick gain and loss of the trait might be highly associated with ecological foraging behaviours (Barbosa & Moreno, 1999). It is also possible that the evolution of the ruddy turnstone was not rapid and long enough, since its sensory pit numbers are close to the number of *Numenius*.

In addition to Scolopacidae, bill-tip organs have been discovered in kiwi (Apterygidae) and ibises (Threskiornithidae) (Cunningham *et al.*, 2010; Cunningham *et al.*, 2013). Different taxa might have evolved the organs through convergent evolution from similar selection pressures. Similarly, within other archosaurs it has been proposed that crocodilians have integumentary sensory organs (ISOs)—tiny (0.2–1.2 mm) dome-shaped spots with mechanoreceptors on their skin—to help them detect prey with tactile cues in water (Schneider, Gracheva, & Bagriantsev, 2016). However, despite the external structures similar to the bill tip organ of birds, ISOs are considered unique complex sensory nervous systems in semi-aquatic crocodylians (Di-Poï & Milinkovitch, 2013). Furthermore, a bill-tip organ has been documented in the fossil of an extinct palaeognathous bird in the family Lithornithidae in the Cretaceous (du Toit, Chinsamy, & Cunningham, 2020). There was also evidence of mechanoreceptors within foramina, likely occupied by Herbst corpuscles or similar ISOs, on the distal portion of rostra for tactile foraging early in the non-avian theropods (Carr *et al.*, 2017) and pterosaurs (Martill *et al.*, 2021) in the Cretaceous. More studies of genetics,

neuroscience and palaeontology will be required to clarify the evolutionary history of the sensory pits.

The ER (equal-rates) model is the simplest evolutionary model that fits the taxonomic distribution of presence of micro tongue tip spines. The phylogeny with ancestral state reconstruction showed that the spines were likely absent at the root and gained twice separately. The spines have never been lost after they have been gained. It is suggested that shanks, terek sandpiper, ruddy turnstone, and calidrid sandpipers share a common ancestor that had spines. The strong phylogenetic signal also suggests that the trait in the descendent is associated with this common ancestor. This is consistent with the idea of phylogenetic dependency of Kuwae *et al.* (2012). It seems that the spines have evolved independently in plovers and in the clade of sandpipers. The spines have also been documented in some other plover species (Kuwae *et al.*, 2012; Withington, 2015). However, the possibility of sister clades with a shared derived trait cannot be excluded.

The ARD (all-rates-different) model is a more complex model than the ER model to fit the taxonomic distribution of presence of distal rhynchokinesis. The phylogeny with ancestral state reconstruction showed that rhynchokinesis was likely present in the common ancestor to all the species and has been lost two to six times in this study. It is suggested that the rhynchokinesis has been lost in an ancestor to pied stilt (*Himantopus himantopus*) and South Island pied oystercatcher (SIPO) (*Haematopus finschi*), in an ancestor to *Tringa*, and again separately in ancestors to black-fronted dotterel, Australian pratincole (*Stiltia isabella*), whimbrel (*Numenius phaeopus*), and ruddy turnstone. There is no significant evidence of phylogenetic signal, so it is likely that the trait has been lost multiple times independently. Because the rhynchokinesis has never re-appeared after it has been lost, the ARD model provides an explanation that the different transition rates might relate to the fact that the trait is lost faster than it is gained. Previous studies have proposed different potential functions of distal rhynchokinesis, such as grabbing and enhancing feeding efficiency with the surface tension transport (STT) feeding (Elner *et al.*, 2005; Estrella & Masero, 2007; Zusi, 1984). Therefore, it is possible that different species have retained distal rhynchokinesis for different purposes. Estrella and Masero (2007) also suggested that distal rhynchokinesis broadens the habitat types the species can feed in.

The fact that different traits of this study better fit to different evolutionary models raises the possibility of interactions between these traits in the adaptations to different dietary niches, leading to the complex foraging strategies among shorebirds. To explore more about

the evolution of feeding apparatuses in shorebirds, future studies will be needed to investigate how variation in these morphological traits affects feeding and to build larger and more robust data sets, better with fossil records for complete phylogeny and model testing. The study of the function and mechanism of the micro tongue tip spines in different species is also needed.

6 General discussion

6.1 Morphological traits

6.1.1 Gross measurements of bodies (shape, length and size)

My results demonstrate that geometric morphometrics can provide useful information for analysing the major interspecific variation of skull shape. The selection of the views and landmarks is crucial to the questions we would like to answer. In this study, the results of the dorsal and right lateral views provide relatively more information than the ventral view in regard to foraging strategy. The geometric morphometrics results indicate that the bill length was the major interspecific variation of the skull shape among the shorebirds studied here. In addition, other variations include the structure of the bill, the head length, the skull width, the distances between the tip of premaxilla and the rostral end of the external nares, and between the rostral end of the external nares and the proximal-most point of the bill, and the expansion of the orbit.

Bill length generally increases with body mass and head length, but there are also other sources of variation localised to particular genera or species. The functional relationships between species' bill morphology and diet are probably strong. It has long been suggested that bill length is related to prey species and sizes buried at different depths in a mudflat (van de Kam *et al.*, 2004). The interspecific variation of the bill length in relation to head length has been suggested to relate to the feeding habit of each species (Barbosa & Moreno, 1999; Burton, 1974; Colwell, 2010). There is considerable variation in body size (mass) between species in the same genus of shorebirds. *Calidris* (calidrid sandpipers) and *Tringa* (shanks) species have a range of various body sizes. Small *Calidris* are similar to or even slightly smaller than plovers. The thin plate spline (TPS) results show that some species with sturdy bills and closely attached rhamphothecae (South Island pied oystercatcher (SIPO) (*Haematopus finschi*), ruddy turnstone (*Arenaria interpres*) and Australian pratincole (*Stiltia isabella*)) have relatively long heads, which may provide a rigid base for use of the powerful bills, whereas some species with relatively long bills (e.g. bar-tailed godwit (*Limosa lapponica*), curlew sandpiper (*Calidris ferruginea*) and terek sandpiper (*Xenus cinereus*)) have flexible bills.

In general, most shorebirds take invertebrates or small fish as their major prey. I found similar gross structures of the tongues and palates in them, structures that have been proposed to help with manipulating prey and preventing regurgitation (Johnston, 2014). These structures include the elongated tongue body within the long bill and the papillae around the rear of the tongue body, the tongue base and the choanal cleft. However, it seems that the species with powerful sturdy bills tend to have short tongues.

6.1.2 Tactile vs. visual foraging

There is considerable interspecific variation in the number of sensory pits for tactile sensation between and within genera of shorebirds. All birds have at least a few sensory pits and Herbst corpuscles embedded in the bony premaxilla, so even the species with no bill-tip organ with dense pits can still use direct touch (Heppleston, 1970). However, remote touch foraging has been suggested to be more efficient than direct touch (van de Kam *et al.*, 2004). This variation of the number of sensory pits in the bill-tip organ has been suggested to relate to the substrates of the foraging habitat (Cunningham *et al.*, 2010; van de Kam *et al.*, 2004). The ruddy turnstone and little whimbrel (*Numenius minutus*), species that prefer terrestrial areas, have low sensory pit numbers in their bill-tip organs. However, other aquatic species have various pit numbers (e.g. the sharp-tailed sandpiper (*Ca. acuminata*) has 549 pits, whereas the terek sandpiper has 192–220 pits). There are possibilities that the number of pits is related to prey types and / or foraging behaviours.

The fact that all birds have sensory pits embedded in their bill tips suggest that the pits are likely present in a common ancestor of all birds. However, the species of the family Scolopacidae are quite different from other shorebird families because of their obvious bill-tip organs with large sensory pit numbers in them. Although the bill-tip organ with concentrated sensory pits has been found in other modern and extinct avian groups (du Toit, Chinsamy, & Cunningham, 2020), testing the taxonomic distribution of sensory pit numbers in evolutionary models suggested that the large sensory pit numbers of the bill-tip organ have evolved an common ancestor to Scolopacidae.

The TPS deformation grid results showed that the bulging orbits were present in both some visual foragers and tactile foragers. The little whimbrel and wood sandpiper (*Tringa glareola*) are the species with bulging orbits but considered to be using less visual and more tactile cues. On the other hand, the red-kneed dotterel (*Erythrogonys cinctus*) and SIPO are

considered visual foragers but with no obvious bulging orbit. In addition, the plover species and the red knot (*Ca. canutus*) are small birds with similar orbit sizes, but the former uses more visual cues, and the latter uses more tactile cues. These results agree with the idea of R. J. Thomas *et al.* (2006) that the visual foragers do not always have larger eyes than the tactile foragers. The bulging orbit is not completely related to visual or tactile foraging.

6.1.3 Nocturnal foraging

It has been suggested that shorebirds feeding at night are mostly visual foragers with great night vision from relatively larger eyes (Martin & Piersma, 2009; R. J. Thomas *et al.*, 2006; van de Kam *et al.*, 2004). Some studies mentioned the habitat switching of some shorebirds at night (Dann, 1999; Rohweder & Baverstock, 1996; Sitters *et al.*, 2001). It has been suggested that tactile foragers tended to stay at the same tidal flats day and night, while visual foragers change habitats at night (van de Kam *et al.*, 2004). However, recent studies showed that the mechanism of habitat switching is much more complex (Jourdan *et al.*, 2021; Rohweder & Baverstock, 1996; Sitters *et al.*, 2001). Furthermore, the TPS deformation grid results and the comparison of the diameter of orbita (OD) from Schäfer and Schmitz (2016) indicate that nocturnal feeding is not absolutely associated with large eye size. In addition to comparing eye sizes between birds, electroretinograms (ERGs) and histological observations of the photoreceptors imply that plovers and stilts have good night vision (Rojas *et al.*, 1999). Instead of relying on a single sense, some birds like whimbrels (*N. phaeopus*), pied stilts (*Himantopus himantopus*) and shanks were suggested to switch between or use both tactile and visual cues to feed at night (Battley *et al.*, 2003; Rojas *et al.*, 1999; Turpie & Hockey, 1993). Most birds may use multiple sensory cues to compensate and support them feeding in disadvantageous low light environments. Even in the daylight, some species may have rather flexible diets. For example, it has been noted that the genera *Calidris* and *Tringa* use variable foraging methods in different situations (Barbosa & Moreno, 1999). It is unclear whether there is a relationship between sensory pits and nocturnal foraging.

6.1.4 Micro tongue tip structures

My scanning electron microscope (SEM) results demonstrated that the micro tongue tip spines can be well preserved for the examination for many years if the specimens are kept in proper condition. Besides the species that have been mentioned before in Kuwae *et al.* (2012) and Withington (2015), the spines were first documented in the black-fronted dotterel (*Elseyornis melanops*) and curlew sandpiper in this study. The species with tongue tip spines in my study are consistent with the proposition of Kuwae *et al.* (2012) that the spines tend to be present in small birds (mass not heavier than common greenshank (*T. nebularia*)). The combined data with other studies suggests the common presence of micro tongue tip spines in shanks, terek sandpipers, ruddy turnstones, and calidrid sandpipers (Kuwae *et al.*, 2012; Withington, 2015). The evolutionary test of this study suggests that the presence of tongue tip spines were likely derived traits in an ancestor shared by shanks, terek sandpipers, ruddy turnstones, and calidrid sandpipers, and in another ancestor of some plovers.

Although the association between the presence of tongue tip spines and biofilm feeding has been suggested by many studies in different aspects (Beninger & Elner, 2020; Elner *et al.*, 2005; Kuwae *et al.*, 2008; Kuwae *et al.*, 2012), the presence of the spines in different species raise the possibility that the tongue tip spines with their small sizes could be applied to feeding functions of filtering or sticking.

Surface pecking has been considered a common behaviour for the species with tongue tip spines to graze on biofilms (Kuwae *et al.*, 2012). This is suggested by my study that all the species here with spines can do surface pecking with short to medium length bills (e.g. terek sandpiper). It is also suggested by the short gaps between tongue tip and mandible tip in some plovers, terek sandpipers and calidrid sandpipers, which may allow their tongues to reach and transport biofilms easily.

6.1.5 Distal rhynchokinesis

The fact that the geometric morphometrics results indicated the variation of the distances between the tip of premaxilla and the rostral end of the external nares may relate to the importance of distal rhynchokinesis in some species. Distal rhynchokinesis has been suggested to give long-distance migratory shorebirds more opportunities to feed on

different habitats and/or prey types with their flexible bills (Estrella & Masero, 2007). Distal rhynchokinesis may relate to more than just one single foraging behaviour, though it seems less related to scything behaviour. Distal rhynchokinesis was also likely present in a common ancestor to all the species and has been later lost in some of them.

6.1.6 Phylogenetic analysis

The fact that different traits are suggested to be explained by different evolutionary models shows that the foraging strategy of a species can be a complex result of several traits interacting together with environments. For example, the short bill-tip organ with concentrated sensory pits in the bar-tailed godwit, terek sandpiper and *Calidris* may allow them to use remote touch foraging, but at the same time retain distal rhynchokinesis for grabbing. Distal rhynchokinesis may increase the feeding efficiency on biofilms through surface tension transport with pecking.

The taxonomic distribution of the morphological traits, especially sensory pit numbers and presence of micro tongue tip spines, seems to be consistent with the phylogenetic trees built from the molecular data. Note the recent rapid evolution of *Tringa* and *Calidris*–most species are small and medium-sized Arctic migratory birds. Interspecific competition for food sources is suggested to be great on the non-breeding grounds (Colwell, 2010), and smaller species might have developed feeding strategies different from those of the large migratory birds to avoid conflicts (Kuwae *et al.*, 2012). The relatively quick gain and loss of the morphological traits related to foraging over evolutionary timescales may reflect variable ecological conditions experienced during migration. Overall, several morphological changes were likely to occur in Scolopacidae over a short period of time. The relatively high diversification rate of Scolopacidae has been mentioned by Barbosa and Moreno (1999), but they also mentioned the high rate of stilts and avocets (Recurvirostrinae), and the low rate of plovers (Charadriinae), which have not been tested with enough species and behavioural data in this study.

6.2 Features of specific birds

The species of the genus *Calidris* generally have a short bill with a large number of sensory pits (376–549 pits) in the bill-tip organ. The pit density decreases with longer organ length in larger birds. Note that the tiny red-necked stint (*Ca. ruficollis*) has a short bill with a high pit density. This does not suggest the coevolution between long bill lengths and tactile feeding of Barbosa and Moreno (1999).

The species of the genus *Tringa* generally have a medium length bill (28.4–53.1 mm in this study) with the organ (pits) taking up much more of its bill length. The bill is rigid and thick dorso-ventrally. It has a smaller number of sensory pits (241–375 pits) than *Calidris* species but larger than the bar-tailed godwit. The pit numbers increase with bill-tip organ length, but the pit density decreases. Those features of the shanks' bills may relate to their foraging behaviours.

A foraging behaviour that may relate to the elongated bill-tip organ of shanks is ploughing for fish. Birds run with their bill partially immersed in the water, often as a line of birds to concentrate fish together (Battley *et al.*, 2003). Thus, a long sensory organ along the distal part of the bill may enable shanks to detect the movement of fish through remote touch from any direction in water.

The distal part of the bill is also submerged in water when scything. Scything behaviour is the sweeping of the bill horizontally from one side to the other in muddy substrates or water (Hockey & Douie, 1995; Rico-Guevara *et al.*, 2019). Scything is commonly used by shanks and terek sandpipers. Besides pecking, here I propose scything as a potential foraging behaviour for grazing biofilms with tongue tip spines. The distances between the tongue tip and mandible tip in shanks are not as short as in calidrid sandpipers, but scything provides a possible way for shanks to use their tongue spines regardless. This proposition is suggested by the spines of the terek sandpiper and wood sandpiper being distributed broadly along the long tongue bodies. In addition, it is suggested that the wrybill (*Anarhynchus frontalis*) (a plover) may use this scything strategy as well based on their spine forms and characteristic sideways sweeps of their bill in soft mud (Withington, 2015).

Moreover, there are species with similar numbers of pits, or fewer, than *Tringa.* Grey-tailed tattler (*T. brevipes*) pit numbers (241–244 pits), for instance, overlap with those of the bar-tailed godwit (201–250 pits). Note that these species with small pit numbers in their bill-tip organs, including grey-tailed tattlers, terek sandpipers, bar-tailed godwits, and whimbrels,

having diets that include crabs and polychaetes gained by probing. The terek sandpiper has a slightly upcurved long bill and bill-tip organ similar to godwits, but with micro tongue tip spines similar to shanks. It can peck surfaces, scythe, and may even be capable of using multiple foraging methods in different environments. Also note that the North Island brown kiwi (*Apteryx mantelli*) has a long bill with sensory pit numbers (251 pits) of the bill-tip organ similar to the shorebirds above (Cunningham *et al.*, 2013). Hence, those pit numbers may relate to deep probing foraging.

Ruddy turnstone is an interesting species that can use multiple foraging strategies. It has a short wedge-shape bill (21.1 mm) that is rigid but still retains some sensory pits. The sensory pit form is shallow and looks quite different from those of other shorebirds; Schäfer and Schmitz (2016), for instance, classified they ruddy turnstone as lacking pits (Fig. 3.7). Its organ (pits) takes up large proportion of its bill length, like those of the shanks. The number of pits (149 pits) is small. With its bill, it can feed on a variety of terrestrial and aquatic invertebrates through searching them by flicking and pushing obstacles, probing mud crab burrows, pecking on surface, smashing barnacles, and cutting the adductor muscle of gastropods. The OD of the ruddy turnstone is similar to the one of plovers and red knots (Schäfer & Schmitz, 2016). The ruddy turnstone may rely on both tactile and visual senses. In addition, it has micro tongue tip spines, which may increase its feeding capabilities.

6.3 Future research

While my dataset covered a wide range of shorebird diversity, it lacked species of medium to large body mass (such as grey plovers (*Pluvialis squatarola*) and Pacific golden plovers (*Pluvialis fulva*)). Furthermore, there are branches in the phylogeny of the order Charadriiformes that I lacked samples for. The species with bill-tip organs of the family Scolopacidae has been a major clade of this study. Other birds of this family that have not been documented include the genus *Bartramia* (upland sandpipers), *Limnodromus* (dowitchers), *Scolopax* (woodcocks), *Coenocorypha* (austral snipes), *Gallinago* (snipes), *Phalaropus* (phalaropes), and *Actitis* (Gibson & Baker, 2012). The range can be widened to the suborder Scolopaci containing the families Scolopacidae, Jacanidae (jacanas), Rostratulidae (painted snipes), Thinocoridae (seedsnipes), and Pedionomidae (plains-wanderers) (Gibson & Baker, 2012; Mayr, 2011). The other two suborders of the Charadriiformes are Lari and Charadrii, and both of them have many species that have not been studied using the methods here yet (Mayr, 2011).

For the associated ecological information, there is not enough information on nocturnal foraging of some species. The situation of habitat selection at night can be complex with documented intraspecific competition. In addition, it is still unclear where some birds stay at night. The question may be solved with new tracking techniques and night vision equipment.

For the cranial morphology, creating 3D geometric morphometrics model with a fusion of the landmarks from different views may provide different information for future studies. For the sensory pits, there are different forms of the pits, such as different total numbers, densities and distributions, on the bill tip of shorebirds. Although I have proposed some potential behaviours associated with those forms, the mechanism of different pit forms will need further confirmation. In this study I have demonstrated that it is possible to observe the micro tongue tip structure of a well-preserved specimen under SEM. There are still some species, especially common greenshank and plovers, that need to be evaluated for the presence of the tongue tip spines. To clearly study the function of these tongue tip spines, more analyses of the keratinised structures from different perspectives with large sample sizes and detailed descriptions, will be needed. Furthermore, to approach the association between the evolution of the trait above and ecological changes, further studies will need to be done in genetics, neuroscience, palaeontology, and behavioural ecology. It would be interesting to test the evolutionary rate of traits against the diversification rates of the species.

7 Reference

Abdi, H., & Williams, L. J. (2010). Principal component analysis. *WIREs Computational Statistics, 2*(4), 433-459. https://doi.org/10.1002/wics.101

Adams, D. C., Collyer, M., Kaliontzopoulou, A., & Sherratt, E. (2016). Geomorph: software for geometric morphometric analyses (Version 4.0.2) [R package]. Retrieved from https://hdl.handle.net/1959.11/21330

Ajayi, A., Edjomariegwe, O., & Iselaiye, O. T. (2016). A review of bone preparation techniques for anatomical studies. *Malaya Journal of Biosciences, 3*(2), 76-80.

Armitage, I. (2017). Black-fronted dotterel. *New Zealand Birds Online.* Retrieved from https://nzbirdsonline.org.nz/species/black-fronted-dotterel

Baker, M. C. (1979). Morphological correlates of habitat selection in a community of shorebirds (Charadriiformes). *Oikos, 33*(1), 121-126. 10.2307/3544520

Balu, S., Bhunia, S., Gachhui, R., & Mukherjee, J. (2020). Assessment of polycyclic aromatic hydrocarbon contamination in the Sundarbans, the world's largest tidal mangrove forest and indigenous microbial mixed biofilm-based removal of the contaminants. *Environmental Pollution, 266*, 115270. https://doi.org/10.1016/j.envpol.2020.115270

Banks, R. C., Cicero, C., Dunn, J. L., Kratter, A. W., Rasmussen, P. C., Remsen, J. V., Jr., . . . Stotz, D. F. (2006). Forty-seventh supplement to the American ornithologists' union check-list of North American birds. *The Auk, 123*(3), 926-936. 10.1093/auk/123.3.926

Barbosa, A., & Moreno, E. (1999). Evolution of foraging strategies in shorebirds: an ecomorphological approach. *The Auk, 116*(3), 712-725. 10.2307/4089332

Battley, P. F. (2017). Great knot. *New Zealand Birds Online.* Retrieved from https://nzbirdsonline.org.nz/species/great-knot

Battley, P. F. (2022). Red knot | huahou. *New Zealand Birds Online.* Retrieved from https://nzbirdsonline.org.nz/species/lesser-knot

Battley, P. F., Poot, M., Wiersma, P., Gordon, C., Ntiamoa-Baidu, Y., & Piersma, T. (2003). Social foraging by waterbirds in shallow coastal lagoons in Ghana. *Waterbirds, 26*(1), 26-34.

Beninger, P. G., & Elner, R. W. (2020). On the tip of the tongue: natural history observations that transformed shorebird ecology. *Ecosphere, 11*(5). 10.1002/ecs2.3133

Berkhoudt, H. (1979). The morphology and distribution of cutaneous mechanoreceptors (Herbst and Grandry corpuscles) in bill and tongue of the mallard (*Anas platyrhynchos* L.). *Netherlands Journal of Zoology, 30*(1), 1-34. https://doi.org/10.1163/002829680X00014

Birdlife Australia. (2022a). *Wood Sandpiper.* Retrieved from https://www.birdlife.org.au/bird-profile/wood-sandpiper

Birdlife Australia. (2022b). *Australian pratincole.* Retrieved from https://www.birdlife.org.au/bird-profile/australian-pratincole

Both, C., Edelaar, P., & Renema, W. (2003). Interference between the sexes in foraging bar-tailed godwits *Limosa lapponica*. *Ardea, 91*, 268.

Bright, J. A., Marugán-Lobón, J., Rayfield, E. J., & Cobb, S. N. (2019). The multifactorial nature of beak and skull shape evolution in parrots and cockatoos (Psittaciformes). *BMC Evolutionary Biology, 19*(1), 104. 10.1186/s12862-019-1432-1

Burnham, K. P., & Anderson, D. R. (2002). *Model selection and multimodel inference : a practical information-theoretic approach* (2nd ed.): Springer.

Burton, P. J. K. (1974). *Feeding and the feeding apparatus in waders: A study of anatomy and adaptations in the Charadrii*: British Museum (Natural History). Publication; no. 719.

Carr, T. D., Varricchio, D. J., Sedlmayr, J. C., Roberts, E. M., & Moore, J. R. (2017). A new tyrannosaur with evidence for anagenesis and crocodile-like facial sensory system. *Scientific Reports, 7*(1), 44942. 10.1038/srep44942

Cavalli-Sforza, L. L., & Edwards, A. W. (1967). Phylogenetic analysis. Models and estimation procedures. *American journal of human genetics, 19*(3 Pt 1), 233-257.

Choi, C.-Y., Battley, P. F., Potter, M. A., Ma, Z., Melville, D. S., & Sukkaewmanee, P. (2017). How migratory shorebirds selectively exploit prey at a staging site dominated by a single prey species. *The Auk, 134*(1), 76-91. 10.1642/AUK-16-58.1

Christian, P. D., Christidis, L., & Schodde, R. (1992). Biochemical systematics of the Charadriiformes (shorebirds) - relationships between the Charadrii, Scolopaci and Lari. *Australian Journal of Zoology, 40*(3), 291-302. https://doi.org/10.1071/ZO9920291

Colwell, M. A. (2010). *Shorebird ecology, conservation, and management*. Berkeley: University of California Press.

Conklin, J. R., Battley, P. F., Potter, M. A., & Ruthrauff, D. R. (2011). Geographic variation in morphology of Alaska-breeding bar-tailed godwits (*Limosa lapponica*) is not maintained on their nonbreeding grounds in New Zealand. *The Auk, 128*(2), 363-373. 10.1525/auk.2011.10231

Conklin, J. R., Lisovski, S., & Battley, P. F. (2021). Advancement in long-distance bird migration through individual plasticity in departure. *Nature Communications, 12*(1), 4780. 10.1038/s41467-021-25022-7

Cunningham, S. J., Alley, M. R., Castro, I., Potter, M. A., Cunningham, M., & Pyne, M. J. (2010). Bill morphology of ibises suggests a remote-tactile sensory system for prey detection. *The Auk, 127*(2), 308-316. 10.1525/auk.2009.09117

Cunningham, S. J., Corfield, J. R., Iwaniuk, A. N., Castro, I., Alley, M. R., Birkhead, T. R., & Parsons, S. (2013). The anatomy of the bill tip of kiwi and associated somatosensory regions of the brain: comparisons with shorebirds. *PLoS ONE, 8*(11), e80036. 10.1371/journal.pone.0080036

Dann, P. (1987). The feeding behaviour and ecology of shorebirds. In *Shorebirds in Australia* (pp. 10-20). Melbourne, Australia: Nelson Publishers.

Dann, P. (1999). Feeding periods and supratidal feeding of red-necked stints and curlew sandpipers in Western Port, Victoria. *Emu - Austral Ornithology, 99*(3), 218-222. 10.1071/MU99025A

Davidson, N. C., Townsend, D. J., Pienkowski, M. W., & Speakman, J. R. (1986). Why do curlews *Numenius* have decurved bills? *Bird Study, 33*(2), 61-69. 10.1080/00063658609476896

Di-Poï, N., & Milinkovitch, M. C. (2013). Crocodylians evolved scattered multi-sensory micro-organs. *EvoDevo, 4*(1), 19. 10.1186/2041-9139-4-19

Dit Durell, S. E. A. L. V., & Goss-Custard, J. D. (1984). Prey selection within a size-class of mussels, *Mytilus edulis*, by oystercatchers, *Haematopus ostralegus*. *Animal Behaviour, 32*(4), 1197-1203. https://doi.org/10.1016/S0003-3472(84)80237-7

Dowding, J. E. (2022). Variable oystercatcher | Tōrea pango. *New Zealand Birds Online.* Retrieved from https://nzbirdsonline.org.nz/species/variable-oystercatcher

du Toit, C. J., Chinsamy, A., & Cunningham, S. J. (2020). Cretaceous origins of the vibrotactile bill-tip organ in birds. *Proc. R. Soc. B, 287*(1940), 20202322. 10.1098/rspb.2020.2322

Duijns, S., Hidayati, N. A., & Piersma, T. (2013). Bar-tailed godwits *Limosa l. lapponica* eat polychaete worms wherever they winter in Europe. *Bird Study, 60*(4), 509-517. 10.1080/00063657.2013.836153

Dunlap, M., & Adaskaveg, J. E. (1997). Introduction to the scanning electron microscope. *Theory, practice, & procedures. Facility for Advance Instrumentation. UC Davis, 52*.

Elner, R. W., Beninger, P. G., Jackson, D. L., & Potter, T. M. (2005). Evidence of a new feeding mode in western sandpiper (*Calidris mauri*) and dunlin (*Calidris alpina*) based on bill and tongue morphology and ultrastructure. *Marine Biology, 146*(6), 1223-1234. 10.1007/s00227-004-1521-5

Elsheikh, E. H., & Al-Zahaby, S. A. (2014). Light and scanning electron microscopical studies of the tongue in the hooded crow (Aves: *Corvus corone cornix*). *The Journal of Basic & Applied Zoology, 67*(3), 83-90. https://doi.org/10.1016/j.jobaz.2014.08.004

Emura, S. (2016). Scanning electron microscopic study on the tongues of seven avian species. *Okajimas Folia Anatomica Japonica, 93*(2), 41-51. 10.2535/ofaj.93.41

Erdoğan, S., & Iwasaki, S.-i. (2014). Function-related morphological characteristics and specialized structures of the avian tongue. *Annals of Anatomy - Anatomischer Anzeiger, 196*(2), 75-87. https://doi.org/10.1016/j.aanat.2013.09.005

Erdoğan, S., & Perez, W. (2015). Anatomical and scanning electron microscopic characteristics of the oropharyngeal cavity (tongue, palate and laryngeal entrance) in the southern lapwing (Charadriidae: *Vanellus chilensis*, Molina 1782). *ACTA ZOOLOGICA, 96*(2), 264-272. 10.1111/azo.12075

Esselink, P., & Zwarts, L. (1989). Seasonal trend in burrow depth and tidal variation in feeding activity of *Nereis diversicolor*. *Marine Ecology Progress Series, 56*, 243-254. 10.3354/meps056243

Estrella, S. M., & Masero, J. A. (2007). The use of distal rhynchokinesis by birds feeding in water. *Journal of Experimental Biology, 210*(21), 3757. 10.1242/jeb.007690

Felice, R. N., & Goswami, A. (2018). Developmental origins of mosaic evolution in the avian cranium. *Proceedings of the National Academy of Sciences, 115*(3), 555. 10.1073/pnas.1716437115

Felice, R. N., Tobias, J. A., Pigot, A. L., & Goswami, A. (2019). Dietary niche and the evolution of cranial morphology in birds. *Proceedings of the Royal Society B: Biological Sciences, 286*(1897), 20182677. 10.1098/rspb.2018.2677

Ferns, P. N., & Siman, H. Y. (1994). Utility of the curved bill of the curlew *Numenius arquata* as a foraging tool. *Bird Study, 41*(2), 102-109. 10.1080/00063659409477205

Gibson, R., & Baker, A. (2012). Multiple gene sequences resolve phylogenetic relationships in the shorebird suborder Scolopaci (Aves: Charadriiformes). *Molecular Phylogenetics and Evolution, 64*(1), 66-72. 10.1016/j.ympev.2012.03.008

Griffin, P. (2013). Red-capped plover. *New Zealand Birds Online.* Retrieved from https://nzbirdsonline.org.nz/species/red-capped-plover

Gussekloo, S. W., Vosselman, M. G., & Bout, R. G. (2001). Three-dimensional kinematics of skeletal elements in avian prokinetic and rhynchokinetic skulls determined by Roentgen stereophotogrammetry. *Journal of Experimental Biology, 204*(10), 1735-1744. 10.1242/jeb.204.10.1735

Hammond, P. (2013). Little whimbrel. *New Zealand Birds* Retrieved from https://nzbirdsonline.org.nz/species/little-whimbrel

Hayman, P., Marchant, J., & Prater, A. J. (1986). *Shorebirds : an identification guide to the waders of the world*. London: Croom Helm.

Heppleston, P. B. (1970). Anatomical observations on the bill of the Oystercatcher (*Haematopus ostralegus occidentalis*) in relation to feeding behaviour. *Journal of Zoology, 161*(2), 519-524. https://doi.org/10.1111/j.1469-7998.1970.tb02053.x

Hockey, P. A. R., & Douie, C. (1995). *Waders of southern Africa*. Cape Town: Struik Winchester.

Hughes, A. L. (2015). Evolution of supraorbital ossification in Charadriiformes. *The Auk, 132*(3), 685-696.

Hulscher, J. B. (1982). The oystercatcher *Haematopus ostralegus* as a predator of the bivalve *Macoma balthica* in the Dutch Wadden Sea. *Ardea, 55*(1–2), 89-152.

Iwasaki, S.-i. (1992). Fine structure of the dorsal lingual epithelium of the little tern, S*terna albifrons* Pallas (Aves, Lari). *Journal of Morphology, 212*(1), 13-26. https://doi.org/10.1002/jmor.1052120103

Iwasaki, S.-i. (2002). Evolution of the structure and function of the vertebrate tongue. *Journal of Anatomy, 201*(1), 1-13. https://doi.org/10.1046/j.1469-7580.2002.00073.x

Iwasaki, S.-i., Asami, T., & Chiba, A. (1997). Ultrastructural study of the keratinization of the dorsal epithelium of the tongue of Middendorff's bean goose, *Anser fabalis middendorffii* (Anseres, Antidae). *The Anatomical Record, 247*(2), 149-163. https://onlinelibrary.wiley.com/doi/10.1002/(SICI)1097-0185(199702)247:2%3C149::AID-AR1%3E3.0.CO;2-T

Jetz, W., Thomas, G. H., Joy, J. B., Hartmann, K., & Mooers, A. O. (2012). The global diversity of birds in space and time. *Nature, 491*(7424), 444-448. 10.1038/nature11631

Jetz, W., Thomas, G. H., Joy, J. B., Hartmann, K., & Mooers, A. O. (2014). A global phylogeny of birds. Retrieved from https://birdtree.org/

Johnson, R. (1984). The cranial and cervical osteology of the European oystercatcher *Haematopus ostralegus* L. *Journal of Morphology, 182*(2), 227-244. https://doi.org/10.1002/jmor.1051820209

Johnston, N. E. (2014). The avian tongue. In.

Jourdan, C., Fort, J., Pinaud, D., Delaporte, P., Gernigon, J., Lachaussée, N., . . . Bocher, P. (2021). Nycthemeral movements of wintering shorebirds reveal important differences in habitat uses of feeding areas and roosts. *Estuaries and Coasts, 44*(5), 1454-1468. 10.1007/s12237-020-00871-5

Kamilar, J. M., & Cooper, N. (2013). Phylogenetic signal in primate behaviour, ecology and life history. *Philosophical Transactions of the Royal Society B: Biological Sciences, 368*(1618), 20120341. 10.1098/rstb.2012.0341

Kass, N., Montalti, D., & Acosta Hospitaleche, C. (2018). Comparison of the skull of Brown Skua (*Catharacta antarctica lonnbergi*) and South Polar Skua (*Catharacta maccormicki*): differentiation source identification and discriminant analysis. *Polar Biology, 41*(5), 1049-1053. 10.1007/s00300-018-2268-7

Krupa, M., Ściborsk, M., Krupa, R., Popis, R., & Wołoszyn, J. (2009). Differences in foraging ecology of wood sandpiper *Tringa glareola* and ruff *Philomachus pugnax* during spring migration in Sajna River Valley (Northern Poland). *Ornis Svecica, 19*, 90-96.

Kuhl, H., Frankl-Vilches, C., Bakker, A., Mayr, G., Nikolaus, G., Boerno, S. T., . . . Gahr, M. (2021). An unbiased molecular approach using 3 ´ -UTRs resolves the avian family-level tree of life. *Molecular Biology and Evolution, 38*(1), 108-127. 10.1093/molbev/msaa191

Kulemeyer, C., Asbahr, K., Gunz, P., Frahnert, S., & Bairlein, F. (2009). Functional morphology and integration of corvid skulls – a 3D geometric morphometric approach. *Frontiers in Zoology, 6*(1), 2. 10.1186/1742-9994-6-2

Kuwae, T., Beninger, P. G., Decottignies, P., Mathot, K. J., Lund, D. R., & Elner, R. W. (2008). Biofilm grazing in a higher vertebrate: the western sandpiper, *Calidris mauri*. *Ecology, 89*(3), 599-606. 10.1890/07-1442.1

Kuwae, T., Miyoshi, E., Hosokawa, S., Ichimi, K., Hosoya, J., Amano, T., . . . Elner, R. W. (2012). Variable and complex food web structures revealed by exploring missing trophic links between birds and biofilm. *Ecology Letters, 15*(4), 347-356. 10.1111/j.1461-0248.2012.01744.x

Kuznetsova, A., Brockhoff, P. B., & Christensen, R. H. B. (2017). lmerTest Package: tests in linear mixed effects models. *Journal of Statistical Software, 82*(13), 1 - 26. 10.18637/jss.v082.i13

Lopez, D., Vlamakis, H., & Kolter, R. (2010). Biofilms. *Cold Spring Harbor perspectives in biology, 2*, a000398. 10.1101/cshperspect.a000398

Lourenço, P. M., Catry, T., Piersma, T., & Granadeiro, J. P. (2016). Comparative feeding ecology of shorebirds wintering at Banc d'Arguin, Mauritania. *Estuaries and Coasts, 39*(3), 855-865. 10.1007/s12237-015-0029-1

Mancini, P. L., Bond, A. L., Hobson, K. A., Duarte, L. S., & Bugoni, L. (2013). Foraging segregation in tropical and polar seabirds: testing the intersexual competition hypothesis. *Journal of Experimental Marine Biology and Ecology, 449*, 186-193. https://doi.org/10.1016/j.jembe.2013.09.011

Martill, D. M., Smith, R. E., Longrich, N., & Brown, J. (2021). Evidence for tactile foraging in pterosaurs: a sensitive tip to the beak of *Lonchodraco giganteus* (Pterosauria, Lonchodectidae) from the Upper Cretaceous of southern England. *Cretaceous Research, 117*, 104637. https://doi.org/10.1016/j.cretres.2020.104637

Martin, G. R. (2017). *The sensory ecology of birds*. doi:10.1093/oso/9780199694532.001.0001

Martin, G. R., & Brooke, M. d. L. (1991). The eye of a Procellariiform seabird, the Manx shearwater, *Puffinus puffinus*: visual fields and optical structure. *Brain, Behavior and Evolution, 37*(2), 65-78. 10.1159/000114347

Martin, G. R., & Piersma, T. (2009). Vision and touch in relation to foraging and predator detection: insightful contrasts between a plover and a sandpiper. *Proceedings of the Royal Society B: Biological Sciences, 276*(1656), 437-445. 10.1098/rspb.2008.1110

Mathot, K. J., Lund, D. R., & Elner, R. W. (2010). Sediment in stomach contents of western sandpipers and dunlin provide evidence of biofilm feeding. *Waterbirds: The International Journal of Waterbird Biology, 33*(3), 300-306.

Mayr, G. (2011). The phylogeny of charadriiform birds (shorebirds and allies) - reassessing the conflict between morphology and molecules. *Zoological Journal of the Linnean Society, 161*(4), 916-934. 10.1111/j.1096-3642.2010.00654.x

McCormack, C. A., Lo Gullo, R., Kalra, M. K., Louissaint, A., & Stone, J. R. (2016). Reliability of body size measurements obtained at autopsy: impact on the pathologic assessment of the heart. *Forensic Science, Medicine, and Pathology, 12*(2), 139-145. 10.1007/s12024-016-9773-1

Medway, D. G. (2000). *The Reed field guide to common New Zealand shorebirds*. Auckland, N.Z.: Reed.

Melville, D. S. (2022). Eurasian whimbrel. *New Zealand Birds Online.* Retrieved from https://nzbirdsonline.org.nz/species/whimbrel

Mitteroecker, P., & Gunz, P. (2009). Advances in geometric morphometrics. *Evolutionary Biology, 36*(2), 235-247. 10.1007/s11692-009-9055-x

Münkemüller, T., Lavergne, S., Bzeznik, B., Dray, S., Jombart, T., Schiffers, K., & Thuiller, W. (2012). How to measure and test phylogenetic signal. *Methods in Ecology and Evolution, 3*(4), 743-756. https://doi.org/10.1111/j.2041-210X.2012.00196.x

Nebel, S., Jackson, D. L., & Elner, R. W. (2005). Functional association of bill morphology and foraging behaviour in calidrid sandpipers. *Animal Biology, 55*(3), 235-243. 10.1163/1570756054472818

Nebel, S., & Thompson, G. (2011). The evolution of sexual bill-size dimorphism in shorebirds: a morphometric test of the resource partitioning hypothesis. *Evolutionary Ecology Research, 13*, 35-44.

Ntiamoa-Baidu, Y. A. A., Piersma, T., Wiersma, P., Poot, M., Battley, P., & Gordon, C. (1998). Water depth selection, daily feeding routines and diets of waterbirds in coastal lagoons in Ghana. *Ibis, 140*(1), 89-103. https://doi.org/10.1111/j.1474-919X.1998.tb04545.x

Pagel, M. (1999). Inferring the historical patterns of biological evolution. *Nature, 401*(6756), 877-884. 10.1038/44766

Paradis, E., & Schliep, K. (2019). ape 5.0: an environment for modern phylogenetics and evolutionary analyses in R. *Bioinformatics, 35*(3), 526-528. 10.1093/bioinformatics/bty633

Passarelli, C., Meziane, T., Thiney, N., Boeuf, D., Jesus, B., Ruivo, M., . . . Hubas, C. (2015). Seasonal variations of the composition of microbial biofilms in sandy tidal flats: focus of fatty acids, pigments and exopolymers. *Estuarine, Coastal and Shelf Science, 153*, 29-37. 10.1016/j.ecss.2014.11.013

Pecsics, T., Laczi, M., Nagy, G., Kondor, T., & Csörgő, T. (2020). Skull morphometric characters in parrots (Psittaciformes). *Ornis Hungarica, 28*(1), 104-120. doi:10.2478/orhu-2020-0008

Pennell, M. W., Eastman, J. M., Slater, G. J., Brown, J. W., Uyeda, J. C., FitzJohn, R. G., . . . Harmon, L. J. (2014). geiger v2.0: an expanded suite of methods for fitting macroevolutionary models to phylogenetic trees. *Bioinformatics, 30*(15), 2216-2218. 10.1093/bioinformatics/btu181

Pierce, R. J. (1985). Feeding methods of stilts (*Himantopus* spp.). *New Zealand Journal of Zoology, 12*(4), 467-472. 10.1080/03014223.1985.10428298

Pierre, J. P. (1994). Effects of sexual dimorphism on feeding behaviour of the bar-tailed godwit (*Limosa lapponica*) at a Southern Hemisphere wintering site. *New Zealand Natural Sciences, 21*, 109-112. http://dx.doi.org/10.26021/680

Piersma, T., Aelst, R. v., Kurk, K., Berkhoudt, H., & Maas, L. R. M. (1998). A new pressure sensory mechanism for prey detection in birds: the use of principles of seabed dynamics? *Proceedings of the Royal Society of London. Series B: Biological Sciences, 265*(1404), 1377-1383. 10.1098/rspb.1998.0445

Powlesland, R. G. (1998). *New Zealand's migrant waders*. Auckland, N.Z.: Penguin in association with Dept. of Conservation.

Profico, A., Piras, P., Buzi, C., Del Bove, A., Melchionna, M., Senczuk, G., . . . Manzi, G. (2019). Seeing the wood through the trees. Combining shape information from different landmark configurations. *Hystrix, the Italian Journal of Mammalogy, 30*(2), 157-165. 10.4404/hystrix-00206-2019

Rasband, W. S. (2020). ImageJ (Version 1.53e). Bethesda, Maryland, USA: U.S. National Institutes of Health. Retrieved from https://imagej.nih.gov/ij/

Revell, L. J. (2012). phytools: an R package for phylogenetic comparative biology (and other things). *Methods in Ecology and Evolution, 3*(2), 217-223. https://doi.org/10.1111/j.2041-210X.2011.00169.x

Rico-Guevara, A., Sustaita, D., Gussekloo, S., Olsen, A., Bright, J., Corbin, C., & Dudley, R. (2019). Feeding in birds: thriving in terrestrial, aquatic, and aerial niches. In V. Bels & I. Q. Whishaw (Eds.), *Feeding in Vertebrates: Evolution, Morphology, Behavior, Biomechanics* (pp. 643-693). Cham: Springer International Publishing.

Robertson, H. A. (2017). Red-kneed dotterel. *New Zealand Birds Online.* Retrieved from https://nzbirdsonline.org.nz/species/red-kneed-dotterel

Rohlf, F. J. (2018a). tpsDig (Version 2.31). State University of New York, Stony Brook, USA: Department of Ecology and Evolution.

Rohlf, F. J. (2018b). tpsUtil (Version 2.31). State University of New York, Stony Brook, USA: Department of Ecology and Evolution.

Rohweder, D., & Baverstock, P. (1996). Preliminary investigation of nocturnal habitat use by migratory waders (Order Charadriformes) in northern New South Wales. *Wildlife Research, 23*(2), 169-183. https://doi.org/10.1071/WR9960169

Rojas, L. M., McNeil, R., Cabana, T., & Lachapelle, P. (1999). Diurnal and nocturnal visual capabilities in shorebirds as a function of their feeding strategies. *Brain, Behavior and Evolution, 53*(1), 29-43. 10.1159/000006580

Ross, T. A. (2018). *The roles of morphology, individuality and arrival from migration in the foraging ecology of bar-tailed godwits at the Manawatū River estuary : a thesis presented in partial fulfilment of the requirements for the degree of Master of Science in Zoology at Massey University, Manawatū, New Zealand.* (Master of Science (MSc) Masters). Massey University, Retrieved from http://hdl.handle.net/10179/15003

Royston, P. (1995). Remark AS R94: a remark on algorithm AS 181: The W-test for normality. *Journal of the Royal Statistical Society. Series C (Applied Statistics), 44*(4), 547-551. 10.2307/2986146

Rubega, M. A., & Obst, B. S. (1993). Surface-tension feeding in phalaropes: discovery of a novel feeding mechanism. *The Auk, 110*(2), 169-178. 10.1093/auk/110.2.169

Sagar, P. M. (2022). South Island pied oystercatcher | Tōrea. *New Zealand Birds Online.* Retrieved from https://nzbirdsonline.org.nz/species/south-island-pied-oystercatcher

Savriama, Y. (2018). A step-by-step guide for geometric morphometrics of floral symmetry. *Frontiers in Plant Science, 9*. 10.3389/fpls.2018.01433

Schäfer, F., & Schmitz, G. (2016). Skull identification key for Central European shorebirds (Aves: Charadriiformes: Scolopaci and Charadrii). *Stuttgarter Beiträge zur Naturkunde A, 9*(1), 267-282. 10.18476/sbna.v9.a16

Scheiffarth, G., Wahls, S., Ketzenberg, C., & Exo, K.-M. (2002). Spring migration strategies of two populations of bar-tailed godwits, *Limosa lapponica*, in the Wadden Sea: time minimizers or energy minimizers? *Oikos, 96*(2), 346-354. https://doi.org/10.1034/j.1600-0706.2002.960216.x

Schneider, E. R., Gracheva, E. O., & Bagriantsev, S. N. (2016). Evolutionary specialization of tactile perception in vertebrates. *Physiology, 31*(3), 193-200. 10.1152/physiol.00036.2015

Sitters, H. P., González, P. M., Piersma, T., Baker, A. J., & Price, D. J. (2001). Day and night feeding habitat of red knots in Patagonia: profitability versus safety? *Journal of Field Ornithology, 72*(1), 86-95.

Steed, C. (2017). Grey-tailed tattler. *New Zealand Birds Online.* Retrieved from https://nzbirdsonline.org.nz/species/grey-tailed-tattler

Stuart, A., Wooding, L., & Takurou, H. (2015). Nocturnal foraging by grey-tailed tattlers *Tringa brevipes*. *Stilt, 67*, 28-30.

Sun, Y., Si, G., Wang, X., Wang, K., & Zhang, Z. (2018). Geometric morphometric analysis of skull shape in the Accipitridae. *Zoomorphology, 137*. 10.1007/s00435-018-0406-y

Sutherland, T. F., Shepherd, P. C. F., & Elner, R. W. (2000). Predation on meiofaunal and macrofaunal invertebrates by western sandpipers (*Calidris mauri*): evidence for dual foraging modes. *Marine Biology: International Journal on Life in Oceans and Coastal Waters, 137*(5-6), 983-993. 10.1007/s002270000406

Swennen, C., De Bruijn, L. L. M., Duiven, P., Leopold, M. F., & Marteijn, E. C. L. (1983). Differences in bill form of the oystercatcher *Haematopus ostralegus*; a dynamic adaptation to specific foraging techniques. *Netherlands Journal of Sea Research, 17*(1), 57-83. https://doi.org/10.1016/0077-7579(83)90006-6

Thomas, G. H., & Freckleton, R. P. (2012). MOTMOT: models of trait macroevolution on trees. *Methods in Ecology and Evolution, 3*(1), 145-151. https://doi.org/10.1111/j.2041-210X.2011.00132.x

Thomas, R. J., Székely, T., Powell, R. F., & Cuthill, I. C. (2006). Eye size, foraging methods and the timing of foraging in shorebirds. *Functional Ecology, 20*(1), 157-165.

Tukey, J. W. (1977). *Exploratory data analysis*. Reading, MA: Addison-Wesley Pub. Co.

Tulp, I., & Degoeij, P. (1994). Evaluating wader habitats in Roebuck Bay (North-western Australia) as a springboard for Northbound migration in waders, with a focus on great knots. *Emu, 94*, 78-95. 10.1071/MU9940078

Turpie, J. K., & Hockey, P. A. R. (1993). Comparative diurnal and nocturnal foraging behaviour and energy intake of premigratory grey plovers *Pluvialis squatarola* and whimbrels *Numenius phaeopus* in South Africa. *Ibis, 135*(2), 156-165. https://doi.org/10.1111/j.1474-919X.1993.tb02827.x

van de Kam, J., Ens, B., Piersma, T., & Zwarts, L. (2004). *Shorebirds an illustrated behavioural ecology* (English updated edition ed.). Utrecht, The Netherlands: KNNV.

van, T. G., Vestjens, W., & Slater, E. (1969). Orange runway lighting as a method for reducing bird strike damage to aircraft. *CSIRO Wildlife Research, 14*(2), 129-151. https://doi.org/10.1071/CWR9690129

Webster, M., & Sheets, H. D. (2010). A practical introduction to landmark-based geometric morphometrics. *The Paleontological Society Papers, 16*, 163-188. 10.1017/S1089332600001868

Whitfield, D. P. (1990). Individual feeding specializations of wintering turnstone *Arenaria interpres*. *Journal of Animal Ecology, 59*(1), 193-211. 10.2307/5168

Withington, R. J. (2015). *The foraging ecology of non-breeding Wrybills (Anarhynchus frontalis) in the Firth of Thames: a thesis presented in partial fulfilment of the requirements for the degree of Master of Science in Ecology at Massey University, Palmerston North, New Zealand.* (Master of Science (MSc) Masters). Massey University, Retrieved from http://hdl.handle.net/10179/7898

Woodley, K. (2022). Bar-tailed godwit | Kuaka. *New Zealand Birds Online.* Retrieved from https://nzbirdsonline.org.nz/species/bar-tailed-godwit

Yang, H.-Y., Chen, B., Ma, Z., Hua, N., van Gils, J., Zhang, Z.-W., & Piersma, T. (2013). Economic design in a long-distance migrating molluscivore: how fast-fuelling red knots in Bohai Bay, China, get away with small gizzards. *The Journal of experimental biology, 216*, 3627-3636. 10.1242/jeb.083576

Zhang, X., Hua, N., Ma, Q., Xue, W., Feng, X., Wu, W., . . . Ma, Z. (2011). Diet of great knots (*Calidris tenuirostris*) during spring stopover at Chongming Dongtan, China. *Chinese Birds, 2*. 10.5122/cbirds.2011.0003

Zharikov, Y., & Skilleter, G. (2011). Sex-specific intertidal habitat use in subtropically wintering bar-tailed Godwits. *Canadian Journal of Zoology, 80*. 10.1139/z02-178

Zusi, R. L. (1984). A functional and evolutionary analysis of rhynchokinesis in birds. *Smithsonian contributions to zoology*.

Zwarts, L., Anne-Marie, B., & Roelof, H. (1990). Increase of feeding time in waders preparing for spring migration from the Banc D'Arguin, Mauritania. *Ardea, 55*(1–2), 237-256. 10.5253/arde.v78.p237

Zwarts, L., & Blomert, A.-M. (1992). Why knot *Calidris canutus* take medium-sized *Macoma balthica* when six prey species are available. *Marine Ecology Progress Series, 83*(2/3), 113-128.

Appendices

Appendix 1

Table 1.1: The first three principal components (PC1, PC2, and PC3) of the principal component analysis (PCA) of the dorsal view.

	Comp1	Comp2	Comp3
1.X	-0.57683	0.027332	-0.00303
1.Y	-0.0002	-0.00986	0.015302
2.X	0.227727	-0.49999	0.0377
2.Y	0.048648	-0.04396	0.069711
3.X	0.233011	-0.46446	0.037477
3.Y	-0.05556	0.039921	-0.05596
4.X	0.188602	0.079302	0.159357
4.Y	0.047644	-0.08484	-0.00862
5.X	0.189044	0.081181	0.143424
5.Y	-0.04721	0.086502	-0.00655
6.X	0.217263	0.132525	0.125301
6.Y	0.111535	-0.1587	0.055482
7.X	0.222487	0.133086	0.107385
7.Y	-0.11128	0.165385	-0.07205
8.X	0.083297	0.184858	-0.56541
8.Y	0.040338	-0.07623	-0.12105
9.X	0.084069	0.182204	-0.57268
9.Y	-0.03269	0.104027	0.095112
10.X	-0.12655	0.131786	0.242261
10.Y	0.195297	0.038166	-0.15073
11.X	-0.124	0.140349	0.224817
11.Y	-0.19464	-0.04133	0.157894
12.X	-0.13933	0.122991	0.108606
12.Y	0.200693	0.25501	0.14298
13.X	-0.1429	0.111482	0.097652
13.Y	-0.20316	-0.25673	-0.12988
14.X	-0.33591	-0.36264	-0.14286
14.Y	0.000578	-0.01736	0.008357

Table 1.2: The first three principal components (PC1, PC2, and PC3) of the principal component analysis (PCA) of the right lateral view.

	Comp1	Comp2	Comp3
1.X	0.202129	0.651415	-0.13807
1.Y	0.038914	0.086153	0.137506
2.X	0.393739	-0.68195	0.166064
2.Y	-0.01929	-0.01329	0.18488
3.X	-0.42626	0.106578	0.333046
3.Y	-0.04602	-0.039	-0.06014
4.X	-0.31036	-0.03837	0.093381
4.Y	-0.13446	-0.08475	-0.03072
5.X	-0.02895	-0.08676	-0.31452
5.Y	0.171228	0.06581	-0.13559
6.X	-0.29509	-0.01898	0.131286
6.Y	-0.10503	-0.06835	-0.18962
7.X	-0.01107	0.071916	0.210169
7.Y	-0.27124	-0.07977	-0.05079
8.X	0.091301	0.051493	-0.00658
8.Y	-0.03683	-0.00578	-0.21602
9.X	0.072162	-0.01792	-0.27661
9.Y	0.01358	0.003571	0.222189
10.X	0.043727	-0.0357	-0.32527
10.Y	0.097881	0.003956	0.099946
11.X	0.054034	-0.06365	-0.15372
11.Y	0.180275	0.086356	0.189967
12.X	-0.14283	-0.06521	-0.04397
12.Y	0.125564	0.019211	-0.13272
13.X	-0.09668	-0.05236	-0.06211
13.Y	0.107404	0.033685	-0.15441
14.X	0.136159	0.042276	0.088266
14.Y	-0.22819	-0.06748	-0.10151
15.X	0.317986	0.137229	0.298649
15.Y	0.106215	0.059676	0.237031

Table 1.3: The first three principal components (PC1, PC2, and PC3) of the principal component analysis (PCA) of the ventral view.

	Comp1	Comp2	Comp3
1.X	0.539995	-0.01827	-0.02261
1.Y	0.001192	-0.00778	-0.01219
2.X	-0.37455	-0.4217	-0.05101
2.Y	-0.05521	-0.01073	0.189171
3.X	-0.37148	-0.42562	-0.04348
3.Y	0.05333	0.014559	-0.17459
4.X	-0.04222	0.248703	0.016309
4.Y	-0.12766	0.130551	0.574004
5.X	-0.03647	0.251152	0.019213
5.Y	0.129066	-0.06064	-0.61915
6.X	0.008918	0.18958	-0.00418
6.Y	-0.18176	0.015628	0.041491
7.X	0.008753	0.181123	0.011717
7.Y	0.183263	-0.02892	-0.02192
8.X	0.052606	0.20542	0.064532
8.Y	-0.12977	-0.06573	0.013413
9.X	0.052688	0.194344	0.054341
9.Y	0.131363	0.049231	-0.01433
10.X	-0.13567	0.117949	-0.23002
10.Y	-0.0608	0.088918	0.066135
11.X	-0.13394	0.122945	-0.22551
11.Y	0.056507	-0.08781	-0.07655
12.X	-0.11093	0.093557	0.011515
12.Y	-0.02486	0.056909	0.021491
13.X	-0.10859	0.09858	-0.01081
13.Y	0.015917	-0.06557	0.021435
14.X	0.054783	-0.09427	0.070239
14.Y	-0.21611	0.171564	-0.04496
15.X	0.053389	-0.08641	0.067751
15.Y	0.22263	-0.16524	0.075401
16.X	0.090899	-0.04854	-0.0612
16.Y	0.000634	-0.01342	-0.00511
17.X	0.202652	-0.24758	0.086091
17.Y	0.000862	-0.01274	-0.02157
18.X	0.249171	-0.36095	0.247108
18.Y	0.001392	-0.0088	-0.01217

Appendix 2

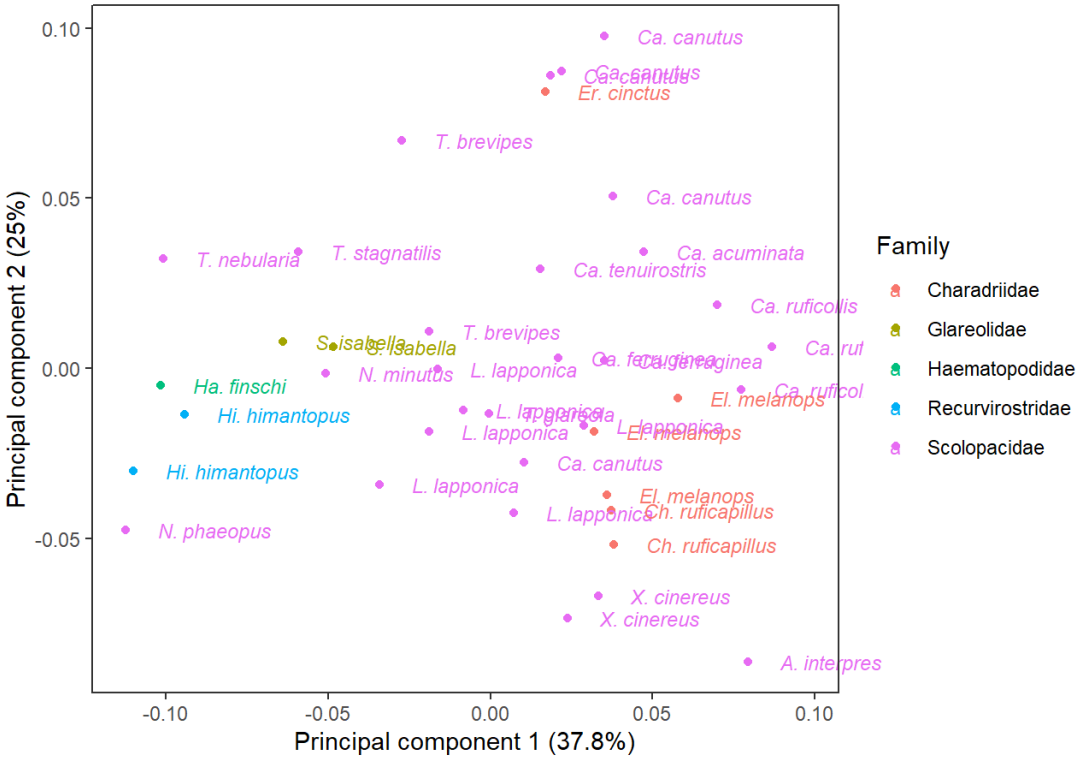

Fig. 2.1: Principal component one and two scores plot of the dorsal view with the landmark No.1 removed. The first two principal components explain 62.8% of the variation in the dataset. The dots are labelled with species and coloured with family.

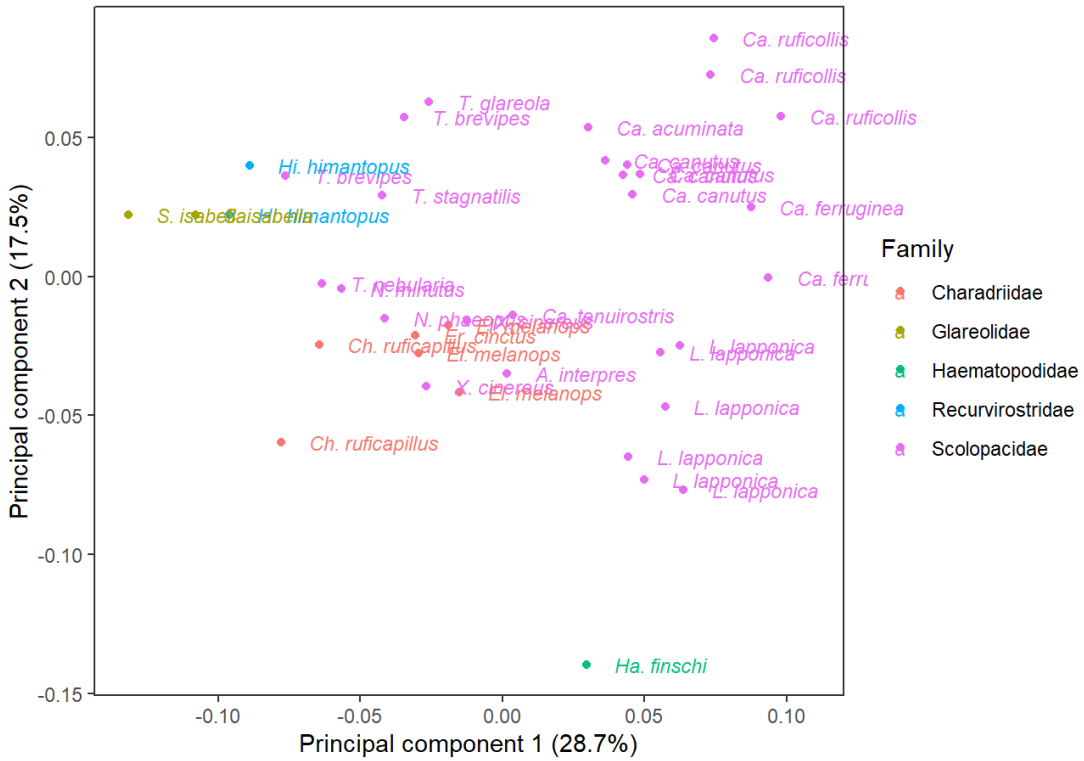

Fig. 2.2: Principal component one and two scores plot of the right lateral view with the landmark No.1&2 removed. The first two principal components explain 46.2% of the variation in the dataset. The dots are labelled with species and coloured with family.

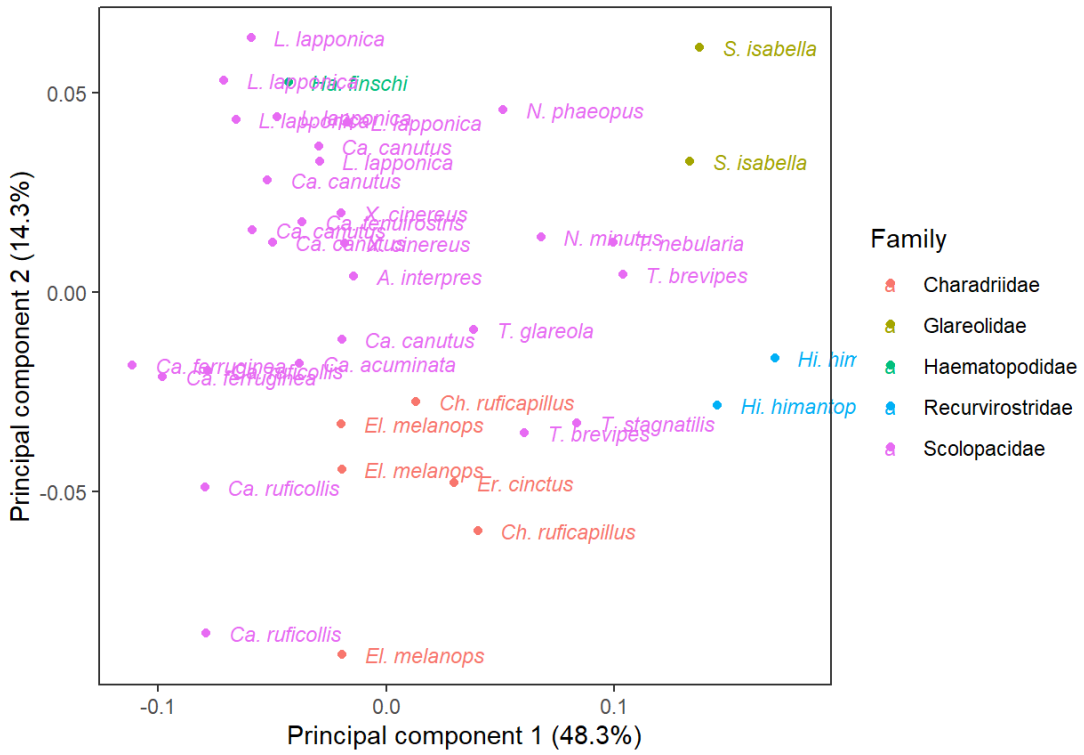

Fig. 2.3: Principal component one and two scores plot of the ventral view with the landmark No.1 removed. The first two principal components explain 62.6% of the variation in the dataset. The dots are labelled with species and coloured with family.

Table 2.1: The first three principal components (PC1, PC2, and PC3) of the principal component analysis (PCA) of the dorsal view with the landmark No.1 removed.

	Comp1	Comp2	Comp3
1.X	-0.49135	0.150266	-0.18161
1.Y	-0.0345	0.034794	-0.13469
2.X	-0.46064	0.148653	-0.17493
2.Y	0.018993	-0.00728	0.142582
3.X	0.115726	0.09628	0.035898
3.Y	-0.03117	0.009211	0.06905
4.X	0.113779	0.081874	0.030158
4.Y	0.029643	-0.01541	-0.08746
5.X	0.259201	0.126249	0.182463
5.Y	-0.1199	0.130217	0.257906
6.X	0.25946	0.118416	0.213469
6.Y	0.117613	-0.1349	-0.30113
7.X	0.013725	-0.61388	-0.08895
7.Y	-0.1289	-0.0708	0.21717
8.X	0.01056	-0.61712	-0.07057
8.Y	0.155124	0.053925	-0.18459
9.X	0.122548	0.160873	-0.34412
9.Y	0.048533	-0.12495	0.278908
10.X	0.122647	0.156883	-0.3048
10.Y	-0.04117	0.114801	-0.26676
11.X	0.138949	0.100038	0.182852
11.Y	0.255474	0.063166	-0.09239
12.X	0.12561	0.100238	0.193057
12.Y	-0.26346	-0.05986	0.07829
13.X	-0.33022	-0.00877	0.327066
13.Y	-0.00628	0.007078	0.023117

Table 2.2: The first three principal components (PC1, PC2, and PC3) of the principal component analysis (PCA) of the right lateral view with the landmark No.1&2 removed.

	Comp1	Comp2	Comp3
1.X	-0.517	0.102325	-0.27895
1.Y	-0.12299	0.156992	-0.12493
2.X	-0.0292	0.088895	0.150408
2.Y	0.09201	-0.09974	-0.36328
3.X	0.200895	-0.03387	0.247102
3.Y	-0.04151	0.109643	0.016865
4.X	-0.13942	0.210942	0.049
4.Y	0.025098	-0.05172	0.087286
5.X	-0.15569	-0.00411	0.022524
5.Y	-0.09421	-0.02615	0.304134
6.X	0.043896	0.166711	0.079209
6.Y	0.259197	0.035522	0.14241
7.X	0.336195	0.504868	-0.20997
7.Y	-0.25641	-0.30944	0.351532
8.X	0.179234	0.025684	0.219895
8.Y	-0.088	0.124306	0.154665
9.X	0.084699	-0.18559	0.226982
9.Y	-0.19454	0.064758	-0.00047
10.X	0.139407	-0.45785	-0.25132
10.Y	-0.0843	0.245408	-0.0707
11.X	0.136563	-0.25979	0.043962
11.Y	0.080442	-0.03309	-0.16244
12.X	0.08263	0.014076	-0.12678
12.Y	0.204246	0.064654	0.021284
13.X	-0.3622	-0.1723	-0.17208
13.Y	0.220973	-0.28115	-0.35636

Table 2.3: The first three principal components (PC1, PC2, and PC3) of the principal component analysis (PCA) of the ventral view with the landmark No.1 removed.

	Comp1	Comp2	Comp3
1.X	0.447185	0.012631	-0.00976
1.Y	-0.05551	0.257512	0.044448
2.X	0.449667	0.027667	-0.00998
2.Y	0.050611	-0.25754	-0.02832
3.X	-0.19969	-0.17604	-0.13448
3.Y	-0.18924	0.396628	-0.37875
4.X	-0.20322	-0.14752	-0.12362
4.Y	0.157328	-0.49638	0.324721
5.X	-0.16055	-0.16478	-0.14233
5.Y	-0.03001	-0.00927	0.108274
6.X	-0.14687	-0.14838	-0.15405
6.Y	0.042359	0.028875	-0.13034
7.X	-0.21755	-0.01548	-0.04356
7.Y	0.114249	-0.22652	-0.07998
8.X	-0.20964	-0.01381	-0.00914
8.Y	-0.09732	0.235612	0.075221
9.X	-0.14509	0.087473	0.323984
9.Y	-0.10819	0.097915	0.002283
10.X	-0.14338	0.08646	0.31233
10.Y	0.118275	-0.10404	0.003658
11.X	-0.10711	0.018109	0.105313
11.Y	-0.05441	0.049326	0.023209
12.X	-0.10776	0.008565	0.111285
12.Y	0.059663	-0.03378	-0.02082
13.X	0.135623	-0.06887	-0.35406
13.Y	-0.14931	-0.13936	0.027918
14.X	0.140647	-0.07788	-0.35314
14.Y	0.119183	0.209202	0.012156
15.X	0.002516	0.049784	0.313344
15.Y	0.010962	0.002963	-0.00176
16.X	0.175208	0.272763	0.221058
16.Y	0.009886	-0.00864	0.007318
17.X	0.290001	0.24931	-0.05319
17.Y	0.001475	-0.0025	0.010759

Appendix 3

Fig. 3.1: The right lateral view of the dentary bill-tip organ of a whimbrel. Note that the pits were aligned along the elongated curved mandible.

Appendix 4

Fig. 4.1: The dorsal view of the tongue of a red knot. The yellow double-headed arrow shows the length of glottis. The blue arrow shows the width of glottis.

Fig. 4.2: The left lateral view of the tongue of a red knot. The yellow double-headed arrow shows the thickness of the papillary crest.

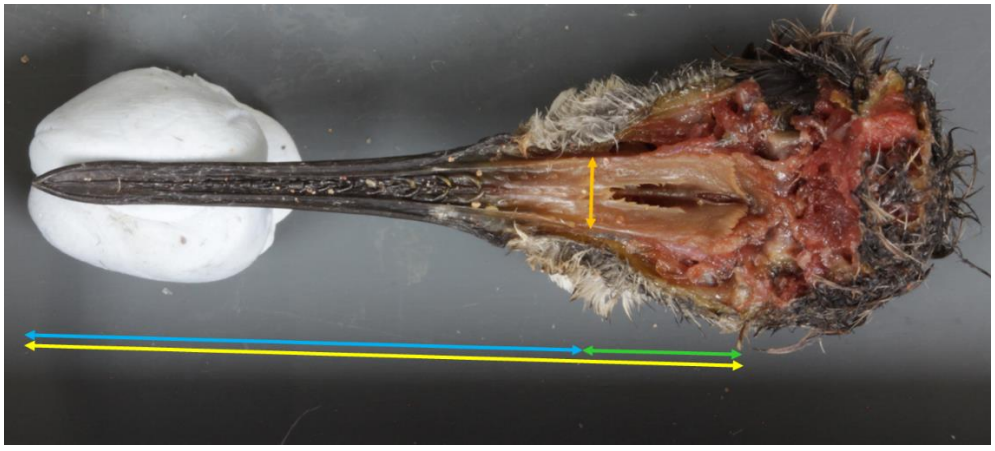

Fig. 4.3: The ventral view of the tongue of a red knot. The yellow double-headed arrow shows the palate length. The blue arrow shows the distance between the palate tip and the row of the palatine conical papillae. The orange arrow shows the width of the row of the palatine conical papillae. The green arrow shows the length of choanal cleft.

Table 4.1: The data of the gross anatomy of oropharyngeal cavities. (Mean±1SD)

	Tongue								Palate			
Species name **Sample size**	Distance between the mandible tip and the tongue tip (mm)	Tongue length (mm)	Distance between the tongue tip and the papillary crest (mm)	Distance between the papillary crest and the rear of tongue (mm)	Width of the papillary crest (mm)	Thickness of the papillary crest (mm)	Length of glottis (mm)	Width of glottis (mm)	Palate length (mm)	Distance between the palate tip and the row of the palatine conical papillae (mm)	Width of the row of the palatin conical papillae (mm)	Length of choanal cleft (mm)
Bar-tailed godwit (*Limosa lapponica*) n=6	50.50 ±5.00	62.85 ±4.65	47.37 ±4.03	18.13 ±1.92	4.47 ±0.29	3.72 ±0.28	6.53 ±1.36	1.27 ±0.56	121.50 ±9.01	109.88 ±9.68	6.43 ±0.63	20.45 ±2.18
Red knot (*Calidris canutus*) n=5	5.08 ±1.46	38.18 ±1.65	25.02 ±1.43	14.32 ±1.06	2.96 ±0.29	3.06 ±0.16	5.18 ±0.78	1.06 ±0.26	46.50 ±1.30	37.45 ±1.34	4.43 ±0.20	7.86 ±1.17
Great knot (*Calidris tenuirostris*) n=1	9.20	43.80	29.50	16.00	3.50	3.10	5.90	1.30	59.30	48.20	6.10	16.50
Red-necked stint (*Calidris ruficollis*) n= 3	3.50 ±0.43	22.33 ±0.45	15.57 ±0.66	7.57 ±1.22	1.43 ±0.21	2.23 ±0.31	3.10 ±0.22	0.67 ±0.05	27.93 ±1.18	22.03 ±0.90	2.17 ±0.25	3.60 ±0.75
Curlew sandpiper (*Calidris ferruginea*) n=2	4.85 ±0.55	38.20 ±3.00	28.45 ±2.45	10.95 ±0.65	2.45 ±0.05	2.55 ±0.05	3.95 ±0.15	0.80 ±0.10	46.85 ±3.05	40.05 ±2.85	3.65 ±0.15	4.20 ±1.10
Sharp-tailed sandpiper (*Calidris acuminata*) n=1	4.40	30.20	21.50	10.00	2.30	2.40	3.70	1.00	38.50	31.00	3.40	14.30
Little curlew (*Numenius minutus*) n=2	33.40 ±1.20	28.90 ±0.60	18.85 ±1.05	13.45 ±0.25	4.25 ±0.05	2.50 ±0.60	6.05 ±0.15	1.20 ±0.30	67.80 ±2.60	57.95 ±1.75	5.70 ±0.30	20.80 ±0.30
Whimbrel (*Numenius phaeopus*) n=1	50.30	39.50	26.10	16.90	5.20	4.00	7.00	2.00	100.60	89.10	7.20	27.70
Grey-tailed tattler (*Tringa brevipes*) n=2	13.15 ±1.05	34.70 ±0.40	24.00 ±0.00	12.40 ±0.30	3.15 ±0.05	2.50 ±0.00	4.60 ±0.10	1.00 ±0.00	53.85 ±1.15	44.30 ±0.90	5.15 ±0.15	17.15 ±0.25
Common greenshank (*Tringa nebularia*) n=1	29.60	39.40	26.90	14.30	3.60	2.90	5.10	1.00	71.90	62.10	5.90	20.40

Table 4.1 continued.

	Tongue								Palate			
Species name **Sample size**	Distance between the mandible tip and the tongue tip (mm)	Tongue length (mm)	Distance between the tongue tip and the papillary crest (mm)	Distance between the papillary crest and the rear of tongue (mm)	Width of the papillary crest (mm)	Thickness of the papillary crest (mm)	Length of glottis (mm)	Width of glottis (mm)	Palate length (mm)	Distance between the palate tip and the row of the palatine conical papillae (mm)	Width of the row of the palatin conical papillae (mm)	Length of choanal cleft (mm)
Wood sandpiper (*Tringa glareola*) n=1	8.40	31.70	23.30	9.20	2.00	1.70	4.40	1.20	43.50	35.40	2.00	13.80
Marsh sandpiper (*Tringa stagnatilis*) n=1	17.20	32.80	24.40	9.90	2.30	2.20	3.50	0.40	54.80	46.80	3.70	8.90
Terek sandpiper (*Xenus cinereus*) n=2	10.00 ±2.60	51.05 ±0.85	39.65 ±0.35	13.25 ±0.85	2.90 ±0.10	3.15 ±0.25	4.65 ±0.15	1.05 ±0.25	64.45 ±1.45	55.95 ±1.45	5.20 ±0.20	9.45 ±0.25
Ruddy turnstone (*Arenaria interpres*) n=1	4.40	28.00	17.30	12.40	3.10	1.60	4.40	0.60	37.70	29.10	5.20	13.90
Australian pratincole (*Stiltia isabella*) =2	8.65 ±0.05	22.20 ±0.10	13.35 ±0.15	10.15 ±0.45	3.15 ±0.25	1.80 ±0.00	3.75 ±0.55	1.10 ±0.00	34.65 ±0.25	26.25 ±0.65	4.60 ±0.10	16.95 ±0.15
Red-capped plover (*Charadrius ruficapillus*) n=2	4.15 ±0.95	21.75 ±2.15	12.60 ±0.30	10.35 ±1.75	2.45 ±0.05	2.10 ±0.10	3.00 ±0.10	0.45 ±0.05	27.90 ±0.10	21.05 ±0.25	3.95 ±0.15	6.75 ±0.95
Black-fronted dotterel (*Elseyornis melanops*) n=3	4.73 ±0.57	16.90 ±0.78	10.50 ±0.45	7.57 ±0.37	1.93 ±0.25	2.00 ±0.24	2.60 ±0.08	0.60 ±0.08	24.83 ±1.31	19.10 ±1.24	3.20 ±0.29	10.77 ±0.52
Red-kneed dotterel (*Erythrogonys cinc*tus) n=1	5.70	26.00	15.20	11.90	1.90	3.00	3.40	0.30	34.10	26.30	3.40	14.20
Pied stilt (*Himantopus himanto*pus) n=2	34.00 ±2.80	43.60 ±0.30	29.70 ±0.40	16.00 ±0.20	4.25 ±0.05	2.95 ±0.35	3.60 ±0.10	0.65 ±0.05	84.05 ±0.35	72.20 ±0.40	5.60 ±0.20	13.80 ±0.70
South Island pied oystercatcher (SIPO) (*Haematopus finschi*) n=1	72.70	33.20	21.40	14.60	5.90	2.80	6.60	1.50	111.70	100.50	8.80	24.50